8-23-2024

Embryotoxicity of Chemotherapeutic Agents Tested Using Engineered Cardiac Organoids

Meng Chai
Syracuse University

Abstract

Medication use during pregnancy presents complex considerations due to its potential for causing congenital malformations and its implications for maternal and fetal health. With approximately 90% of pregnant women consuming at least one pharmaceutical agent, there is a critical need for comprehensive developmental toxicity screening, particularly for cancer treatments during pregnancy. Pluripotent stem cell (PSC) models, specifically iPSC-derived organoids, offer promising approaches for assessing drug toxicity and efficacy during pregnancy. This study introduces an embryotoxicity screening platform using biomaterial-engineered 3D cardiac organoids created through micropatterning techniques. The platform aims to characterize the response of six pharmaceutical agents across pregnancy risk categories, focusing on four chemotherapeutic compounds, based on the measurements of cardiac physiology and tissue morphology. The engineered cardiac organoids serve as a model for characterizing embryonic cardiac development and physiology, holding the potential to enhance diagnostic capabilities for chemotherapy-induced cardiotoxicity. This well-defined 3D structure is proposed as a pre-validation model for early-stage cardiotoxicity assessment, potentially contributing to an updated pregnancy risk classification system.

Embryotoxicity of Chemotherapeutic Agents Tested Using Engineered Cardiac Organoids

by

Meng Chai

B.S., China University of Petroleum (East China), 2019

M.S. University of Miami, 2021

Thesis

Submitted in partial fulfillment of the requirements for the degree of

Master of Science in Bioengineering

Syracuse University

August 2024

Acknowledgments

My heartfelt thanks go to my thesis advisor, Dr. Zhen Ma, who's been a guiding light on my academic journey, supported me throughout my master's program, and saved me from my thesis before the deadline. I'm especially grateful for encouraging me to gain valuable industry experience as an intern in my last academic year.

To my thesis committee - Dr. Qin Zhao, Mary Beth Monroe, and Era Jain - thank you for your time, insights, and valuable feedback. A special shout-out to Dr. Julia M Hasenwinkel - congratulations on your new role! Dr. Monroe, your quick response and willingness to step in were lifesavers. Dr. Jain, your drug delivery course was inspiring and laid the foundation for much of my thesis work.

To my lab family - Shiyang, you're a saint for patiently explaining lab techniques to me time and time again. Chenyan Wang, Tackla Winston, Huaiyu Shi, Dr. Yuanhui Song, Nhu Y Mai, Andy Kowalczewski, and Susan Moradi Nasab - you've all played a part in this journey. Chenyan and Tackla, thanks for the job application help. Huaiyu and Dr. Song, my cells (and I) appreciate your constant care. Y and Andy, thanks for being all available in and out of the lab. Can't wait to see what the new STEMa lab members bring to the table!

A big thank you to my internship manager for reinforcing my research mindset and showing me the ropes of the biotech industry. Also grateful to my company for allowing me to approach my thesis with an industry perspective. To my new manager, I'm thrilled and feel honored to continue exploring my interest in organoids in a real-world industrial setting.

Last but not least, to my family and friends - your mix of doubt and support has kept me grounded and determined in my research career. To my partner, thank you for being my rock through the emotional rollercoaster of thesis writing. And to Poopa, the best cat in the world, my

furry stressbuster and loyal thesis companion - those late nights wouldn't have been the same without you!

Table of Contents

List of Figures

List of Tables

1 CHAPTER 1 INTRODUCTION

1.1 Drug Embryotoxicity and Developmental Toxicity

Congenital anomalies represent a significant global health issue, imposing substantial treatment costs and considerable financial and emotional strain on families and societies. Approximately 6% of newborns worldwide are affected by congenital disorders, leading to hundreds of thousands of associated fatalities annually. [1] A 2023 survey by the World Health Organization (WHO) across 193 countries estimated that congenital disorders result in the deaths of around 240,000 newborns within the first 28 days of life each year.[2] The administration of medication during pregnancy presents complex considerations, given its significant potential to contribute to congenital malformations and its contentious implications for maternal and fetal health outcomes. Epidemiological data suggest that approximately 90% of pregnant women consume at least one pharmaceutical agent.[3] Notably, 80% of pregnant individuals report medication use during the first trimester, a period of critical importance known as organogenesis.[4] On average, pregnant women are exposed to 2.6 pharmacological agents, encompassing both prescription and over-the-counter medications, throughout the course of pregnancy. This high prevalence of pharmaceutical exposure underscores the importance of continually updated clinical guidelines to ensure the safety and efficacy of medications used during pregnancy.[5] Avoiding exposure to harmful substances has become the primary part of preventing and managing severe congenital anomalies during pregnancy, as most of the teratogen-induced anomalies are preventable.[6]

Embryonic development is highly sensitive and can be disrupted by toxic external molecules. Extensive research has demonstrated that toxicants can transfer from maternal blood to the

developing embryo or fetus through the placenta, leading to developmental toxicity. [6] In the United States, environmental or iatrogenic teratogens are responsible for 2–3% of the 3–5% of children born with birth defects. [7] Teratogens may pose the greatest risk during the organogenesis period, which occurs between the 3rd and 8th weeks of fetal development **(Figure 1).** [8] During this critical phase, tissues and organs are forming, and the rapidly dividing cells are particularly susceptible to the harmful effects of these toxic agents. [6] Embryotoxicity describes the detrimental effects of various substances on the critical phase of embryonic development, potentially resulting in malformations, growth retardation, or other abnormalities in the developing fetus. [8] Factors contributing to embryotoxicity mainly lie in the exposure to teratogenic agents during critical stages of embryonic development.[9] Studies have highlighted that exposure to teratogenic agents such as chemicals, viruses, environmental factors, physical factors like X-rays, and drugs, can contribute to approximately 10% of congenital anomalies. [10] These agents can disrupt normal cellular processes, interfere with organogenesis, and affect fetal growth, ultimately causing structural or functional abnormalities in the embryo.

Drugs can have direct teratogenic effects on the developing embryo, potentially causing malformations or embryo-fetal demise. They may impair fetal development by disrupting the transplacental transfer of essential nutrients and oxygen from the mother, thereby reducing fetal blood supply. This disruption can also induce premature myometrial contractions, leading to preterm birth. [11] Furthermore, drugs can influence the intrauterine development of gene-encoding proteins, altering transcriptional regulation signals and adversely impacting embryogenesis. [12] For many drugs, particularly new ones, the limit of human exposure data necessitates reliance on animal studies, in vitro tests, or information on related compounds for

risk assessment. Regulatory authorities like the U.S. Food and Drug Administration (FDA) and the European Medicines Agency (EMA) require that medications potentially used by pregnant women be tracked through pregnancy registries.[7] Research indicates that drug exposure during pregnancy can result in various congenital anomalies, such as cardiovascular defects, neural tube defects, and facial clefts. [13] Nowadays, pharmaceutical agents have emerged as a primary focus in the assessment of developmental toxicity risk, particularly in the context of pregnancy safety evaluation. This focus not only underscores the critical necessity for comprehensive monitoring of drug safety profiles in pregnant populations but also necessitates the development and implementation of innovative methodologies for large-scale developmental toxicity screening of both novel and existing pharmaceutical compounds.[14]

The thalidomide tragedy served as a pivotal moment in pharmacovigilance, catalyzing global awareness regarding the teratogenic potential of pharmaceutical agents. Thalidomide, notorious for its teratogenic effects, exerts its impact by binding to cereblon (CRBN) and inhibiting its ubiquitin ligase activity, which is essential for protein degradation and various cellular processes critical for normal development. This inhibition disrupts CRBN function, triggering a series of events that interfere with key signaling pathways involved in limb development and neovascularization, leading to limb deformities and other congenital anomalies. Thalidomide-induced embryotoxicity also includes the prevention of angiogenic outgrowth during early limb formation, resulting in vessel loss that precedes alterations in limb morphogenesis and gene expression. [15] Given these profound developmental impacts, it is imperative to monitor and assess drug utilization patterns among pregnant women to mitigate fetal exposure to teratogenic agents.[16] Concurrently, elucidating the relationship between drug exposure and congenital

anomalies is of critical importance for healthcare providers to make informed decisions regarding pharmacological interventions during pregnancy.

1.2 Pluripotent Stem Cell-based Embryotoxicity Testing

Although mammalian models are considered the gold standard in toxicological studies and have been extensively utilized for pre-clinical drug toxicity testing, in vivo experiments are characterized by low throughput, high costs, intensive labor, lengthy durations, and significant ethical concerns.[17] Zebrafish were introduced four decades ago as a model for studying developmental biology [18] due to their small size, easy maintenance, and rapid development. Recently, zebrafish have garnered increased interest in toxicological studies and pharmaceutical screening (**Figure 2a**). Their transparent embryos and external development from the mother facilitate the assessment of teratogenic and embryotoxic effects.[19] Additionally, zebrafish are suitable for large-scale screenings; for instance, testing 100 biologically active substances on zebrafish at 2 days post-fertilization revealed that 18 substances induced cardiotoxicity in zebrafish, while 23 are known to cause adverse cardiac effects in humans. [20] However, despite the high similarity between the zebrafish and human genomes, results from zebrafish studies can be controversial due to inherent interspecies differences and the lack of complex human-like responses to stimuli.[21]

Embryonic stem cells (hESCs) and induced pluripotent stem cells (iPSCs) have become the most widely used tools in the pharmaceutical industry for pre-clinical developmental toxicity screening. The embryonic period is particularly vulnerable due to the organisms' extensive proliferative capacity, pluripotency, and cytogenetic stability. Embryonic stem cells, in

particular, offer significant advantages in toxicity assessment, including their ability to mimic early developmental stages and their responsiveness to various toxic agents.[9] An in vitro assay to assess embryotoxicity was proposed by Spielmann et al. in 1997.[22] This mouse Embryonic Stem Cell Test (mEST) leverages the ability of mouse embryonic stem cells (mESCs) to differentiate into various cell types in culture. This assay evaluates three toxicological endpoints following 10-day exposure to chemicals: cytotoxicity assessment across two cell lines, non-differentiated mESCs, and mouse 3T3 fibroblasts, and is conducted over two endpoints to determine the IC50 of the agent. Additionally, the ID50 is calculated based on the other endpoint evaluating the efficiency of mESC differentiation into contracting myocardial cells. (**Figure 2b**). [23] The mEST demonstrated equal or superior accuracy (78%) compared to other in vitro embryotoxicity assays.[24] In 2004, mEST was validated by the National European Centre for the Validation of Alternative Methods (ECVAM) to classify chemicals according to their embryotoxic potential for regulatory purposes.[25] However, the mEST exhibits limitations in its ability to accurately replicate the human physiological environment, potentially yielding drug response profiles that diverge from those observed in human subjects. The logical alternative of employing human embryonic stem cells (hESCs), derived from human embryos, presents significant ethical challenges. This approach remains controversial, particularly among those who ascribe equivalent moral status to human embryos and adult humans. The debate encompasses concerns regarding the ethical implications of manipulating human embryonic development in the pursuit of research objectives. [26]

Induced pluripotent stem cells (iPSCs), generated by reprogramming adult somatic cells with the four Yamanaka transcription factors, exhibit similarities to hESCs in terms of morphology,

proliferation, feeder dependence, surface antigens, gene expression, epigenetic status, telomerase activity, and pluripotency.[27] However, iPSCs encounter fewer ethical concerns compared to hESCs. Following this groundbreaking development, research has focused on producing genetically modified differentiated cells such as neurons, cardiomyocytes, endothelial cells, and hepatocytes, which are suitable for large-scale toxicology screenings.[28] The development of spontaneously contracting CMs from iPSCs has emerged as a novel method for developing cardiotoxicity assay using physiologically relevant human cell models (**Figure 2c**).[29] [30] Multi-dimensional function assays for drug toxicity screening are developed using orthogonal techniques in a high throughput fashion, allowing efficient and extensive drug toxicity characterization (**Figure 2d**). [31] iPSC-derived CMs expressed cardiac contractile proteins and major ion channels, mimicking the physical contraction observed in native CMs (**Figure 2f**), [32] which provides a more accurate evaluation of developmental toxicity that closely recapitulates human physiology. Compared to the traditional mEST, iPSCs offer enhanced versatility in their capacity to be directed towards specific differentiation, and identify the drug-induced toxicity at early stages of human development by enabling the evaluation of impacts on differentiation processes. This capability suggests that iPSC-based models represent a promising and potentially more predictive tool for developmental toxicity assessment.

1.3 Organoid Technology for Embryotoxicity and Developmental Toxicity Testing

The 2D monolayer model's feasibility and relative simplicity underscore its primary limitation: the lack of structural complexity, dynamic growth, diverse cell types, organ-level intricacy, in vivo environment, vascularization, and maturity. Critics have doubted the validity of studying isolated cells outside an intact system, as physiological pathways, drug responses, and

phenotypic outcomes cannot be accurately replicated in a manner that mirrors in vivo human conditions. This limitation raises concerns about the model's ability to reflect the true biological environment necessary for precise drug testing and disease modeling.[33] Organoids have long been acknowledged as complex three-dimensional structures that replicate the architecture and functionality of in vivo organs, which are developed from stem cells or organ-specific progenitors through a self-organization process.[34] They exhibit a composition and behavior closely aligned with physiological cells, maintain a more stable genome, and provide improved adaptability for biological transfection and high-throughput screening applications.[35]

Compared to two-dimensional models, three-dimensional (3D) model systems are better equipped to accurately replicate the physiological environments and cellular interactions found in living organisms. iPSC-derived organoids can be regarded as minimal systems that emulate human developmental mechanisms and disorders in vitro, as these intrinsic processes are often challenging to identify in vivo.[36] Both hESCs and iPSCs have the capacity to spontaneously aggregate, forming structures known as embryoid bodies (EBs). These EBs can differentiate into derivatives of the three primary germ layers: ectoderm, mesoderm, and endoderm, thereby simulating the early stages of embryogenesis.[37] Consequently, EBs or EB-derived organoids serve as a valuable model for investigating human embryonic development and assessing the embryotoxicity of various chemicals that pose risks to the fetus through assays that measure abnormalities in cellular proliferation and differentiation (**Figure 3a**). The study of human development and organogenesis, traditionally limited by the scarce availability of human embryonic and fetal tissues and ethical concerns, stands to benefit significantly from the use of hiPSC-derived organoids.[36]

Evaluations of developmental toxicity are crucial for both preclinical screening of drug candidates and studying human embryo development. Organoids derived from iPSCs present a promising platform for these applications due to their capacity to closely replicate endogenous cell organization and organ structures. This fidelity enables researchers to examine cell-cell interactions within a context that closely mirrors human physiology and development, providing more reliable assessments compared to traditional 2D cell models or animal models.[38] These organoids have been developed for different organ systems, such as the digestive system, liver, kidney, brain, and retina (**Figure 3, b-g**) [39–42] Compared to organoids derived from adult stem cells, iPSC-derived organoids offer a significant advantage in their ability to recapitulate the structural and functional characteristics of fetal organs. This capability provides valuable opportunities for modeling genetic or environmentally induced toxicity at various developmental stages or during specific phases of organogenesis.

As previously noted, approximately 1% of congenital anomalies are associated with pharmaceutical exposure.[43] Beyond replicating key aspects of human development, organoid technology enables researchers to examine the impact of drugs on specific cell types and tissues involved in fetal growth and maturation. This specificity is crucial for identifying potential teratogenic effects that could affect the developing fetus. Consequently, organoid models offer valuable insights for regulatory agencies and healthcare providers, aiding in the assessment of pharmaceutical compound safety during pregnancy.

Kidney organoids, which feature nephron-like tubular structures, have been extensively produced and display a high degree of similarity to first-trimester human kidneys. [40] [33,44]These tubular organoids exhibit kidney injury molecule-1 (KIM-1) expression following nephrotoxic chemical injury. Nephrotoxicity can be evaluated by assessing the KIM-1 expression and cellular apoptosis induced by nephrotoxicants, such as gentamicin and cisplatin, in proximal tubules (**Figure 4a**). [44–46] A novel human testis organoid, incorporating peritubular cells, Sertoli cells, Leydig cells, and spermatogonia stem cells, has been developed as an advanced screening tool for assessing the reproductive toxicity of chemotherapeutic drugs such as cisplatin, etoposide, doxorubicin, and busulfan (**Figure 4b**). The 3D testis organoids exhibited dose-dependent responses and maintained IC50 values that were significantly higher than those observed in 2D cultures, allowing for a more physiologically relevant assessment of gonad toxicity compared to traditional 2D cultures.[47]

In addition to pharmaceutical compounds, *in utero* exposure to illicit drugs poses a threat to fetus development. Indeed, most drugs of abuse can easily cross the placenta and pose significant risks to nervous system development. However, classic clinical studies on fetal exposure often fall short in detecting induced deficits in brain formation and function[48]. Among these illicit substances, cocaine exposure during fetal development is consistently linked to impairments in fetal head growth and subsequent neurobehavioral deficits. [49] This highlights the critical need for comprehensive research to fully understand the nuanced impacts of such exposures on fetal development. Notably, prenatal cocaine exposure has been linked to impaired neurobehavioral function through disruption of frontal cortical development. [50,51] Kindberg et al. demonstrated cocaine-induced premature neuronal differentiation in various cortical neuronal subtypes,

impaired neocortical patterning, and increased reactive oxygen species (ROS) formation with a 3D EB-based neocortical model.[52] Furthermore, by employing 3D neocortical organoids with a single cortex-like unit, Lee et. al identified a specific human cytochrome P450 isoform, CYP3A5, as responsible for cocaine-induced developmental abnormalities in the human neocortex. These abnormalities include a proliferation deficit and premature differentiation of neuroepithelial progenitors, along with a significant reduction in cortical plate formation in the organoids.[53]

Besides the drug-induced developmental toxicity, organoid models have also been applied to examine the embryotoxicity of other chemical substances, such as environmental pollutants. As one of the most significant teratogens, environmental toxins are not only associated with respiratory symptoms and diseases but also with severe adverse birth outcomes following prenatal exposure.[54,55] Researchers have utilized iPSC-derived alveolar organoids to investigate the developmental toxicity associated with diesel PM2.5 exposure,[56] demonstrating that high levels of dPM2.5 exposure disrupt the development of alveolar epithelial cells, rendering them more susceptible to infections.

As many new or existing drugs have been found to cause unexpected adverse cardiac effects, cardiotoxicity has become a critical area in toxicity assessment. These cardiac adverse effects are often identified late in the traditional drug discovery pipeline or, in some cases, only after the drugs have been released to the market. [19,57] Therefore, it is necessary to conduct early and comprehensive cardiac safety evaluations during drug development. Doxorubicin is known to exhibit severe cytotoxic effects on cardiac organoids, evidenced by decreased cell viability,

elevated expression of apoptosis-related and inflammatory factors, and alterations in beating frequency **(Figure 4c**).[58] [59] Recently, Chen's group demonstrated that doxorubicin induces severe cytotoxicity in cardiac organoids, evidenced by reduced cell viability, increased inflammation, and disrupted mitochondrial functions.[60] Additionally, doxorubicin treatment significantly elevated the lactate dehydrogenase (LDH) level in the organoid culture medium, consistent with the previous 2D cell model showing high serum LDH levels in patients with doxorubicin-induced cardiac injury.[61]

Recent studies have demonstrated the power of human organoids as a platform for high-throughput functional screenings in preclinical drug development, as they reduce false positives commonly encountered in traditional 2D screening systems. Mill et al. developed a high-content functional screening system for the assessment of a 5000-compound library. Utilizing human cardiac organoids, they have explored the pathway-regulated cardiomyocyte proliferation in both immature and mature cardiac organoids (**Figure 4d**). [62] Immature organoids were first used for pre-screening the compounds with CM pro-proliferative effects and normal contractile functions, while those inhibiting proliferation or contraction behaviors were both eliminated. Mature organoids were subsequently employed for compound validation and further single RNA-seq profiling of critical pathways that regulate CM proliferation, aiming for the accurate prediction of the potential cardiotoxicities and negative contraction effects on compounds that promote CM proliferation. Meanwhile, simvastatin was demonstrated to inhibit the regulation pathway and, therefore, decrease the CM proliferation and heart size. Indeed, maternal statin use during the first trimester of pregnancy has been linked with congenital heart defects in newborns.[63] In general, human organoid screening assays in a high-throughput fashion hold the promise of

accurately identifying potential therapeutic targets with minimum toxicity and, meanwhile, evaluating the safety of drug use during pregnancy and its potential implications for fetal cardiac development.

1.4 State-of-Art Cardiac Organoids

The heart is the first organ to function in human embryos, collaborating with the circulatory system to ensure the unidirectional and continuous flow of blood, which is crucial for transporting oxygen, nutrients, and hormones throughout the developing body.

Cardiac organoids are three-dimensional self-organized structures that mimic the shape and function of heart tissue. These organoids include major cardiac cell types such as cardiomyocytes (CM), cardiac fibroblasts (CF), and endothelial cells (EC). Recent studies have demonstrated that cardiac organoids can effectively model human cardiac development, showcasing substantial progress in understanding heart formation and function.

Drakhlis's group introduced a method for generating cardiac organoids through Matrigel embedding, modulated by the WNT pathway, to replicate the initial stages of human cardiogenesis (**Figure 5a, 5b**).[64] This study detailed the development of early heart structures from mesoderm formation to the emergence of the foregut endoderm, mirroring the early stages of the native heart prior to heart tube formation. They further demonstrated that NKX2.5, one of the earliest cardiac lineage markers, was expressed in a ring shape, with the inner layer comprising endothelial and foregut-like cells, the middle layer primarily consisting of cardiomyocytes, and the outer layer containing mesenchymal and liver cells. Hofbauer's team established chamber-like cardioids featuring a central cavity to emulate early heart lineage

development (**Figure 5c**).[65] They claimed the cavity formation, attributing it to the intrinsic capabilities of the cardiac mesoderm. [66,67] The formation of these cavities began during the mesoderm stage, with numerous small cavities merging into a single major cavity around Day 3, resembling the early left ventricular heart chamber. To recapitulate the subsequent stage of heart development involving epicardium interaction, Hofbauer et al. co-cultured cardioids, composed of endocardial and cardiomyocyte lineages, with epicardium. This integration extended the cardioid culture to the stage of epicardial tissue formation, enabling the investigations of interactions among the three cardiac lineages.

Lewis et al. described a cost-effective method for generating cardioids by using chemical inhibitors, such as CHIR99021, in combination with exogenous growth factors BMP4 and Activin A. This approach resulted in the robust production of chamber-like heart organoids with well-defined vascular structures (**Figure 5d**). Similar to Hofbauer's study, they optimized conditions to integrate epicardial tissue adjacent to myocardial tissue using distinct differentiation protocols, emphasizing the crucial role of epicardium-myocardium communication in early heart formation. [68,69] Additionally, they further employed this cardioid model to study pregestational diabetes-induced congenital heart disease by culturing the organoids in media with elevated glucose and insulin levels. These findings suggest that heart organoids can model non-genetically induced congenital heart disease, providing a valuable tool for studying disease pathology.

Embryonic organoids, which replicate the morphological and transcriptional features of early embryos, have demonstrated significant potential for studying organogenesis. Rossi et al.

described an embryonic organoid model, termed gastruloids, that mimics early heart development, from the generation of cardiovascular progenitor cells to the specification of the first and second heart fields.[70] By culturing mESCs in a stem cell culture medium containing CHIR99021, followed by a cardiac differentiation medium supplemented with basic fibroblast growth factor (bFGF), L-ascorbic acid phosphate, and vascular endothelial growth factor (VEGF), a crescent-like structure emerged on the gastruloids by Day 6 (**Figure 5e**). The crescent subsequently developed into cardiac tube-like formations on their anterior side, representing the initial beating regions exhibiting Ca^{2+} signaling properties.[71]

Current methods for generating cardiac organoids using supportive matrices or non-adhesive culturing face significant challenges in achieving multiple cell populations within a single tissue. This difficulty arises as specific culture conditions may favor the dominant cell type but be unsuitable for supplementary cell types within the organoids.[72] Additionally, controlling the patterning of these organoids is challenging, often leading to undesired differentiation, and their mechanical fragility exacerbates these issues. [73,74] For example, gel-embedding and suspension culturing protocols leverage the intrinsic tendency of cardiomyocytes to self-assemble or aggregate. [75] However, controlling the shape of organoids within a self-organizing environment poses significant challenges, especially when a defined shape is crucial for clinical applications. Moreover, traditional fabrication techniques have further hindered the clinical application of organoids due to low reproducibility and efficiency.[76] Therefore, it is essential to develop next-generation cardiac organoids by integrating interdisciplinary research from biomaterials, tissue engineering, and stem cell biology [77]. Advances in bioengineering have focused on improving tissue regeneration while simultaneously replicating the complex cellular environments

characteristic of early cardiac morphogenesis in vivo. For example, the inefficient geometric control by gel embedding can be mitigated by employing well-defined tubular cardiac constructs through 3D bioprinting. [78] Arai's team addressed this by integrating the pre-cultured spheroids containing iPSC-derived CM, EC, and CF onto the designed needle arrays with a controlled shape. These spheroids were printed onto a needle array to form tubular structures, and scaffold-free constructs were obtained by removing the needle arrays and allowing the tissues to mature for seven days in a bioreactor. Additionally, another study optimized the ECM formulation, incorporating it into a bioink that directly prints iPSCs, continuously promoting cell proliferation, resulting in high cell density and enhanced cardiac tissue connectivity.[79]

Min's team, this year, developed an engineered human cardiac tissue system that effectively integrates three critical microenvironmental cues from the native heart: cellular components (iPSC-CMs, ECs, and CFs), extracellular matrix derived from decellularized heart tissue, and dynamic flow provided by a microfluidic device.[80] The extracellular matrix hydrogel offers biocompatibility and mechanical support, promoting extensive cell-cell and cell-gel interactions, which result in a more compact and condensed cardiac tissue structure. Meanwhile, dynamic flow ensures the efficient transport of nutrients and oxygen to the developing cardiac tissues. This highly stimulated microenvironment enhances the differentiation and maturity of cardiac tissues compared to conventional culture matrices, leading to increased autonomous contractile activity.

1.5 Overall Goal of the Thesis

In this thesis, I will present an embryotoxicity screening platform utilizing the self-organization of 3D cardiac organoids through a biomaterial-based approach. This advanced system

incorporates micropatterning techniques to confine iPSC colonies within precisely defined micropatterns, which are fabricated utilizing polyethylene glycol (PEG) hydrogel with the aid of molded polydimethylsiloxane (PDMS) stencils etched on the solid tissue culture substrate. The grafted PEG hydrogel structure imparts geometric constraints to the iPSC colonies, thereby facilitating cellular organization and alignment during cardiac differentiation process. This engineered microenvironment more faithfully recapitulates the spatial dynamics characteristic of native cardiac development. The primary objectives of this thesis are: 1) To generate self-organized cardiac organoids with geometric constraints; 2) To apply these engineered cardiac organoids for embryotoxicity screening using six drugs with varying profiles in FDA Pregnancy Risk Categories; and 3) To characterize the drug responses of 3D cardiac organoids in terms of cardiac differentiation and contractile functions. Chapter 2 will detail the micropatterning of the biomaterial substrate for 3D cardiac organoid generation. Chapter 3 will investigate drug-induced embryotoxicity on the cardiac organoids. Chapter 4 will conclude the thesis by summarizing the advantages of this platform in generating 3D cardiac tissues and discussing the system limitations and future work for the development of embryotoxicity screening assay.

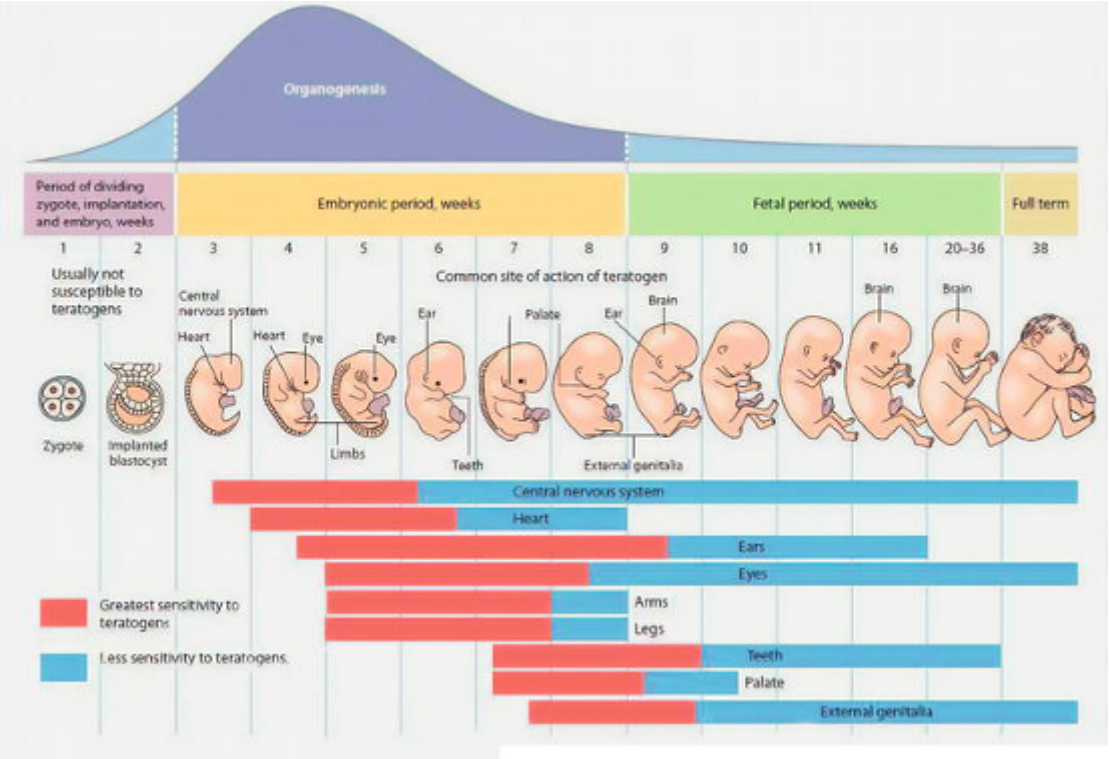

Figure 1. Sensitivity to teratogens during pregnancy. The developmental stage of organogenesis, occurred during the first trimester of pregnancy (3-8 weeks), is recognized as the most susceptible period to adverse effects from teratogens.[6]

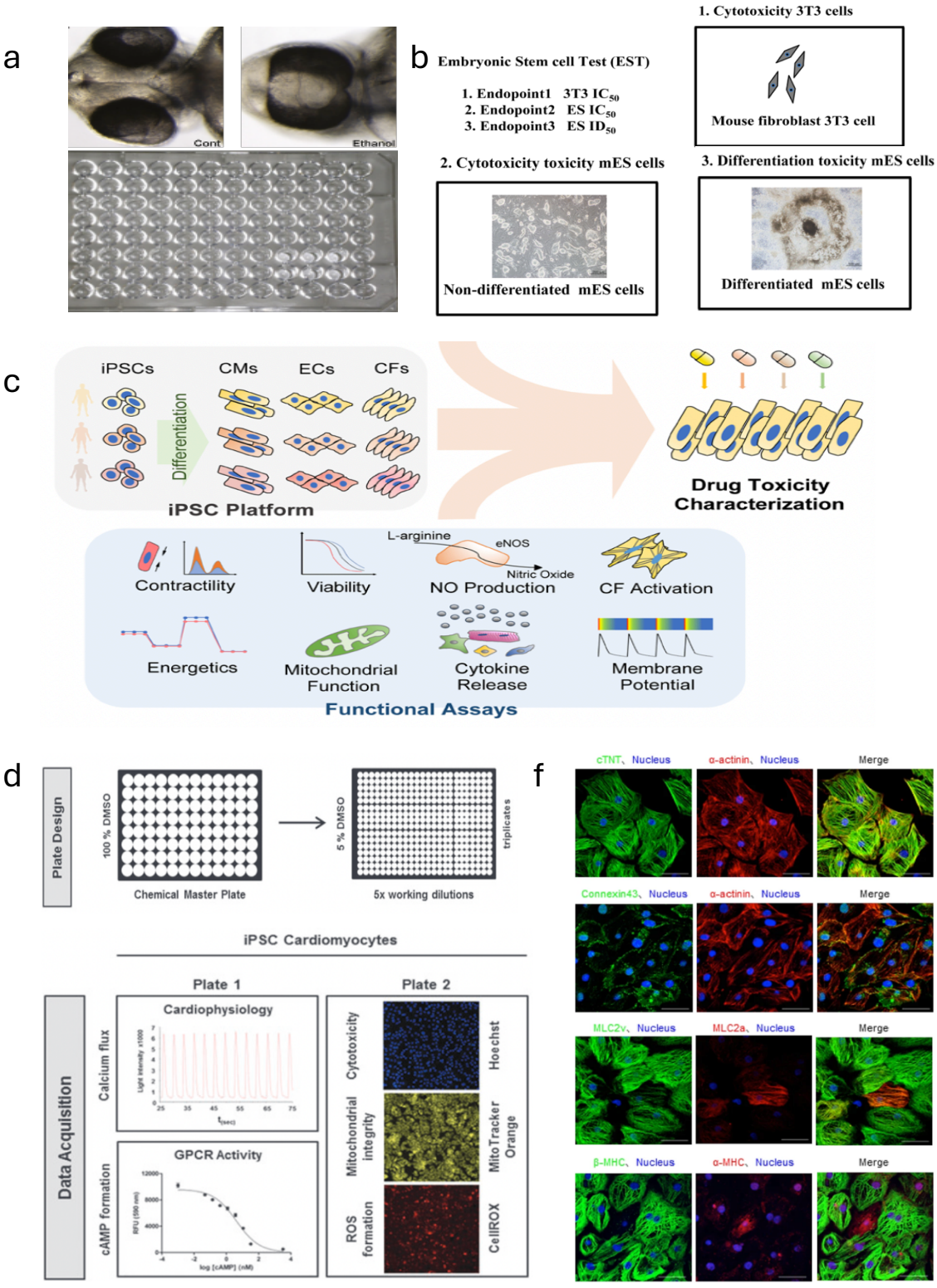

Figure 2. Pluripotent stem cell technology for developmental toxicity screening. (a) Small and transparent zebrafish embryos serve as a toxicological model. Ethanol exposure induces

craniofacial abnormalities 48 hours post-fertilization.[19] (b) Schematic overview of the ECVAM-validated mEST method, including the principle and the endpoints of the mEST method to assess the developmental toxicity using permanent cell lines: mouse 3T3 fibroblasts and mouse ES cells.[23] (c) Human induced pluripotent stem cell (iPSC) platforms for the characterization of drug-induced cardiotoxicity. Various independent methods are employed to develop functional assays for preclinical toxicity screening and prediction.[30] (d) High-content cardiotoxicity screening assays using iPSC-derived cardiomyocytes (iPSC-CMs) with multiple orthogonal techniques, including assessments of calcium flux, G-protein-coupled receptor activity, cytotoxicity, mitochondrial integrity, and reactive oxygen species (ROS) formation.[31] (f) The structure and morphology of iPSC-CMs. Immunolabeling demonstrates the expression of cardiac-specific proteins, such as cardiac troponin T (green) and α-actinin (red), connexin-43 (green) and α-actinin (red), MLC2V (green) and MLC2A (red), and β-MHC (green) and α-MHC (red).[32] All figures are reproduced with copyright permission.

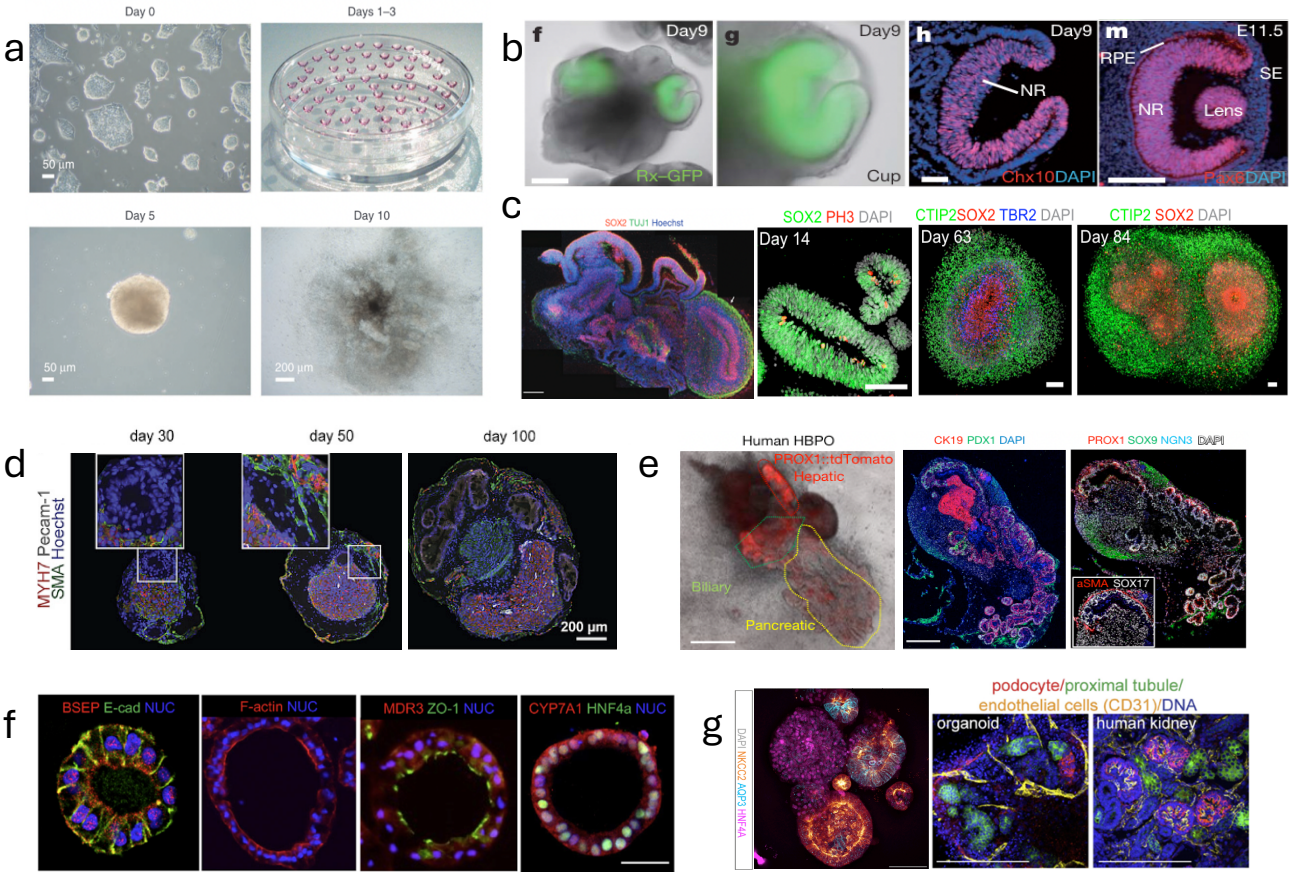

Figure 3. Pluripotent stem cell (PSC)-derived 3D organoids. (a) Stages of mouse embryonic stem cell (mESC) development into embryoid bodies by Day 5 and beating cardiomyocytes by Day 10.[24] (b) Self-organized optic-cup-like structure by mESC aggregates, exhibiting early neural retina (NR) and retinal pigment epithelium (RPE) expression.[81] (c) Early human whole cerebral organoid with heterogeneous regions containing neural progenitors and neurons (Left) and forebrain-specific organoid maturation into a stratified structure (Right).[82] (d) Hepato-biliary-pancreatic organoid exhibiting foregut-midgut boundary at Day 90.[83] (e) Multi-lineage cardiac-gut organoid with interstitial tissue and pre-vascular networks in between.[84] (f) Human tubuloid with mature tubular cells[40] and vascular structure[45] resembling human kidney section. (g) Human liver organoid demonstrating the luminal structure. [85] All figures are reproduced with copyright permission.

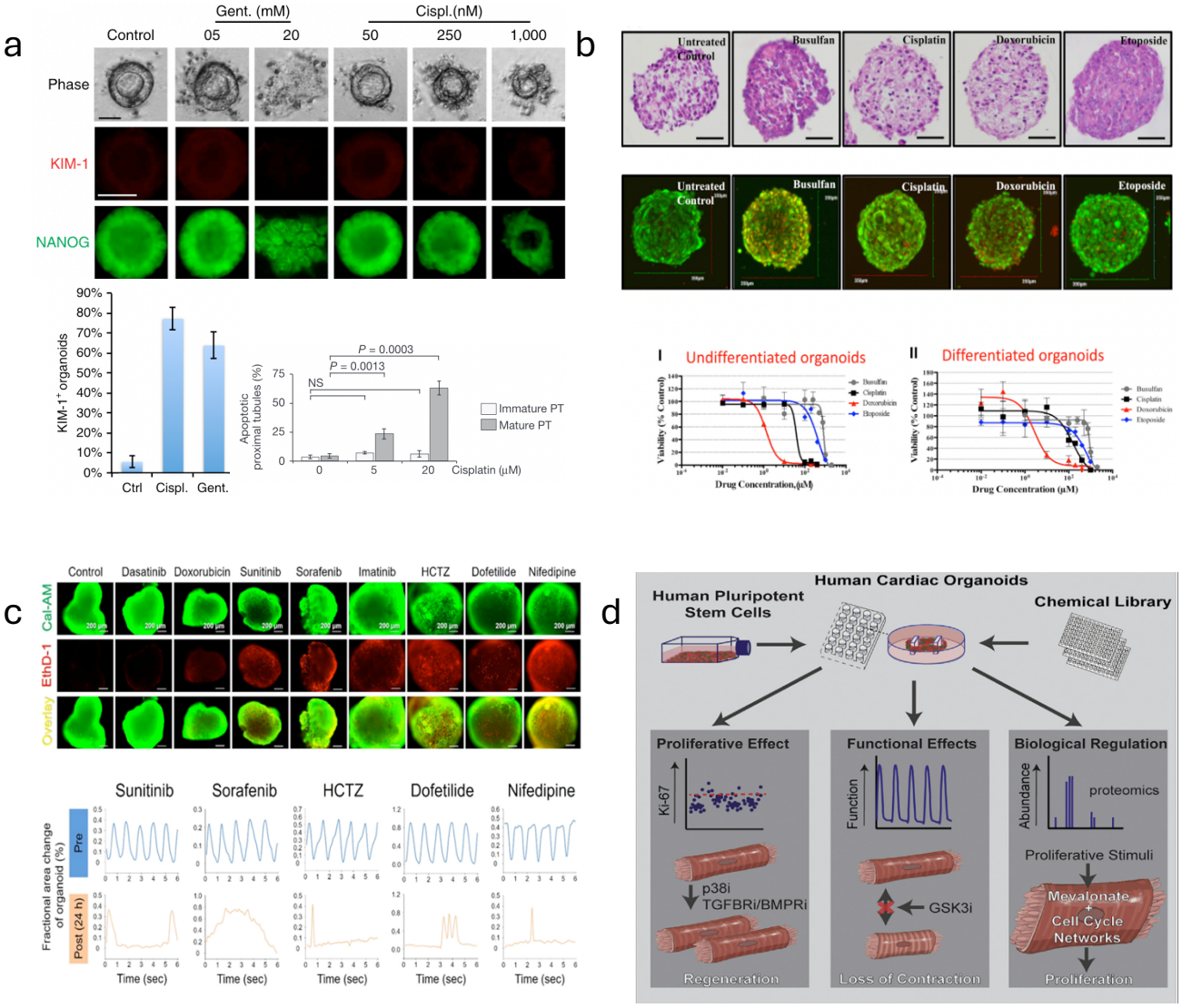

Figure 4. iPSC-derived organoid assays for drug-induced developmental toxicity screening. (a) Tubular organoid model for kidney nephrotoxicity studies, quantified by KIM-1 expression and cytotoxicity to proximal tubules.[44,86] (b) Quantification of human testicular organoid post-drug exposure.[47] (c) High-throughput screening design for method optimization and drug-induced cardiotoxicity screening, characterized by cytotoxicity and physiological tests.[59] (d) Preclinical compound screening and system approaches to identify therapeutic targets in a high-throughput fashion.[62] All figures are reproduced with copyright permission.

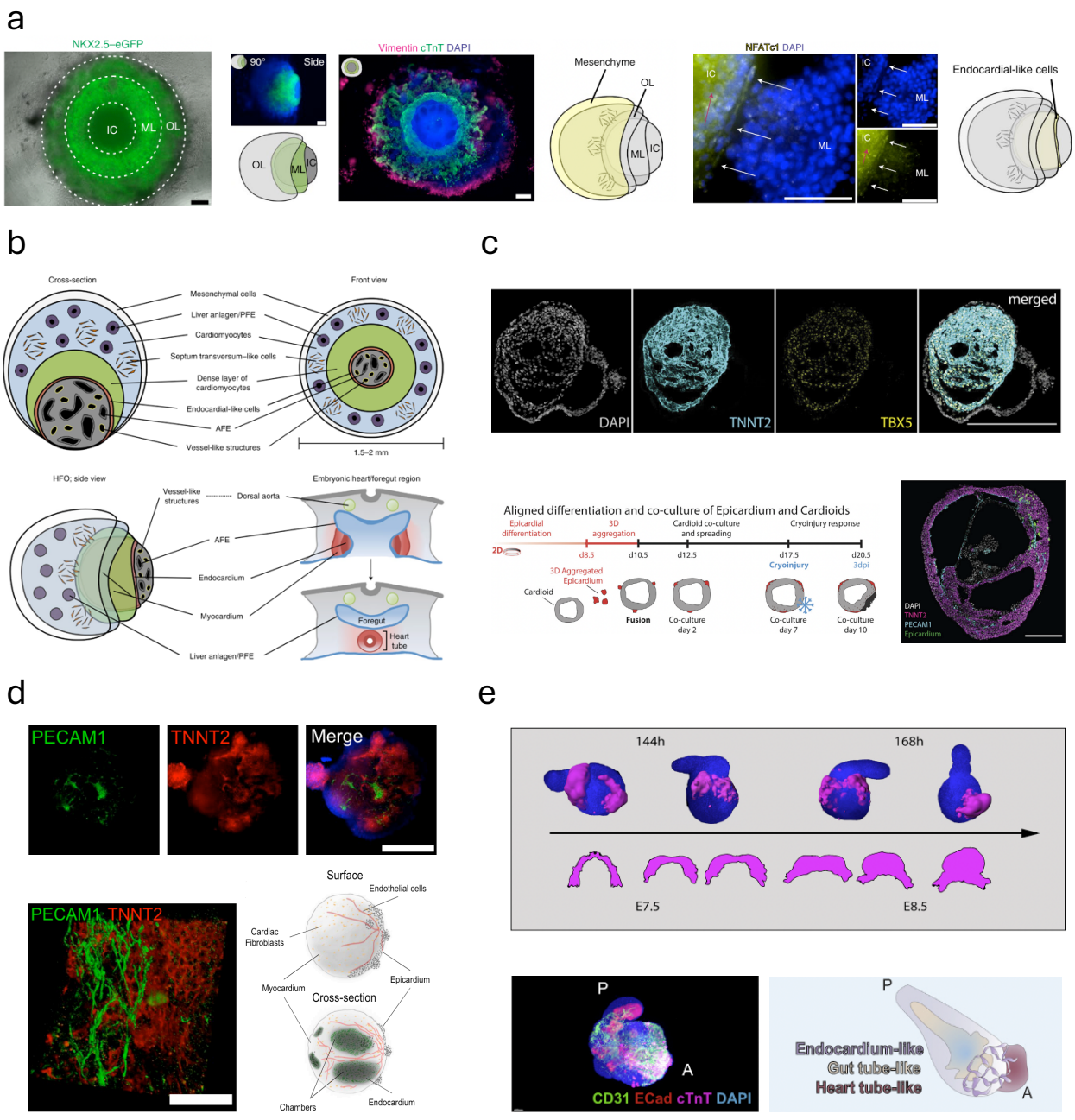

Figure 5. State-of-art human cardiac organoids. (a-b) Human cardiac organoids recapitulate early cardiomyogenesis.[64] (a) Formation of ring-like cardiac lineages (inner core, myocardial layer, outer layer, left), outermost mesenchymal cell layer (middle), and endocardial-like cells in between (right). (b) A scheme of human cardiac organoids in comparison of early embryonic heart/foregut region. (c) Chamber-like cardioids indicate the self-organization of small cavities in

the cardiac mesoderm (top); intrinsic self-organization of co-cultured cardioids with epicardium aggregates into patterned layers resembling the early human left ventricular heart chamber (bottom).[65] (d) Composition of self-assembled human cardiac organoids with vascular structure.[37] (e) Gastruloids mimic early embryogenesis and formation of early heart crescent and heart tube-like domains.[70] All figures are reproduced with copyright permission.

2 CHAPTER 2 METHODS

2.1 Introduction: Cell Micropatterning Techniques

Micropatterning has been extensively utilized in cell and tissue culture applications, demonstrating that confining the geometric space of cell colonies can establish biophysical gradients within the patterns, thereby promoting cell organization and alignment. Commercial solutions, such as those provided by CYTOO, aim to balance the quality and quantity of screening in the pharmaceutical industry by enhancing the physiological relevance of cellular models through the use of micropatterned tissue culture plates. These advancements have facilitated high-throughput screening in pharmaceutical research and development, ensuring that data is not only comprehensive but also reproducible and reliable[87].

Warmflash's team developed an innovative technique for culturing human embryonic stem cells (hESCs) under micropatterned environments, which involves restricting cell colony geometries and promoting cell-cell interactions.[88] When exposed to BMP4, cells were confined with circular micropatterns and spontaneously organized into a disk-like area containing the three germ layers (endoderm, mesoderm, ectoderm), thereby recapitulating the gastrulation stage of mammalian embryonic development. The study also observed dynamic cell migration within the primitive streak region, suggesting an epithelial-mesenchymal transition as specific cells migrated inward. Additionally, the research demonstrated a size-dependent differentiation pattern by controlling the outer edges of the micropatterns. Etoc and colleagues further described BMP4 signaling activity being regulated by its own inhibitor NOGGIN, which restricted pattern expansion from the colony edge, highlighting the crucial role of NOGGIN in positioning cell

fates within the confined patterns.[89] These findings underscore the significance and association of biophysical cues and biochemical signals for cell self-organization within the colonies, suggesting that micropatterning holds great promise in becoming the standard practice for pluripotent stem cell differentiation.

While these studies applied geometric confinement to embryonic pattern culturing, they remained limited to a 2D approach with a restricted range of cell types and tissue structures. Recently, material-based methods have gained attention for their ability to impose 3D spatial boundary control, enabling cellular self-organization into complex, functional, multilayered tissues that better mimic in vivo arrangements. 3D micropatterning seeks to create single-layer 3D microenvironments that spatially confine cell populations, incorporating the physical properties and architecture of the extracellular matrix (ECM), thereby enhancing the reproducibility of tissue development.[90]

Micropatterning substrates and microdevices offer a promising approach to enhancing cardiomyocyte functionality by precisely controlling the topographical features and spatial distribution of surface molecules.[91] Studies indicate that 3D micropatterned hydrogels enhance cardiomyocyte proliferation, alignment, contractility, and intercellular communication. This is attributed to the elastic mechanical support provided by the hydrogels, which closely replicate the dynamic mechanical properties of the extracellular matrix (ECM) found in vivo.[92] As the patterns arise in a self-organized manner, micropatterned cardiac organoid culture offers a promising platform for dynamic studies of human embryogenesis and preclinical drug toxicology. A 3D biomaterial-based micropatterning method was introduced to generate cardiac

microchambers facilitated by the regulation of WNT signaling.[93] These iPSC-derived cardiac organoids demonstrated a further developmental stage beyond gastrulation to the stage where the linear heart tube forms before looping. Similarly, the spatial differentiation process confined by non-fouling substrates also promotes cardiac lineage specification, developing into well-defined cardiac microchambers with dense cardiomyocytes at the center surrounded by smooth muscle-like cells at the periphery. Indeed, when colonies are constrained by 3D ECM micropatterns, cell-ECM interactions tend to polarize the colonies during pluripotency. E-cadherin upregulation at the perimeter results in cell proliferation along the boundary, with these regions of high mechanical stress also favoring epithelial-mesenchymal transition (EMT) events.[94]

Various natural and synthetic materials have been utilized for cell micropattern engineering because the self-organization of organoids critically depends on the dynamic tissue remodeling process.[95] Alongside the spatial confinement provided by micropatterns, the designed properties of hydrogels—such as stiffness, density, porosity, and chemical grafting—play a crucial role in controlling stem cell fate differentiation. Achieving this requires a balance between material engineering and tissue reconstitution. Classical photolithography can fabricate micropatterns in various shapes, which can then be replicated in elastomers or hydrogels using soft lithography and coated with specific extracellular matrix (ECM) components on the substrate.[96]

This chapter explores the application of engineering-inspired methodologies to the differentiation of iPSC-derived cardiac organoids. Specifically, we utilized material lithography and micropatterning techniques to engineer polyethylene glycol (PEG) hydrogel-based substrates to provide geometric constraints on the developing cellular structures **(Figure 6a)**. The primary

objective of this methodology is to guide the self-organization process of cardiac organoids through controlled spatial cues. By manipulating the shape and structural properties of the hydrogel substrate, we aim to influence cellular behavior and tissue formation during cardiac differentiation. This approach facilitates the cell self-arrangement process within a confined environment, which we hypothesize more closely recapitulates the structural organization observed in natural embryonic heart tissue.

2.2 Photolithography

Standard photolithography was employed to imprint the silicon wafer with the designed patterns. Initially, 2 mL of SU8 photoresist was dispensed onto the silicon wafer, which was then spun at 500 rpm for 10 seconds, followed by 2000 rpm for 30 seconds, achieving a thickness of 50 μm. Following the spin-coating, the wafer underwent a baking process. Subsequently, the wafer was exposed to UV light for crosslinking, using a CAD-designed photomask with 600 μm circular patterns. The exposed wafer was then placed in a developer solution to dissolve the photoresist from the unexposed areas, resulting in the formation of 600 μm patterns on the silicon wafer.

2.3 Soft lithography

Polydimethylsiloxane (PDMS) pre-polymer and curing agent were mixed in a 10:1 ratio and subsequently placed in a vacuum desiccator for degassing for 1.5 hours. After degassing, the PDMS mixture (0.5 mL) was dispensed and evenly spread in the center of the SU8 wafer. This setup was secured using two paper clips in a sandwich-like structure involving a glass slide and a transparency film. Following an overnight curing process at 60 °C, the PDMS was fully cured and carefully peeled off from the SU8 wafer. To create the PDMS stencils, the entire mask was

cut into smaller squares to fit the dimensions of the cell culture plate. Finally, the stencils were stored in 70% ethanol until their next use **(Figure 6b through 6e)**.

2.4 PEG Hydrogel Preparation

The opened 12-well cell culture plate was first pre-treated with oxygen plasma in a plasma machine for 3 minutes. Meanwhile, the PEG polymer mixture was prepared by combining 150 mg of PEG 1000, 1.8 mL of PEG diacrylate, 14.55 mL of IPA, 40 mg of Irgacure 2959, and 450 µL of MilliQ water. This mixture was vortexed thoroughly while being protected from light. Following preparation, 380 µL of the PEG mixture was transferred into each well of the culture plate and allowed to rest at room temperature, still protected from light. The PEG-coated plate was then subjected to UV crosslinking for 45 seconds and subsequently washed with MilliQ water to remove any residual PEG.

2.5 Plasma Etching

The PDMS stencils were carefully placed and distributed on top of the PEG layer in the culture plate. Afterward, the plate was dried in an oven at 60 °C for 2 hours. Following the drying process, a second 3-minute oxygen plasma treatment was applied to etch away the PEG in the regions not covered by the PDMS. This procedure created a tissue culture plate with a PEG non-fouling layer. Finally, the plate was sterilized with 70% ethanol for 1 hour before being used for cell culture.

2.6 Surface Cleaning and Geltrex Coating

The sterilized tissue culture plate was thoroughly washed three times with Dulbecco's Phosphate-Buffered Saline (DPBS) to remove any residual ethanol. Following this, 0.5 mL of Geltrax was added to each well, ensuring an even coating. The plate was then incubated for 1 hour at 37°C in a 5% CO_2 environment to allow for proper coating and gelation of the Geltrax.

2.7 GCaMP6f hiPSC Culture and Seeding

GCaMP-engineered human induced pluripotent stem cells (hiPSCs) were cultured for at least three passages using E8/mTeSR Plus medium. Once the cells reached confluency, they were dissociated with Accutase and centrifuged. A cell suspension of 7×10^5 cells/mL was prepared, with the addition of 10 μM ROCK inhibitor (ROCKI) to aid cell survival and attachment, and seeded onto the plate after the Geltrax was removed. After 24 hours of cell seeding, the PDMS stencils were carefully removed from the PEG-grafted plate using tweezers. The ROCK inhibitor was then removed by replacing the medium with fresh culture media. The hiPSCs were cultured for an additional two days until the cell patterns reached confluency, at which point cardiac differentiation was initiated.

2.8 Organoid Differentiation

Once the cell patterns reached confluency (Day 0), the culture media was switched to RPMI 1640 basal medium with B27 supplement minus insulin (RPMI/B27 -I) and supplemented with 10 μM CHIR. After incubating for 24 hours, on Day 1, CHIR was removed and replaced with fresh RPMI/B27 -I media for another 24-hour incubation. On Day 2, the media was changed to RPMI/B27 -I containing 5 μM IWP4, and the cells were cultured for an additional 48 hours. On

Day 4, the media was refreshed with RPMI/B27 -I (without any small molecules) and cultured for 2 more days. From Day 6 to Day 20, the cells were maintained in RPMI 1640 with B27 complete supplement (RPMI/B27 +C), with the media being refreshed every two days. The formation of 3D tissue structures was observed from Day 1 after CHIR treatment, and beating cardiac microchambers were visible from Day 8 **(Figure 7)**.

2.9 Bright-field Video Recording and Motion Tracking Analysis

Brightfield video recordings of cardiac organoids were taken on Day 20 to assess their contractile functionality. The organoids were imaged using an onstage microscope incubator (OkoLab Stage Top Incubator, UNO-T-H-CO2), which was maintained at 37°C and 5% CO2 to preserve physiological activities. Contraction videos were recorded at approximately 30 frames per second with a Nikon Ti-E inverted microscope equipped with an Andor Zyla 4.2+ digital CMOS camera. Subsequently, the brightfield videos of the beating cardiac organoids were exported as image sequences and analyzed using Matlab software developed by Huebsch et al.[97] This software implements block matching to compute motion vectors, tracking pixel changes between frames to calculate contraction and relaxation velocities **(Figure 7a)**. The software then reconstructs these pixel changes into a beating waveform, representing the muscle contraction and relaxation cycles of the tissues. The analysis provided functional readouts, including contraction velocity, relaxation velocity, beat rate, and beat duration, thereby offering a comprehensive quantification of the cardiac organoids' functionality (**Figure 7b and 7c)**. Additionally, area ratio was calculated by dividing the selected area of beating cardiac tissue with respect to the entire pattern area of the organoids (**Figure 7g)**.

2.10 Fluorescent Video Recording and Calcium Transient Analysis

Calcium flux tracing through the cardiac organoids was captured using high-speed imaging at the same frame rate (~33 fps) as the brightfield videos for motion analysis. Calcium tracking videos of each organoid under the GFP channel were recorded concurrently with the motion videos under brightfield microscopy using a Nikon Ti-E inverted microscope equipped with an Andor Zyla 4.2+ digital CMOS camera (**Figure 7d)**. The nd2 video files were then transformed into Matlab scripts, which measured the GCaMP fluorescence intensity and motions using optical flow algorithms.[97] Similarly, a GCaMP signal waveform was generated to represent the calcium tracing functionality (**Figure 7e)**. The functional readouts included max signal, t_0, t_{50}, t_{75}, df/f0, and peak time (**Figure 7f)**. The waveforms of Ca^{2+} flux and contractile motion were spatially and temporally correlated, with a slight delay in the calcium waveform following contraction.

2.11 Statistics

All box plots present the minimum, maximum, median, and 25th and 75th percentiles. Statistical analyses were primarily conducted using analysis of variance (ANOVA) coupled with Tukey's multiple comparison test unless noted otherwise. Data were considered significantly different when the p-value was less than 0.05. Significance levels were indicated with *, **, ***, and ****, representing p-values of < 0.05, < 0.01, < 0.001, and < 0.0001, respective

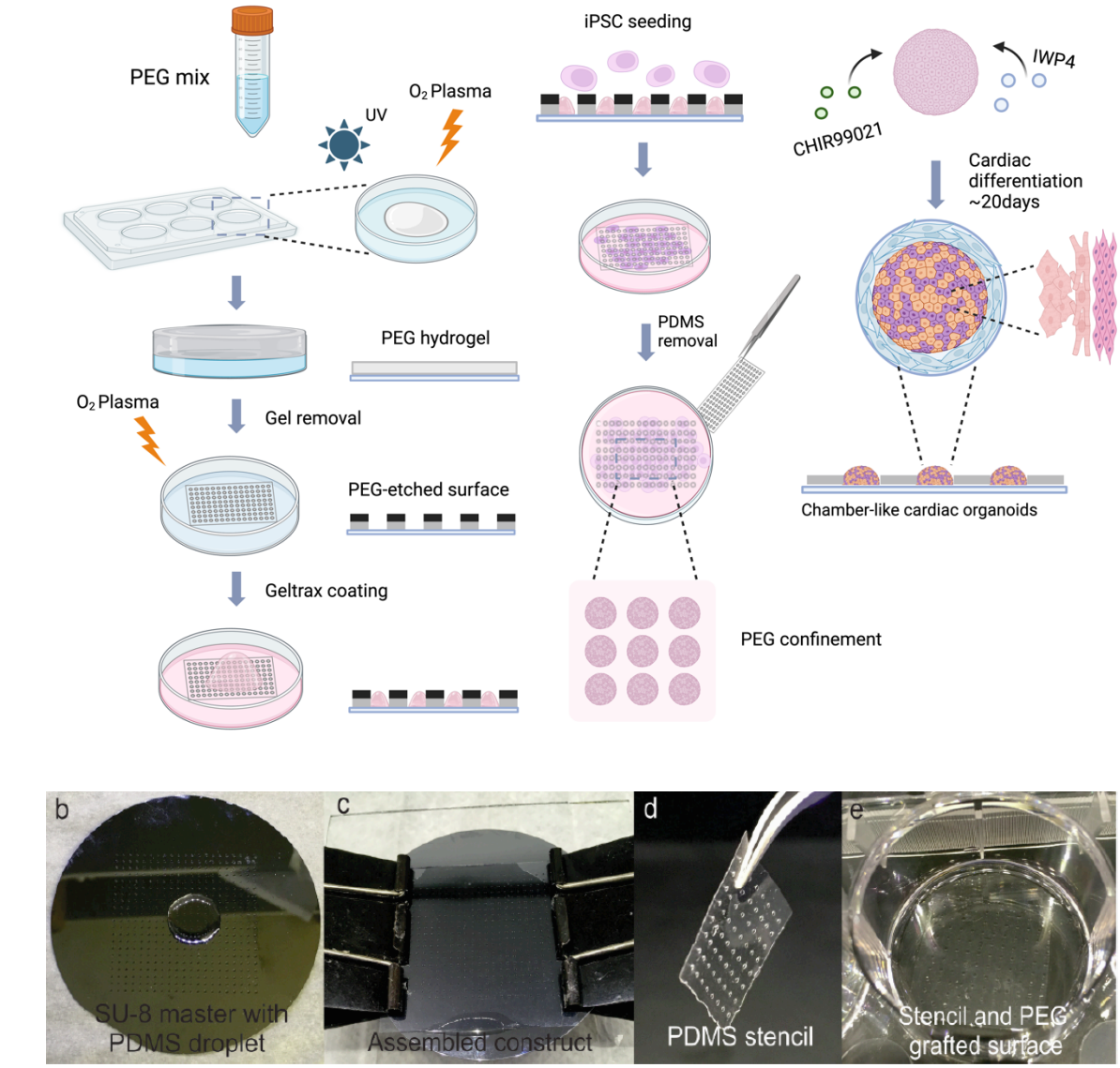

Figure 6. Schematic representation of the PDMS stencil fabrication process. (a) Key steps of the entire procedure. (b) PDMS prepolymer droplets coated onto the SU8 master. (c) Fully assembled construct consisting of the patterned SU8 master, PDMS layer, and transparency glass slide. (d) Cured thin PDMS film was removed from the assembly and placed onto (e) an optically clear PEG-grafted surface. Figures (b-e) are reproduced from the work of Hoang et al. *Nature Protocols*, 2018 with copyright permission. [98]

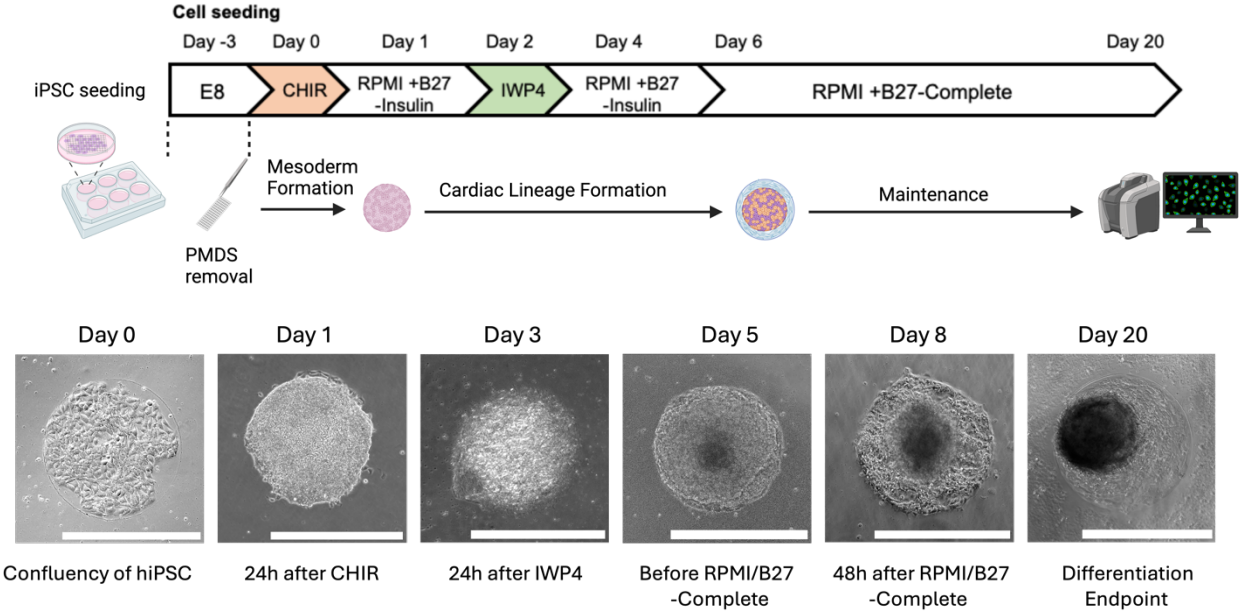

Figure 7. Timeline of WNT-regulated cardiac differentiation. hiPSCs were seeded onto PDMS stencils on Day 3. Upon reaching confluency, the PDMS stencils were removed. Small molecules CHIR and IWP4 were subsequently introduced to promote mesoderm and cardiac lineage formation. From Day 6 onwards, cardiac differentiation was maintained in RPMI + B27 – Complete media until the differentiation endpoint on Day 20. Scale bar: 600 µm.

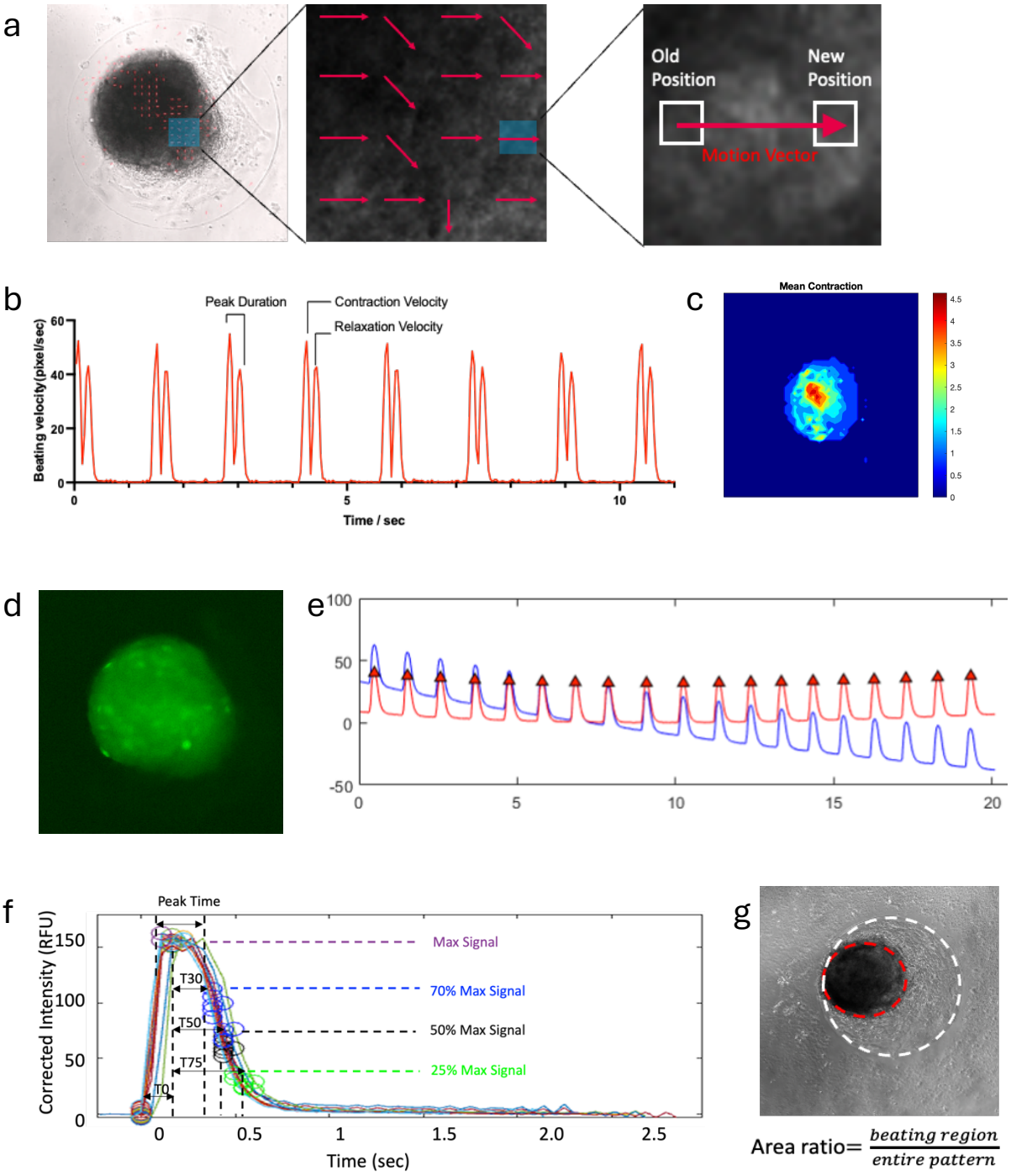

Figure 8. Functional characterization of cardiac organoids. (a) Block-matching algorithms were utilized to analyze the contractility of beating tissue composed of cardiomyocytes. Frames were divided into arrays of pixel macroblocks (blue square, middle). In subsequent frames, the motion of these macroblocks was detected and calculated, with the motion vector (red arrow,

middle) connecting the previous and new positions of the macroblocks (right). (b) Motion tracking of the average velocity for the selected area of cardiac beating tissue. Double peaks representing contraction and relaxation were identified as a single beating cycle, with the duration of the peaks indicating the time interval between contraction and relaxation. (c) Heatmap indicating the contraction intensity, calculated by the motion vectors. (d) Calcium tracing of GCaMP-engineered iPSC in cardiac organoids under the green fluorescence microscope. (e) The original calcium tracing waveform (blue) detected by software; the corrected waveform (red) was generated by subtracting the photobleaching in the background. (f) Single calcium peak with calculated functional parameters indicating calcium signal tracking properties. Starting from the baseline, calcium signals rise, plateau, and then gradually decrease back to the baseline. t_0, t_{30}, t_{50}, and t_{75} represent the times to reach the plateau (maximum signal intensity) and decay by 30%, 50%, and 75% from the maximum signal intensity, respectively. Peak time represents the duration of the signal above 80% of maximum intensity. (g) Area ratio quantifies the beating area of cardiac tissue with respect to the entire shape.

3 CHAPTER 3 RESULTS

3.1 Introduction: Chemo Drugs on Cardiotoxicity and Embryotoxicity

Cancer during pregnancy, although a rare event with an incidence rate between 1 in 1000 to 1 in 1500 pregnancies, presents substantial challenges in the selection of appropriate anticancer drug therapies.[99] This complexity arises primarily due to the potential hazards these treatments may pose to both the mother and the fetus. The estimated risk of congenital anomalies when a single chemotherapy agent is applied during the first trimester ranges from 7.5% to 17%, with the teratogenic risk increasing further when combination chemotherapy is used.[100] Consequently, it is imperative to access comprehensive information regarding the selection of chemotherapeutics for pregnant patients, the safe administration of these potential teratogens during pregnancy, and strategies to mitigate the risks of fetal toxicity.[101] However, there is limited data available on the potential fetotoxicity of new antineoplastic agents, underscoring the need for further research.

The majority of anticancer drugs possess high lipid solubility, allowing them to traverse the placental barrier in both directions via simple diffusion or receptor-mediated ligand binding. Numerous studies have emphasized the detrimental consequences of administering cytotoxic anticancer drugs and molecular-targeted therapies to pregnant women, highlighting significant risks to both maternal and fetal health.[102] For example, antineoplastic drugs employed in the treatment of acute lymphoblastic leukemia have been associated with teratogenic effects, particularly when these agents are administered during the first trimester.[103]

In vitro methods of toxicity prediction rapidly provide a broader understanding of toxic mechanisms and have the potential to replace the current animal models used in predictive

toxicology. While traditional preclinical drug testing methods may not fully capture the complexities of drug interactions in pregnant individuals, novel pluripotent stem cell (PSC) models offer a promising approach for understanding drug-induced interactions during the developmental process, thus providing more accurate and comprehensive assessments of chemotherapeutic drug toxicity and efficacy during pregnancy. Furthermore, the precise recapitulation of drug-regulated biological pathways in PSC models may pave the way for tailored, and even personalized, chemotherapeutic administration for pregnant patients, [101] which will guide the development of evidence-based guidelines for managing cancer in pregnant individuals.

Since 1984, drug risk classification systems have been introduced in the USA. The Food and Drug Administration (FDA) in the United States categorizes drugs into five main categories (A, B, C, D, and X) based on their potential fetal risk. [104] Studies have shown that a notable percentage of pregnant women are exposed to higher-risk medications classified as category D or X during pregnancy.[105] Despite uncertain safety, a significant proportion of chemotherapeutic drugs used during pregnancy fall into categories C, D, or X, with some being exclusively category X drugs.[106] Notably, the utilization of category X drugs during pregnancy has been reported in various countries, ranging from 0.6% to 4.9% of pregnancies[107,108].

This chapter aims to utilize the engineered cardiac organoids from Chapter 2, to conduct a comprehensive examination of six pharmaceutical agents spanning Categories A through X of pregnancy risk classification, with particular emphasis on four widely utilized chemotherapeutic compounds that present potential toxicity risks to embryonic or fetal development. A thorough

literature review will be undertaken, encompassing drug profiles, clinical applications, controversies surrounding pregnancy risks, and analyses of embryotoxicity potentials during gestation based on diverse testing models. To further elucidate drug-induced developmental toxicities, this chapter proposes to implement a novel embryotoxicity assay utilizing iPSC-derived cardiac organoids. This innovative approach aims to characterize the cardiac differentiation toxicity (IC50) of the selected agents, with the ultimate objective of establishing a refined teratogenicity prediction model. This model holds promise as an updated pregnancy risk classification system, potentially categorizing pharmaceuticals as non-embryotoxic, potentially embryotoxic, or strongly embryotoxic based on functional readouts that indicate the toxicity's impact on the physiological properties and cardiac differentiation efficiency of the organoids.

3.2 Drug Profiles of Study

Thiamine (Category A)

Thiamine, also known as vitamin B1, is one of the eight B-complex vitamins essential for metabolic reactions in humans and animals. It naturally occurs in specific foods and is available as a dietary supplement.[109] Therapeutically, thiamine is FDA-approved for intravenous administration to individuals with marginal thiamine status to prevent heart failure. The metabolite of thiamine serves as a cofactor for various enzymes in multiple metabolisms of human body,[110] and there is no evidence indicating toxicity from high intake through food or supplements.

Research indicates that thiamine deficiency (TD) disrupts oxidative phosphorylation, increases oxidative stress, and triggers inflammatory processes, which may result in neurological, cardiac, and gastrointestinal issues.[111] Pregnancy is identified as a condition particularly susceptible to thiamine deficiency, especially during periods of increased thiamine demand such as early pregnancy and the peripartum period.[112] Stem cell studies have further demonstrated that hiPSC-derived neurons exhibit increased cell death and oxidative stress when treated with a thiamine antagonist, while thiamine supplementation significantly reduces neuron death in a dose-dependent manner.[113] Impaired embryogenesis has also been observed in hESCs towards hEB growth, showing cell disintegration and decreased metabolism due to thiamine depletion in the culture media. Disturbed vasculogenesis was also observed from compromised vascular self-renewal structures derived from hEBs.[114] In other embryonic studies, genetically modified zebrafish embryos expressing thiaminase (an enzyme that degrades thiamine) starting at the one-cell stage exhibited embryonic and larval mortality at 5 days post-fertilization, which was partially rescued by thiamine supplementation.[115]

Penicillin (Category B)

Penicillin, a member of the β-lactam antibiotics family, was originally derived from Penicillium molds. Penicillin has a short half-life and is primarily excreted through the kidneys,[116] thus frequent dosing is needed to maintain therapeutic levels in the bloodstream. As one of the most common antibiotics, penicillin can diffuse across the placenta within minutes after maternal administration.[117] The PK properties of penicillin have been reported to be altered during pregnancy due to maternal physiological changes. Research indicates that pregnant women in the second and third trimesters exhibit significant reductions in maximum plasma concentration

(C_{max}) and volume of distribution (Vd), along with an approximate 50% increase in clearance (CL) for penicillin V compared to non-pregnant women. This suggests a need for potential adjustments in penicillin dosage or dosing intervals to maintain optimal drug levels.[118] For infectious diseases like syphilis, penicillin G remains a key treatment for pregnant women. Studies have demonstrated its safety and effectiveness in preventing congenital syphilis without severe adverse reactions.[119] However, selecting appropriate antibiotics for pregnant women is crucial, particularly given the frequent reports of unverified penicillin allergies in this population.[120]

Penicillin is classified as a Category B drug for pregnancy risk, indicating that animal studies have not demonstrated fetal risk, although there are no adequate and well-controlled studies in humans.[118] The use of antibiotics is sometimes essential for pregnant women, however, it is crucial to use antibiotics with well-established efficacy and safety profiles, as there have been occasional reports of teratogenic effects from antibiotics. A study comparing the maternal use of erythromycin and penicillin V revealed a cardiovascular teratogenic effect associated with erythromycin, but not with penicillin.[121] This difference may be due to erythromycin's side effect of inhibiting a specific cardiac potassium current (I_{Kr}) channel, which can result in proarrhythmic potential or lethal arrhythmia, whereas penicillin does not exhibit such proarrhythmic properties.[122,123] However, penicillin hypersensitivity has been reported to induce acute pericarditis in some patients who experience allergic skin reactions to penicillin. Given the uncertainty regarding penicillin allergies reported in pregnant women, alternative antibiotic strategies should be considered to ensure safety.[124]

Penicillin is commonly used as a negative control in various cell-based toxicity evaluation models and has been selected as a default non-embryotoxic chemical even when during the establishment of toxicity prediction models.[24,25,125] To date, penicillin is generally recognized as non-teratogenic in most PD studies conducted in vitro. However, although rare, some studies have suggested potential risks of this antibiotic on embryonic and fetal development. Research has reported that the combination of penicillin and streptomycin adversely affects both proliferation and differentiation in murine embryonic stem cells (ESCs). It has also been recommended to exclude antibiotics from current ESC differentiation protocols due to their negative impact on both growth rates and target mRNA expression levels during ESC differentiation.[126] Human ESC studies indicated that no significant effects were observed in pluripotency markers with antibiotic treatment in their pluripotent state. However, significant cell death was observed during differentiation toward neural and hepatic fates, where the expression of neural stem cell-specific markers was significantly reduced with antibiotics during neural differentiation.[127]

Dacarbazine (Category C)

Dacarbazine is a chemotherapeutic used to treat metastatic malignant melanoma and Hodgkin lymphoma, typically in combination with other antineoplastic agents.[128,129]Due to its poor gastrointestinal absorption, dacarbazine is administered exclusively via intravenous injection or infusion. With minimal binding to plasma proteins, dacarbazine undergoes extensive hepatic metabolism to form an active metabolite.[130] Dacarbazine exerts cytotoxic effects on tumor cells by acting as an alkylating agent that inhibits DNA, RNA, and protein synthesis.[131] Like many chemotherapy drugs, dacarbazine has numerous serious side effects, as it disrupts the growth of

normal cells in addition to cancer cells. Significant adverse effects include birth defects if the drug is used during conception or pregnancy, immune suppression, and possibly permanent sterility. Other developmental toxicities include liver damage and the risk of severe acute hepatic failure.[132] Additionally, cardiotoxicity and thyroid dysfunction have been reported as frequent late effects when dacarbazine is combined with other anthracycline drugs for the treatment of Hodgkin lymphoma.[133–136]

Dacarbazine is classified as a Category C drug in terms of pregnancy risk. Studies have observed independent translocations of sex chromosomes and reduced fertility in female mice.[137] Although comprehensive and well-controlled human studies are lacking, there are some reports of adverse pregnancy outcomes related to dacarbazine chemotherapy. Typically, dacarbazine is used in combination with other chemotherapies to treat advanced Hodgkin lymphoma (HL) during pregnancy. One study indicated that 3% of 123 children born to mothers with HL had major congenital abnormalities, while another 3% had minor abnormalities at birth.[138]The ABVD regimen, which includes doxorubicin, bleomycin, vinblastine, and dacarbazine, is regarded as the optimal therapeutic choice for advanced HL in pregnant women, providing good overall survival rates with low fetotoxicity.[139,140] However, there have been reports of congenital abnormalities, fetal death, and premature births associated with this regimen. Additionally, congenital cardiac dysfunction, such as preserved ejection fraction, has been observed in infants whose mothers underwent ABVD therapy for stage II HL. [141,142]

Although alkylating agents generally exhibit rapid transplacental passage,[143] dacarbazine remains the least studied alkylamine associated with pregnancy, with no human studies in the

literature available on its placental transfer.[102] Additionally, the safety dosage profile of dacarbazine during pregnancy remains unclear due to alterations in maternal pharmacokinetics. Studies have indicated that pregnancy reduces the metabolism of dacarbazine, leading to higher maximum plasma concentrations and lower exposure to its active metabolites, which might result in diminished efficacy.[144] Additionally, individual variations in maternal pharmacokinetics further complexed the use of dacarbazine during pregnancy. Despite being classified as relatively safe during pregnancy and tolerable for the fetus after the first trimester,[143] [145] data on dacarbazine as a standalone treatment is scarce. Most reports involve its use in combination with other anticancer agents, typically as a second or third-line therapy. There have been two reported cases out of five (40%) where exposure to dacarbazine alone resulted in congenital malformations, including pulmonary complications and growth restrictions.[146] This relatively high incidence of adverse outcomes suggests that dacarbazine may possess some degree of teratogenicity.

Doxorubicin (Category D)

Doxorubicin (DOX) is an anthracycline (ANT) drug commonly employed in combined chemotherapy to treat various malignant neoplasms, including leukemia, lymphoma, and some solid tumors. The potent anti-cancer effect of DOX is primarily achieved by inhibiting topoisomerase IIa, an enzyme essential for unwinding DNA during replication and transcription, which results in DNA damage and the death of rapidly proliferating cancer cells. However, like many chemotherapeutic agents, DOX also affects healthy cells with rapid proliferation, such as hematopoietic precursors, the epithelial lining of the intestine, and hair follicle cells.[74]

Doxorubicin (DOX) is classified in pregnancy Category D, which has been demonstrated to be embryo-lethal in rabbits[147] and teratogenic in rats.[148] The dose-related abnormalities observed include gastrointestinal, cardiovascular, urinary, and respiratory defects.[149] In vitro rat whole embryo studies have also confirmed that the primary target tissues as the endoderm of the digestive tract and the caudal mesoderm.[150] In humans, the debate regarding DOX-induced teratogenicity has continued for decades. Although evidence increasingly supports the safety and efficacy of anthracycline-based therapies, certain anthracycline drug classes remain controversial. A study involving 160 patients treated with anthracyclines during pregnancy found that 73% had normal outcomes. However, there were incidences of 27% anomalies, including fetal malformations, deaths, spontaneous abortions, and prematurity. Notably, the risk of severe fetal toxicity increased 30-fold at higher clinical doses of DOX treatment.[151] Another study reported a 10% incidence of congenital anomalies when DOX was administered with other chemotherapeutics during the first trimester,[152,153] where the congenital malformations, including skeletal and cardiac defects, were associated with intrauterine exposure to DOX during this critical developmental period.[154] PK studies emphasized the impact of variations in maternal pharmacokinetics during pregnancy in determining safe dosage, which further complicated the congenital malformations induced by DOX. In comparison to non-pregnant women, the maximum concentration (C_{max}) of doxorubicin (DOX) decreases by 1%, with minor alterations in distribution volumes and clearance.[155] Contrarily, another study highlighted a notably reduced clearance rate in pregnant women.[156] The placenta passage of DOX towards the fetus is facilitated by its amphiphilic nature, low molecular weight (544 g/mol), and high plasma protein binding (70-75%). Detectable levels of DOX have been found in fetal organs such as the

liver, lung, and kidney at concentrations approximately ten times lower than those in the maternal system.[156,157]

Despite it is recognized for its potent efficacy as a chemotherapeutic agent, DOX use is still complicated by significant cardiotoxicity, including acute atrial and ventricular arrhythmias, chronic cardiomyopathy, and heart failure.[158–160] Meanwhile, the potential for DOX-induced fetal cardiotoxicity remains controversial.[161,162] Large-scale retrospective studies have demonstrated that doxorubicin administration during the second and third trimesters does not result in detectable adverse effects on the fetal heart,[163] even with intensive two-week chemotherapy regimens.[164] Multiple mechanisms are involved in DOX-associated cardiotoxicity, including interfering with the cardiac muscle protein, causing the fetal contractile apparatus deficit due to the low force generation of smaller embryonic or fetal myocytes compared to those in adults. Fetal cardiac tissue is especially vulnerable to free radical damage owing to low cardiomyocyte tolerance to changes in the mitochondrial system. [165] Yeh et al. proposed another concept of DOX-induced cardiotoxicity that DOX binds to topoisomerase IIβ (Top2β), which is the predominant Top2 isoform in the heart, to induce cardiomyocyte apoptosis and disrupted mitochondrial biogenesis with the secondary formation of reactive oxygen species (ROS).[166,167] PSC studies further demonstrated the Top2β pathway in altering electrophysiological properties of hiPSC-CMs, manifesting as a time- and dose-dependent reduction in spike amplitude, an increase in beat rate, and a shortening of action potential duration. Notably, electrophysiological effects were detectable at doses as low as 0.25 μM, with immediate onset post-treatment progressing over time. After 20 hours of exposure to 1 μM DOX, the physiological functionality was reduced by 52.1% compared to controls. Cell viability began

to decrease at doses as low as 5 μM, and the cytotoxic concentration is reported as 30.1 μM. Another study identified DOX-induced apoptosis in hiPSC-CMs via a death receptor-mediated pathway, showing a dose-dependent decrease in cell viability with a concentration of 3.5 μM of significant inhibition.[168] Cytotoxic effects were significant at concentrations as low as 450 nM, although below the peak plasma levels seen in humans after IV administration, at which the upregulated death receptors with DOX treatment still lead to impaired beating functionalities of hiPSC-CMs. Cardiac organoid models further confirmed DOX's toxicity by displaying a dose-dependent decrease in cell viability and quantification of abnormal gene expressions of apoptosis, cardiac function, inflammation, and mitochondrial markers, providing a more sensitive detection of cardiotoxicity at DOX concentrations as low as 0.1 μM.[60]

Hydroxyurea (Category D)

Hydroxyurea (HU) is utilized in chemotherapy for treating melanoma, specific leukemias, and various solid tumors. Meanwhile, it is also used for essential thrombocythemia, polycythemia vera, and sickle cell disease.[8] As an antimetabolite, HU acts as a cytostatic agent that disrupts DNA synthesis and repair in cancer cells.[169] Known adverse reactions include skin-related inflammations particularly after prolonged daily use.[170] Additionally, HU is potentially mutagenic and carcinogenic, with reports indicating that 5% to 10% of patients with polycythemia vera and essential thrombocythemia who received HU developed acute leukemia.[8]

The risk of HU during pregnancy is classified as Category D. Studies have shown that HU significantly increases the risk of teratogenic effects on animals. [171,172] During pregnancy, HU is

often used in combination therapies for cancers such as cervix, breast, melanoma, lymphoma, and leukemia, which are frequently diagnosed in pregnant women.[173] Single HU administration is considered palliative for acute and chronic myeloid leukemia (CML) during pregnancy, given the teratogenic potential of conventional tyrosine kinase inhibitors (TKIs).[174–176] However, HU use has been associated with intrauterine deaths, congenital malformations, premature births, and an increased incidence of preeclampsia, particularly in the second and third trimesters.[177] This is partly due to the relatively high recommended dose for resistant CML (20-35 mg/kg per day) compared with other uses, with a reported C_{max} of 52 μg/ml at 35 mg/kg orally.[177] Clinical reports have documented adverse pregnancy outcomes with HU use in various hematologic malignancies and disorders. Review studies indicate that the overall frequency of fetal adverse effects with HU is 30%, with a 29% frequency of use as a single agent.[152] Notably, HU must be taken indefinitely for effectiveness, and exposure-dependent adverse effects have been observed. Nonetheless, there have been reported that more than two dozen apparently normal infants were born to mothers treated with HU during the first trimester.[152]

HU is classified as a Class II teratogen in animals, where embryopathic effects become evident only when the drug dose exceeds a certain threshold. According to the ICH S5(R3) Guideline,[178] the lowest HU dose causing adverse effects on rat embryos is 137 mg/kg, while a dose of 300 mg/kg significantly alters the ultrastructure of neuroepithelial cells.[179] The teratogenic potential of HU in animals is considered clinically relevant since the teratogenic dose in animals (250 mg/kg) is less than 25 times the recommended clinical dose (20-35 mg/kg). Despite HU's classification as a teratogen in animals, the peak plasma concentration at these doses is 5-10 times higher than therapeutic doses in humans.[180] Moreover, teratogenic effects in

animal models based on non-exposure-related evaluations are not particularly useful for categorizing drug teratogenicity by human standards.[181]

The European Centre for the Validation of Alternative Methods (ECVAM) conducted an in vitro validation study of the mouse embryonic stem cell test (mEST), which assessed the test's ability to differentiate chemicals among three classes of embryotoxicity.[25]ECVAM identified HU as a strongly embryotoxic agent in the pre-validation stage, noting that the single endpoint tests for cytotoxic effects (IC50) on both D3 and 3T3 cell lines, as well as the inhibition of differentiation (ID50), were below 10 μg/ml. However, the prediction model suggested an incorrect classification of HU as strongly embryotoxic, with a probability of correct classification below 50%. Instead, one experiment classified HU as weakly embryotoxic. A recent exposure-based teratogenicity assay has explored the drug impact on EB by quantifying the gene expressions associated with the three germ layers, providing human-specific predictions regarding teratogenic mechanisms during early embryonic development.[181] Cytotoxicity assays reported the IC50 for HU of approximately 0.1 mM on Day 7, with exposures lower than the peak plasma concentration in humans (683 nM). Interestingly, HU exhibited a non-teratogenic profile on Day 7 while demonstrating teratogenic effects on Day 5, with significant changes in gene regulation observed across all lineages. However, the machine-learning mode only failed to predict HU’s teratogenicity due to the limited dataset. Consequently, the teratogenic risk of HU in humans tends to be interpreted as inconclusive or unknown.

Methotrexate (Category X)

Methotrexate (MTX) is an antifolate antimetabolite commonly used to treat tumoral pathologies such as acute lymphoblastic leukemias and, in rheumatology, for conditions like rheumatoid arthritis and other chronic inflammatory diseases.[182] MTX functions by inhibiting dihydrofolate reductase, an enzyme crucial for DNA synthesis, leading to impaired DNA synthesis in tumor cells.[183] As a potent autoimmune and anti-cancer agent, MTX is often administered in higher doses alongside other chemotherapeutic agents.[8,102] MTX possesses a high molecular weight and is approximately 50% bound to plasma proteins,[184] with an average C_{max} of 2.14 μg/mL following a single 30 mg/m² dose. The oral bioavailability of MTX tablets is relatively as low as approximately 36%.[185]

In terms of pregnancy risk, MTX is classified as Category X, indicating its teratogenic effects observed in both animal and human studies. In animal studies, the lowest dose causing adverse effects in rats was found to be 0.1 mg/kg.[178] However, MTX is typically administered in a relatively high dose (30-200 mg/kg) for the treatment of neoplasia.[186] The inhibition of DNA synthesis by MTX results in a range of malformations similar to those caused by its derivative, aminopterin, which is known for inducing 100% adverse pregnancy outcomes (APOs),[187] including cranial dysostosis, limb anomalies, and heart defects.[152] In addition, MTX has been identified as multi-organ embryopathatic, causing a variety of malformations such as skeletal defects, growth restriction, and significant pulmonary anomalies.[188] Research indicates that 17% of fetuses exposed to MTX during the first trimester exhibit malformations, and the overall incidence of adverse effects is 28%. Notably, 28% of APOs were recorded with single MTX treatments between 6 and 8 weeks post-conception.[152]

Clinical investigations have reported the complications of MTX-induced cardiomyopathy in healthy adults, showing evidence of myocardial necrosis.[182] High-dose intravenous administration of MTX has been associated with acute cardiac symptoms and arrhythmias.[189] While MTX-induced fetal cardiotoxicity is less frequently reported, there have been cases of congenital cardiac malformations potentially linked to aminopterin syndrome, all exhibiting defects in the pulmonary circulation.[187] One study reported a 69% incidence of congenital heart disease phenotypes, such as atrial septal defects, pulmonary stenosis, and ventricular septal defects, with varied exposure times throughout pregnancy. Notably, 50% of these cases involved exposure during the first trimester. [190] A recent study proposed the MTX-induced cardiotoxicity through disruption of the hypoxia-inducible factor 1 (HIF-1) pathway, leading to increased HIF-1α levels in cardiomyocytes and subsequent nuclear and mitochondrial impairments.[191] HIF-1α, an oxygen-sensitive subunit, is typically upregulated under hypoxic conditions, suggesting that MTX may induce a hypoxic state in cardiomyocytes. The cytotoxic concentration was reported to be 2.2 μM after 48 hours of treatment, resulting in a six-fold increase in HIF-1 levels, a two-fold increase in protein oxidation, and a 24% decrease in total antioxidant capacity. The developing heart, particularly during weeks 6-8 of pregnancy, is highly susceptible to hypoxia-induced damage.[182] The EB-based teratogenicity assay mentioned above [181] indicates the adverse effects from MTX start at concentrations as low as 3.9 nM, with an IC50 of 107 nM, the lowest among tested compounds. MTX exhibited significant teratogenic effects on genes regulating all lineages (ectodermal, endodermal, and mesodermal) during EB differentiation, as well as on PSC self-proliferation at sub-cytotoxic concentrations, without any loss of

pluripotency. Consequently, MTX is classified as strongly embryotoxic with this model, with a total prediction accuracy of 90%.

3.2.1 Experiment procedure

The evaluation of drug-induced embryotoxicity was conducted using a toxicity assay system involving six representative pharmaceuticals from different pregnancy risk categories **(Figure 9)**. These drugs were administered and maintained with organoids throughout the differentiation process, following the cardiac differentiation protocol regulated by the WNT-β pathway. Depending on their solubility, the drugs were initially dissolved in either MilliQ water or DMSO. The drug solutions were sterilized and serially diluted from 1 nM to 1 mM using organoid culture media. Beginning on Day 0, each drug, at eight different concentrations, was administered to the organoids along with vehicle control (0.1% DMSO) throughout the differentiation timeline. At the differentiation endpoint on Day 20, videos of the beating organoids were captured with the microscope and analyzed with MATLAB-based software. The functional analysis included quantitative contractile motion analysis and calcium flux transients reported by the GCaMP-engineered iPSC line, focusing on selected regions of interest (ROIs). Differentiation efficiency was evaluated and normalized by measuring the beating area as a proportion of the entire area of the patterned organoid in pixels, analyzed using ImageJ.

3.2.2 Functional Readouts

Calcium serves as the final integrator of electrical signals generated by the various ion channels contributing to the cardiomyocyte action potential (AP). Alterations in the AP will thus be reflected in intracellular calcium transients. The automated video-based system allows for high-

resolution analysis of intracellular Ca^{2+} dynamics using the GCaMP-reported line, generating waveforms with parameters such as maximum calcium fluorescence intensity (max signal), decay times (t_{30}, t_{50}, t_{75}) indicating the reduction in calcium peak intensity, upstroke duration (t_0) indicating the time to reach plateau, plateau time of peak (peak time), and the ratio of peak fluorescent intensity to baseline intensity (df/f0), indicating relative fluorescence variation. These parameters accurately assess the peak shape in terms of amplitude, peak shoulder and tailing.

The contraction and relaxation kinetics of beating cardiac organoids, a fundamental metric of cardiomyocyte physiological properties, were assessed using a frame-based block-matching algorithm with motion vector analysis. High-speed video imaging analyzed cardiomyocyte contraction to detect subtle changes in response to compounds, including beating rate, peak duration, contraction velocity, and relaxation velocity. These two well-defined cardiac functionality software systems allowed for simultaneous analysis of calcium flux and contraction motions **(Figure 9)**.

3.2.3 Data Analysis

Functional readouts were scaled relative to the main value of each control group. Calculations were performed across several batches separately to balance trends and ensure comparability across batches. For the quantification of drug-induced cardiotoxicity, concentration-effect curves were plotted using GraphPad Prism 9.0, employing nonlinear regression analysis by fitting four parameters into a logistic function. The molar concentration producing 50% inhibition (IC50) of cardiac differentiation was calculated for all functional parameters of each tested drug.

3.3 Results for Six Drugs

3.3.1 Category A

Thiamine

As a dietary supplement ranked as Category A regarding pregnancy risk, thiamine exhibits minimal effects on the differentiation of cardiac organoids **(Figure 10a and 10b)**. In the context of calcium handling, calcium transients in the experimental groups remained relatively consistent with the control group. No significant differences were observed in maximum calcium intensity or time to peak calcium intensity (t0) **(Figure 10c and 10d)**. However, at a higher concentration of 100 μM, there were noticeable changes in the time to 30% and 50% calcium decay (t_{30}, t_{50}) and a moderate increase in the time to 75% decay **(Figure 10e through 10g)**, indicating a tailing-featured peak profile that corresponds with a prolonged plateau time **(Figure 10i)**. Additionally, decreases in relative fluorescence variation (df/f0) were noted in the higher concentration groups (100 μM, 1 mM), which correlated with slight increases in t_0 in these groups **(Figure 10j)**. Nevertheless, according to the Institute of Medicine, there is no established upper limit for thiamine intake that causes toxicity.[109]

For contraction motion, the 1 nM concentration exhibited a significantly higher beating rate compared to the control group **(Figure 10k)**, which was partly reflected by the significantly lower peak time and slightly lower t_0, resulting in a calcium waveform profile with thin peaks, indicating a faster release of intracellular calcium flux. Similar to the prolonged calcium re-uptake time, the 100 μM group showed an increased contraction-to-relaxation peak interval **(Figure 10l)**. No substantial variations were detected in both contraction and relaxation velocities, although a relatively higher standard deviation was observed in the 100 nM group for

both measures **(Figure 10m and 10n)**. Additionally, a slightly lower relaxation velocity was found in the 100 μM group, potentially corresponding with the longer decay time seen in the calcium transients. The area ratio of beating cardiac tissue relative to the entire organoid did not show significant changes, except at the highest concentration (1 mM), which displayed a lower beating area compared to the control group, although this was not significantly different from other concentrations.

Overall, thiamine exhibited limited effects on cardiac organoids in terms of motion behaviors, beating area, and calcium flux transients. Low concentrations of thiamine (1 nM) slightly improved cardiac functionality in both contraction motion and calcium transients, consistent with existing literature.[192] However, it is unable to conclusively state that higher concentrations of thiamine (100 μM, 1 mM) pose significant toxicity to cardiac organoids.

3.3.2 Category B

Penicillin

Penicillin, classified as a Category B agent, is extensively utilized as an antibiotic in cell culture protocols and frequently serves as a default negative control in toxicity assay development. Both analyses detected moderate effects of penicillin on contraction motion and calcium transients from cardiac organoids **(Figure 11a and 11b)**. In comparison to untreated organoids, calcium kinetics demonstrated enhancement under higher penicillin concentrations (100 μM, 1 mM), exhibiting a statistically significant increase in maximum fluorescence intensity **(Figure 11c)**. Despite substantial standard deviations, the lowest data points for both experimental groups were observed to be elevated relative to the control group. Notably, the highest concentration (1 mM)

exhibited a decreased df/f0 **(Figure 11h)**, indicative of a lower relative calcium fluorescence intensity. Given the significant increase in maximum calcium signal observed with 1mM penicillin treatment, the decreased df/f0 may be attributable to an elevated baseline fluorescence intensity (f0), suggesting persistent intracellular calcium activity without complete return to baseline. However, this phenomenon could also potentially be ascribed to insufficient background removal and the presence of photobleaching during video recording. Furthermore, the 1mM treatment group displayed a significantly higher area ratio **(Figure 11j)**, implying an expanded region of calcium transient activity within the cardiac organoids. Although the 100 nM treatment group exhibited a reduced area of beating cardiac tissue, its lowest data point exceeded that of the control group due to the higher variability observed in the latter. In addition, a moderate alteration in calcium re-uptake properties was also noted following penicillin treatment. While no statistically significant changes were observed in t_{30} and t_{75}, a shortened t_{50} was detected in the 10nM group **(Figure 11e through 11g)**. Given that the calcium transient time remained unaffected across all experimental groups, the 10 nM group can be characterized as exhibiting a more peak-shouldering waveform profile.

Regarding the contraction motion tracking, no statistically significant alteration was seen in cardiac tissue beat rate across experimental groups. However, it is noteworthy that the dosed concentrations exhibited increased variability and occasionally displayed elevated beat rates at specific data points **(Figure 11k)**. This observation suggests that the introduction of penicillin may induce a moderate, albeit limited, modification to cardiac motion dynamics. In the higher concentration groups, enhanced motion behaviors were observed, manifested by a reduced interval **(Figure 11l)** between contraction and relaxation cycles (1 mM), as well as improved

contraction and relaxation velocities (100 μM, 100 mM) occurring in a synchronized manner **(Figure 11m and 11n)**. This phenomenon, in conjunction with the elevated calcium fluorescence intensity, potentially indicates accelerated calcium activity and energy transformation in response to higher penicillin concentrations.

Overall, the administration of penicillin at higher concentrations demonstrated relative enhancements in both calcium and motion kinetics, while exhibiting no significant embryotoxic effects on cardiac organoids, aligning with existing literature. The results obtained in this study are consistent with other in vitro and in vivo systems, as well as human data, which collectively suggest that penicillin does not exhibit teratogenic properties within therapeutic concentration ranges.[178,193]

3.3.3 Category C

Dacarbazine

Dacarbazine, classified as a Category C agent, is predominantly employed as a second- or third-line chemotherapeutic in combination with other antineoplastic agents. Well-controlled human studies or clinical cases documenting dacarbazine-induced embryotoxicity are exceedingly scarce.[102] During the dacarbazine treatment **(Figure 12a and 12b)**, cardiac organoids exposed to moderate concentrations (1 nM-10 μM) of dacarbazine survived the entire cardiac differentiation process. However, organoids under high concentrations (100 μM, 1 mM) disintegrated from the pattern following the initial or second addition of IWP4 (Day 1-Day 3). This observation not only confirms the cytotoxicity of dacarbazine but also indicates that the cytotoxic concentration threshold is below 100 μM.

Surviving organoids across all concentrations exhibited impaired morphology, manifesting various degrees of tissue disintegration, cell death, and insufficient differentiation, showing the significantly reduced beating area of cardiac tissue. Calcium transients were notably disrupted, with diminished relative and absolute calcium intensity observed in 1nM, 1μM, and 10 μM dacarbazine treatments **(Figure 12c, 12h; Figure 16)**. The 10 nM and 100 nM groups showed less pronounced effects, albeit with some extremely low data points. The highest concentration permitting organoid survival (10 μM) demonstrated a delayed onset of calcium signaling **(Figure 12d)**, with prolonged time to 30% calcium peak decay **(Figure 12e)** and extended peak plateau duration **(Figure 12i)**. The 1μM concentration group exhibited a significantly extended time for 75% calcium signal decay **(Figure 12g)**. Both higher concentrations displayed shouldered or tailed-peak calcium tracing waveforms, indicating the decelerated calcium activity.

For contractile motion, the 10 nM group exhibited an increased beat rate, while several data points in the 100 nM group also showed elevated beat rates compared to the control **(Figure 12k)**. The duration of contraction and relaxation **(Figure 12l)** was significantly prolonged in the highest concentration group (10 μM), despite high variation, as software vectors failed to detect motion peaks due to impaired motion behaviors. Intriguingly, some organoids treated with 100 nM dacarbazine displayed aberrations in peak regularity of contractile physiology, corresponding to split-peak tracing in their calcium waveform profiles, potentially indicating irregular beat rhythms. Consequently, all concentrations exhibited significantly impaired contraction and relaxation velocities **(Figure 12m and 12n)**.

In conclusion, dacarbazine treatment inhibits cardiac organoid differentiation, manifesting in motion abnormalities, arrhythmia-like responses, and disrupted intracellular calcium flux transients. The averaged IC50 value of all functional readouts for dacarbazine is calculated as 5.3 μM **(Table 1, Figure 16)**. Notably, dacarbazine demonstrated a statistically more potent inhibition of contraction motion compared to calcium response.

3.3.4 Category D

Hydroxyurea

Hydroxyurea, classified as a Category D member, presents a contentious profile regarding its teratogenicity, while the mechanism remains unknown. In this study, cardiac organoids demonstrated viability only up to a 100 μM hydroxyurea treatment, with a limited number surviving the treatment **(Figure 13a and 13b)**. Organoids that persisted through the entire differentiation process exhibited concentration-dependent morphological aberrations, manifesting a dose-dependent reduction in the area of beating tissue. The addition of IWP4 during cardiac differentiation emerged as a critical step as the WNT-β pathway inhibitor, with the highest concentration (1 mM) inducing severe apoptosis and cellular detachment during the second treatment (Day 3). Calcium handling capabilities of cardiac tissue were severely disrupted by hydroxyurea treatment, demonstrating a dose-dependent, statistically significant reduction across all concentrations in maximum calcium signal **(Figure 13c)**, accompanied by delayed onset times **(Figure 13d)** at higher concentrations (10 μM). Higher concentration groups also exhibited prolonged calcium signal decay times (1 μM, 10 μM for t_{30}; 1 μM, 10 μM, 100 μM for t_{50}; 10 μM, 100 μM for t_{75}, **Figure 13e through 13g**), indicative of impaired calcium re-uptake properties. Significantly extended peak times **(Figure 13i)** were observed in higher

concentration groups (1 μM, 10 μM), with a moderate increase and several elevated data points noted in the highest concentration group (100 μM). Analogous to the dramatic decrease in maximum calcium intensity, the relative fluorescence variation displayed a less dose-dependent decrease **(Figure 13h)**.

Hydroxyurea also exerted potent toxic effects on the contractile kinetics of cardiac organoids. Across all concentrations, cardiac organoids exhibited significantly reduced beat rates **(Figure 13k)** and motion velocities **(Figure 13m and 13n)**. Notably, the above-mentioned prolonged calcium decay times observed at higher treatment concentrations, coupled with decreased cardiac relaxation, may manifest as diastolic abnormalities, potentially promoting afterdepolarizations and arrhythmias that contribute to sudden cardiac death. [194,195] Intriguingly, the duration between motions displayed distinct trends of significant alterations **(Figure 13l)**, showing decreases in 10 nM and 100 nM groups, while an increase was observed with 1 μM treatment. This aligns with literature reports of unexpected hydroxyurea interactions that have eluded detection by some prediction models.

In conclusion, hydroxyurea exhibits relatively potent embryotoxic effects on cardiac organoids with respect to calcium dynamics and motion behaviors, potentially inducing diastolic insufficiency and life-threatening cardiac events, with an averaged IC50 value at 896 nM **(Table 1).** These results emphasized the complex nature of hydroxyurea's teratogenic potential and necessitated further investigation into its mechanisms of action in the context of embryonic cardiac development.

Doxorubicin

Doxorubicin, despite its classification as a Category D agent, has been widely recognized as a teratogen associated with congenital cardiac malformations.[149] In this study, the majority of doxorubicin concentrations proved incompatible with cardiac differentiation, with only an extremely limited number of organoids surviving at the lowest concentration of 1 nM. Most organoids underwent apoptosis following the initial RPMI/B27-Insulin treatment, indicative of doxorubicin's potent cytotoxicity as an antineoplastic agent. Even among the survivors at the lowest concentration, many failed to persist through the RPMI recovery phase to the differentiation endpoint. Severe morphological aberrations were observed in the sole treatment group. Rather than cellular disintegration from the pattern, organoids treated with 1 nM doxorubicin exhibited fibrosis-like structures across the pattern, with minimal beating cardiac tissue remaining **(Figure 14j)**. A moderately significant reduction in intracellular calcium peak intensity was observed, while no significant alterations were noted in signal onset time, time to 30% and 75% of signal decay, or relative signal intensity variation **(Figure 14d through 14i)**. In contrast, an unexpected shortening of t_{50} was observed in the experimental group **(Figure 14e)**. This phenomenon could potentially be attributed to high background noise, suggesting that even after background removal, extremely weak calcium tracing may have been obscured by photobleaching effects, limiting software detection capabilities.

Doxorubicin exhibited a more potent inhibition of the physiological properties of cardiac organoids compared to calcium response, manifesting as a significantly decreased beat rate **(Figure 14k)**, reduced motion velocities, and increased motion peak intervals **(Figure 14m and 14n)**. Notably, the motion tracking software was unable to detect minor relocations of motion

vectors due to extremely subtle contractile motion, potentially leading to missed relaxation peaks and consequently, longer statistically displayed peak intervals **(Figure 14l)**.

In conclusion, doxorubicin demonstrated greater inhibition of overall cytotoxicity compared to specific cardiotoxicity, suggesting that cell viability assays may serve as a more sensitive and visible alternative method for evaluating doxorubicin-induced toxicity. However, current data points of differentiation inhibition suggest that while an IC50 value has been identified, the lack of additional reference concentrations limits a reliable evaluation of the dose-response relationship. The calculated IC50 value for doxorubicin (3.08 nM) is insufficient to conclusively determine the drug-induced cardiotoxicity due to the limited availability of reference concentrations **(Table 1)**. Therefore, the range of concentrations inducing cardiotoxicity should be re-evaluated, with 1 nM potentially serving as the upper limit. Future improvements should focus on optimizing algorithms to enhance motion vector detection, improving image resolution and video recording optics, and implementing selective image analysis techniques.

3.3.5 Category X

Methotrexate

Methotrexate, categorized as a Category X agent, is a potent chemotherapeutic with substantial evidence of teratogenicity. While typically associated with skeletal, craniofacial, and limb abnormalities, cardiac malformations are less frequently reported.[187] This system detected the upper limit of methotrexate-induced cardiotoxicity at 10 nM **(Figure 15a and 15b)**, with higher concentrations proving lethal after the second RPMI/B27-Insulin treatment, thus confirming its potent cytotoxicity as a first-line chemotherapeutic. Unexpectedly, 1nM methotrexate treatment

did not induce the anticipated apoptotic response. Despite a significant decrease in the beating cardiac tissue area **(Figure 15j)**, organoid patterns under 1 nM treatment remained relatively intact, preserving the cardiac beating center. In contrast, the 10 nM group exhibited dramatic morphological impairment, presenting only single-layered beating tissue with minimal perimeter surrounding with a limited number of organoid patterns remaining.

Significant reduction in calcium maximum intensity was detected only in the 10 nM group, while the lower concentration (1 nM) showed no statistical difference from the control group but differed significantly from the 10 nM group **(Figure 15c)**. This observation could be attributed to the less severe morphological disruption and relatively intact organoids observed under 1nM methotrexate treatment. This phenomenon could be further reflected in the unaffected calcium onset time with 1nM methotrexate compared to the control group, while a significant increase was observed at 10 nM **(Figure 15d)**. Methotrexate treatment induced moderate alterations in calcium re-uptake properties. Time to 30% calcium signal decay was significantly affected only at 1nM **(Figure 15e)**, while time to 75% calcium decay showed significance at both concentrations **(Figure 15g)**. Notably, t_{50} and calcium peak plateau time remained unaffected **(Figure 15f and 15i)**. The relative calcium intensity variation corresponded to the trend observed in absolute maximum calcium intensity **(Figure 15h)**, suggesting that 1nM methotrexate exerts limited effects on calcium amplitude compared to 10 nM.

Correspondingly, motion tracking software frequently detected peaks with irregularity and complexity, suggesting potential arrhythmia-like responses, and was also reflected in the prolonged motion peak interval under the same concentration **(Figure 15l)**. Surprisingly, the beat

rate of both experimental groups remained unaffected, indicating that the impairment of perimeter tissue did not influence the beat rate of the single-layered cardiac tissue present in the center of the pattern **(Figure 15k)**, however, with significantly lower contractile motion velocities **(Figure 15m and 15n)**.

In conclusion, methotrexate demonstrated visibly strong embryotoxicity through interruption of the cardiac differentiation process, with all functional readouts corroborating each other. However, the quantification of half-inhibitory effects (**Table 1**) may be less accurate or reliable with only two available treatment concentrations. Therefore, the selection of testing concentrations may be re-considered, given the significant variation in functionality observed between 1nM and 10 nM treatment groups.

3.4 Summary and Discussion

The mouse embryonic stem cell test (mEST) stands as one of the prenatal developmental toxicity assays validated by the European Centre for the Validation of Alternative Methods (ECVAM). Despite not achieving regulatory acceptance, the mEST continues to be employed in industrial settings for prescreening and prioritization purposes.[196] Additionally, it serves as a valuable tool in toxicological research into the molecular mechanisms of chemical interference with embryonic cell differentiation.[197] In the context of this study, we have adopted the mEST as the standard against which we evaluate the efficacy of our cardiac organoid model in assessing embryotoxicity.

In comparison with the inhibition to cardiac differentiation observed in the D3 cell line (ID50) in mEST validation study [25] and other EB-based studies using the validated mEST, the four chemotherapeutic agents tested in this study demonstrated lower inhibitory concentrations when implementing the cardiac organoid model. Thiamine and penicillin, categorized as Class A and B for pregnancy risk respectively, exhibited inhibitory concentrations comparable to those observed in mEST models,[25,198] with both drugs and testing models displaying inhibition profiles exceeding 3 mM. These two substances can be validated as non-embryotoxic, exhibiting relatively safe profiles, which aligns with in vivo studies and corresponds to their pregnancy risk categories.

Among the chemotherapeutic agents, dacarbazine exhibited toxicity with a mean IC50 of 5.3 μM, indicating a moderate level of embryotoxicity relative to other anticancer agents. The literature and regulatory data regarding dacarbazine's embryotoxicity, as tested by mESC models, are extremely scarce. The limited available information indicates that approximately 66 μM is sufficient to induce mutagenicity in mouse germ cells, resulting in structural defects manifesting as heritable chromosomal aberrations.[137] Hydroxyurea demonstrated a mean IC50 of 21.4 μM in the mEST validation study, contrasting with the 896 nM observed in this study. However, in the mEST validation study, hydroxyurea exhibited inconsistent classifications across multiple experimental runs. Notably, it was incorrectly categorized as a weakly embryotoxic agent with less than 40% probability of accurate prediction, while the probability of correct classification as strongly embryotoxic was approximately 60%.[25] A later iPSC-based model established alternative criteria for embryotoxicity, categorizing substances as non-

embryotoxic, suspected embryotoxic, or embryotoxic. Under these new criteria, hydroxyurea remained classified as embryotoxic based on data quoted from the mEST database.[199]

According to the literature of mEST-based studies, doxorubicin exhibits cardiotoxic effects within a concentration range of 1 μM to 5 μM.[200–203] Although a standard inhibitory concentration was not established in the validation study, doxorubicin is a well-documented chemotherapeutic agent with a known toxicity profile, including teratogenic effects. Our data, however, indicated an inhibitory concentration of 3.08 nM for doxorubicin treatment. With only the lowest concentration sustaining survival throughout the differentiation process, doxorubicin may not be compatible with the current cardiac differentiation endpoint at Day 20. Moreover, the limited reference concentration constrains the reliability of the data. Methotrexate has been consistently classified as strongly embryotoxic, not only in the mEST validation studies but also in various in vitro models, and has demonstrated a high risk of teratogenicity in animal studies.[25] While the mEST reported an average ID50 of 59 nM, our study revealed a slightly lower embryotoxic concentration of 24.3 nM for methotrexate. Despite this lower value, methotrexate exhibits the closest estimation to the standard mEST inhibition concentration among the chemotherapeutic agents examined.

It is important to note that the reliability of these data may be compromised due to the limited reference concentrations available. The comparatively lower inhibitory concentrations observed in this study may be attributed to the simplified definition of the final inhibitory concentration, which equally weights the IC50 of each parameter. This suggests a need for re-evaluation of the relative importance of various parameters contributing to the overall inhibitory effects. For

instance, the motion-weighted IC50s were found to be significantly lower than the calcium-weighted IC50s across all drugs tested. Given the more potent effects observed in motion properties compared to calcium handling abilities, it may be appropriate to assign higher weighting to motion parameters and lower weighting to calcium parameters. Furthermore, the multidimensional evaluation of embryotoxicity employed in this study fundamentally differs from the single evaluation of contractility in D3 cell-derived CMs, or the sarcomeric protein expression of EB-derived CMs used in the mEST. Additionally, the differentiation endpoint in mEST was analyzed on Day 10, representing less mature properties and a shorter drug exposure time compared to the Day 20 evaluations in our study. This extended exposure period in our model may account for the lower cardiac-inhibitory concentrations observed, as the contractile apparatus is likely more disrupted over a longer exposure duration.

In conclusion, the six pharmaceuticals tested using our cardiac organoid model demonstrate consistency with their respective pregnancy risk categories, exhibiting a decreasing trend in IC50 values as the pregnancy risk increases. Thiamine and penicillin can be validated and classified as non-embryotoxic, while dacarbazine, hydroxyurea, doxorubicin, and methotrexate can be hypothesized as embryotoxic agents. Further validation and investigation into the extent of embryotoxicity for these latter compounds is warranted to establish more definitive conclusions.

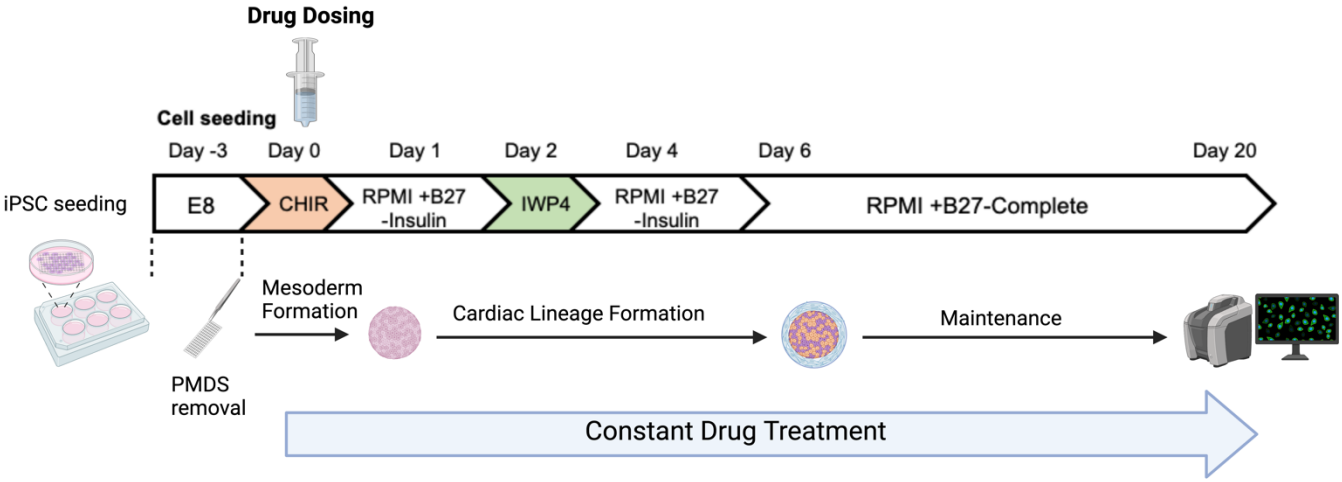

Figure 9. Schematic view of the drug dosing experiment. Drugs are dissolved, sterilized, and serial diluted with cell culture media and then dosed starting from Day 0 following the differentiation process. Upon the differentiation endpoint (Day 20), videos of beating organoids are captured for functional analysis.

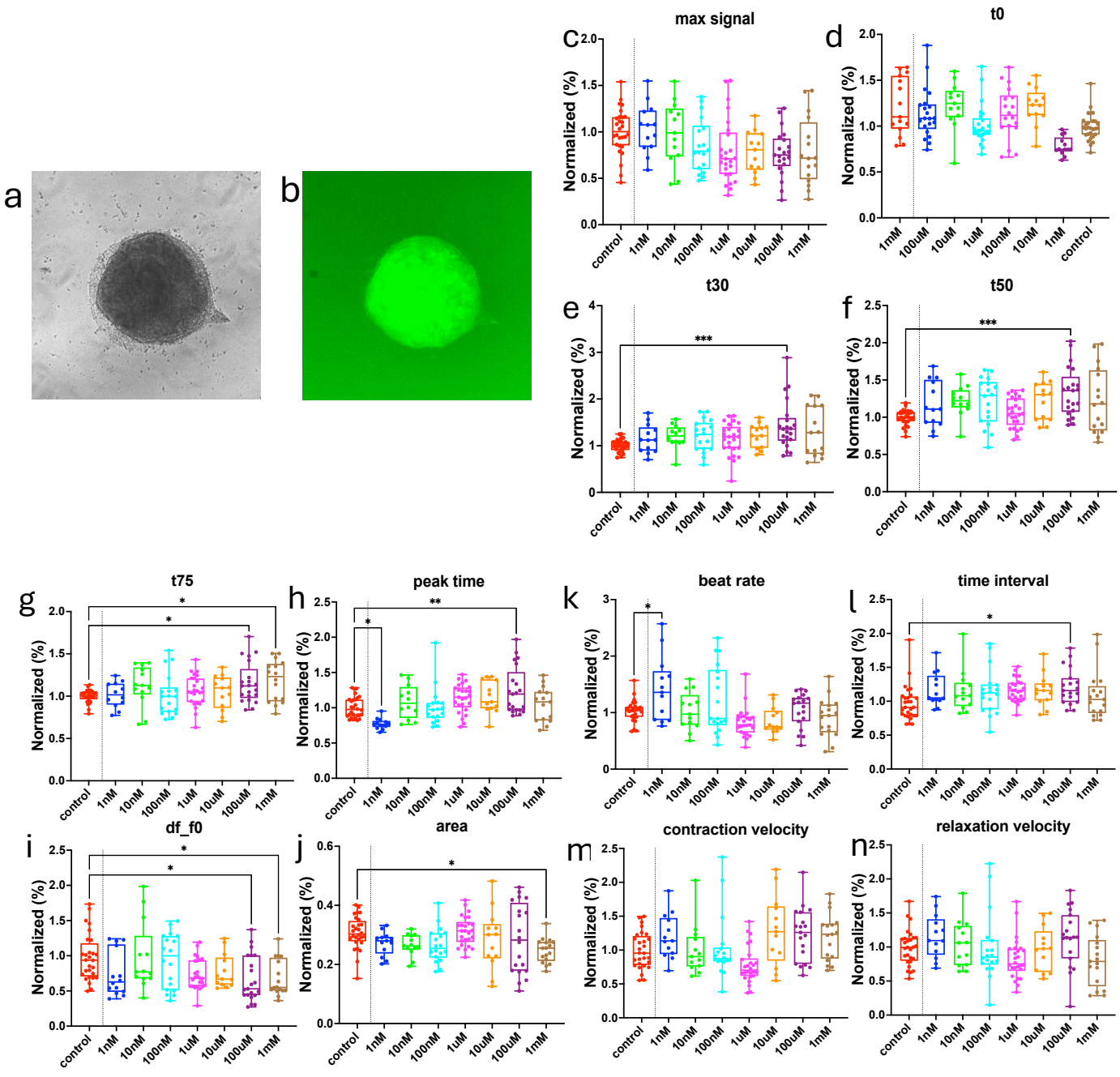

Figure 10. Functionality readouts of cardiac organoids with thiamine treatment. (a-b) Bright-field and GFP fluorescent image of 1mM thiamine-treated cardiac organoid on Day 20. (c-i) Calcium flux functionality showed limited variations upon thiamine treatment. (j) Area ratio of beating cardiac tissue, no significant change was detected except a modest decrease in the 1mM group. (k-n) Motion tracking analysis indicates thiamine exhibits minor effects on cardiac organoids in terms of motion behaviors

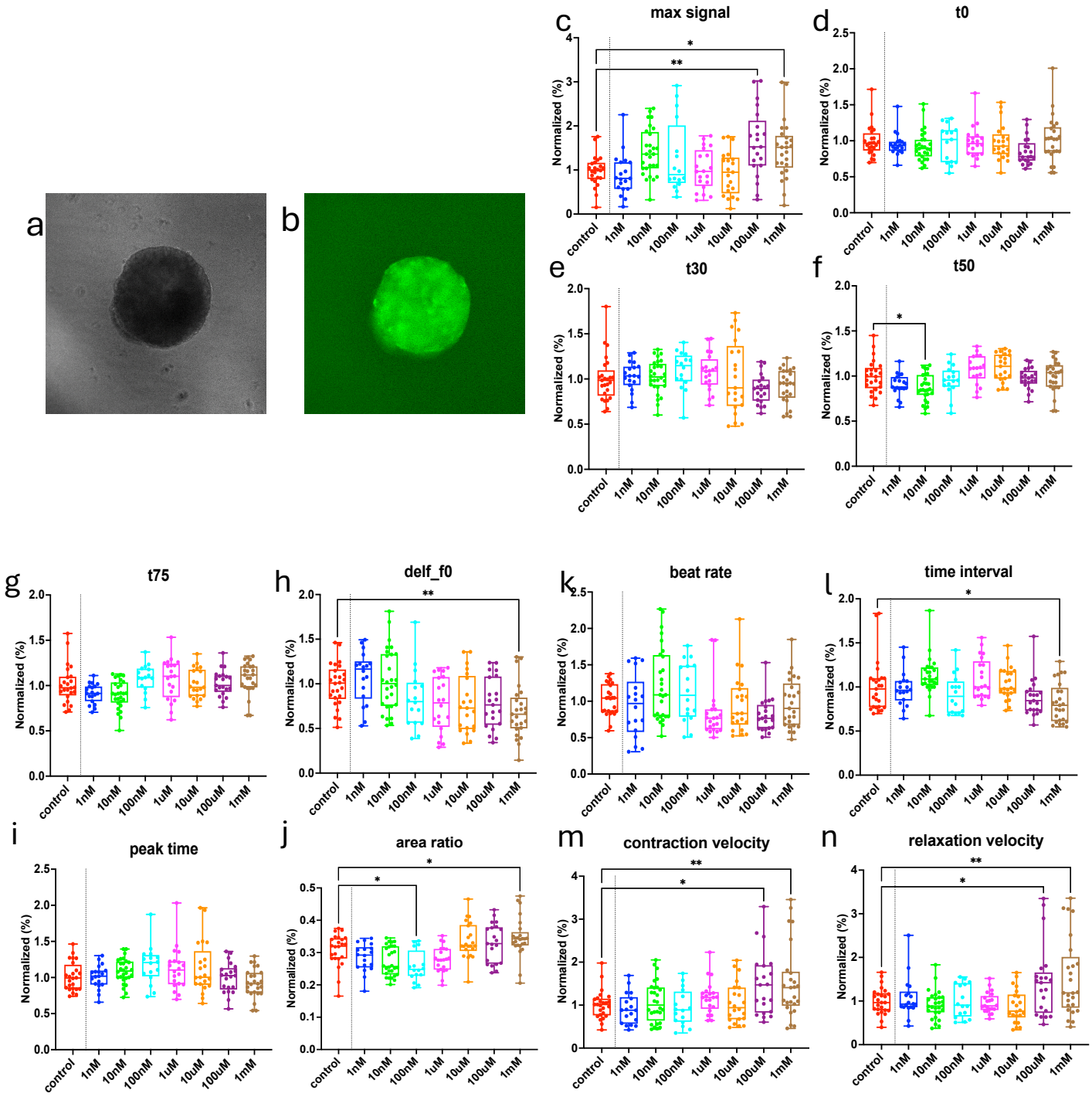

Figure 11. Functionality readouts of cardiac organoids with penicillin treatment. (a-b) Bright-field and GFP fluorescent images of cardiac organoid treated with 1mM penicillin on Day 20. (c-i) Calcium flux activities showed relative enhancements upon penicillin treatment, with (c) higher calcium signal at higher concentrations and similarly, area ratio (j) and motion behaviors (k-n) showed some extent of improvement.

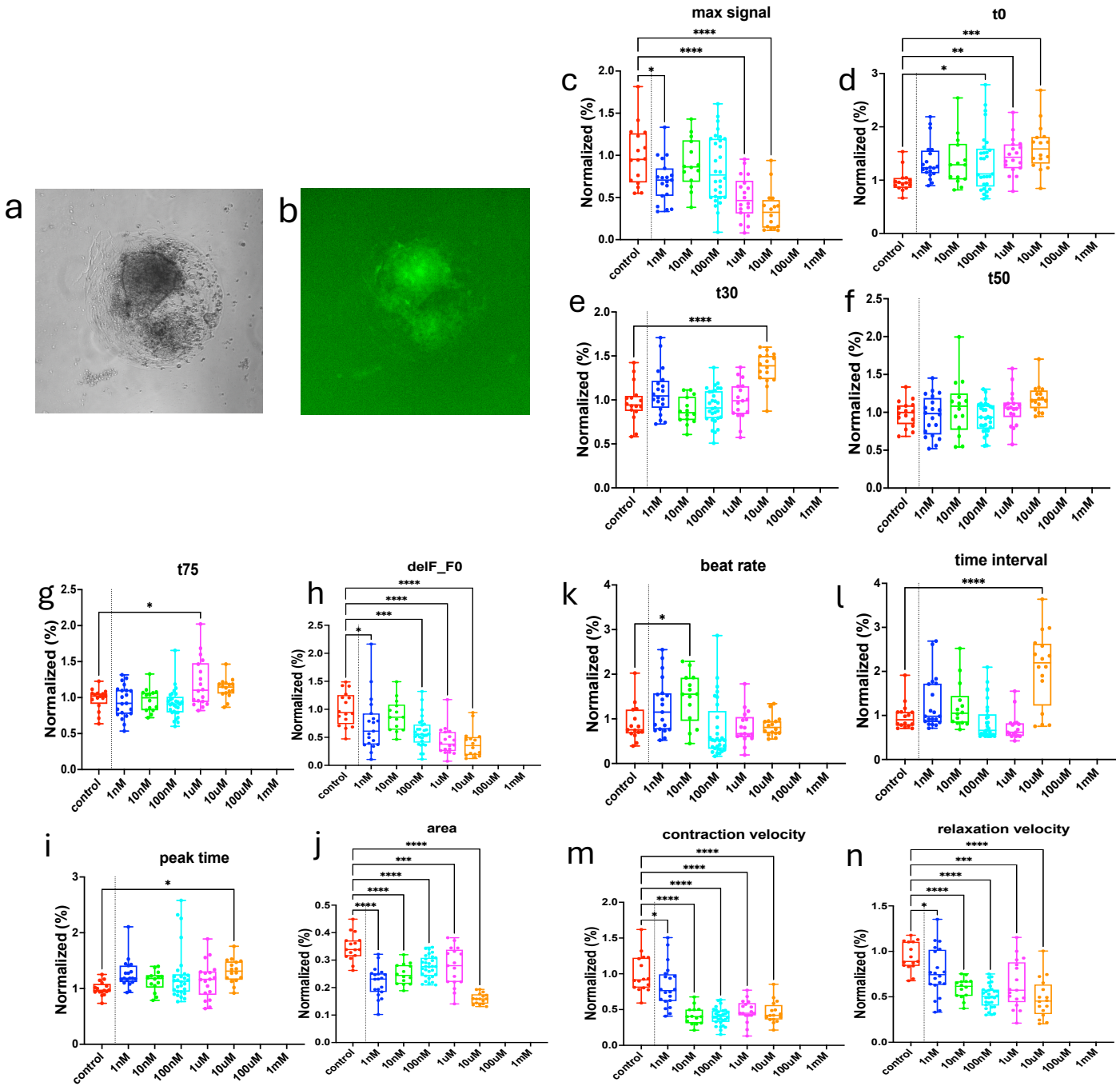

Figure 12. Functionality readouts of cardiac organoids with dacarbazine treatment. (a-b) Bright-field and GFP fluorescent images of cardiac organoids treated with 10 μM dacarbazine. (c-i) Disrupted calcium flux transients post-dacarbazine treatment with significantly decreased calcium intensity (c) and prolonged calcium re-uptake (d-i). (j) Reduced area of beating cardiac tissue. (k-n) Dacarbazine-induced motion abnormalities and arrhythmia-like responses, including (l) prolonged beat duration at the highest concentration and significantly decreased motion velocities across all concentrations.

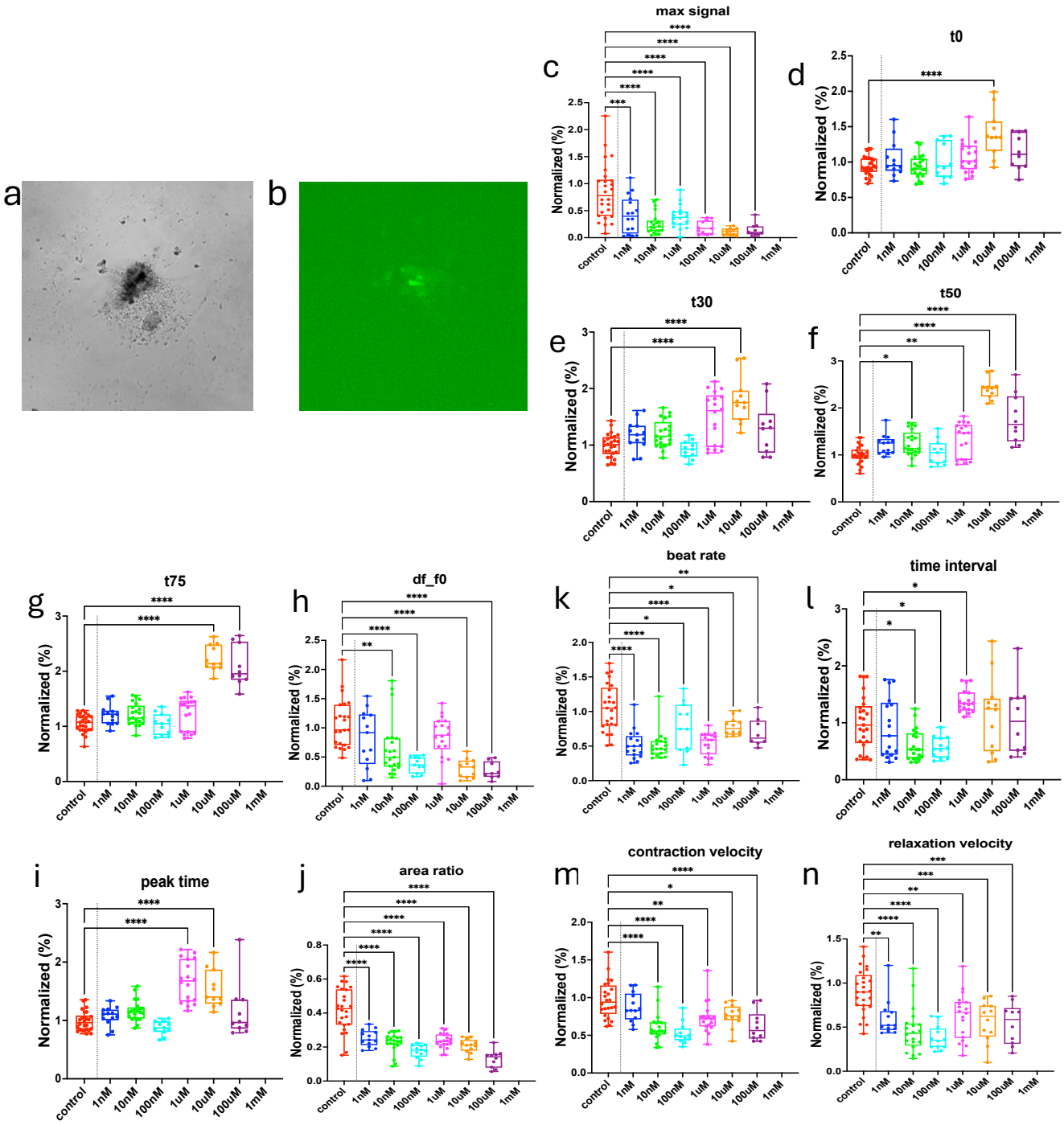

Figure 13. Functionality readouts of cardiac organoids with hydroxyurea treatment. (a-b) Bright-field and GFP fluorescent images with 100 μM hydroxyurea treatment on Day 20. Hydroxyurea exhibits relatively potent embryotoxic effects on cardiac organoids with respect to calcium dynamics (c-i), tissue morphology (j), and motion behaviors (k-n). Disrupted calcium transients manifest significantly as reduced calcium intensities (c and h), prolonged onset time and signal decay time (d-g), and peak plateau time (j) in higher concentrations. Significant motion behavior inhibitory effects include reduced beat rate (k), altered time interval (l), and

decreased contraction and relaxation velocities (m-n) with the potential of inducing diastolic insufficiency.

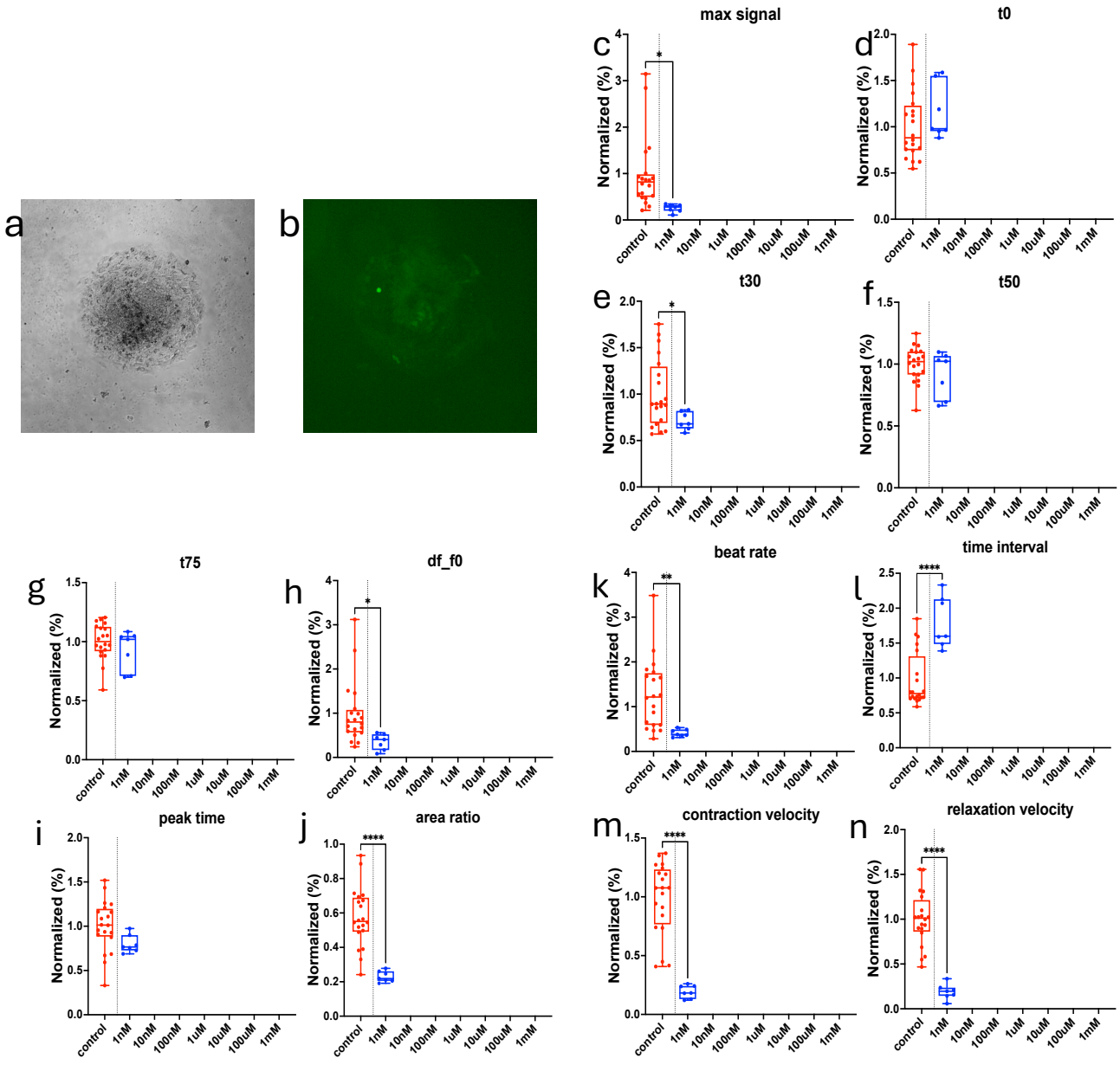

Figure 14. Functionality readouts of cardiac organoids with doxorubicin treatment. (a-b) Bright-field and GFP fluorescent images with 1 nM doxorubicin treatment on Day 20. (c-n) Doxorubicin inhibits overall cytotoxicity compared to specific cardiotoxicity in terms of differentiation. Limited data points suggest the doxorubicin-induced potent cardiotoxicity regarding calcium transients (c-i), cardiac tissue morphology (j), and motion properties (k-n).

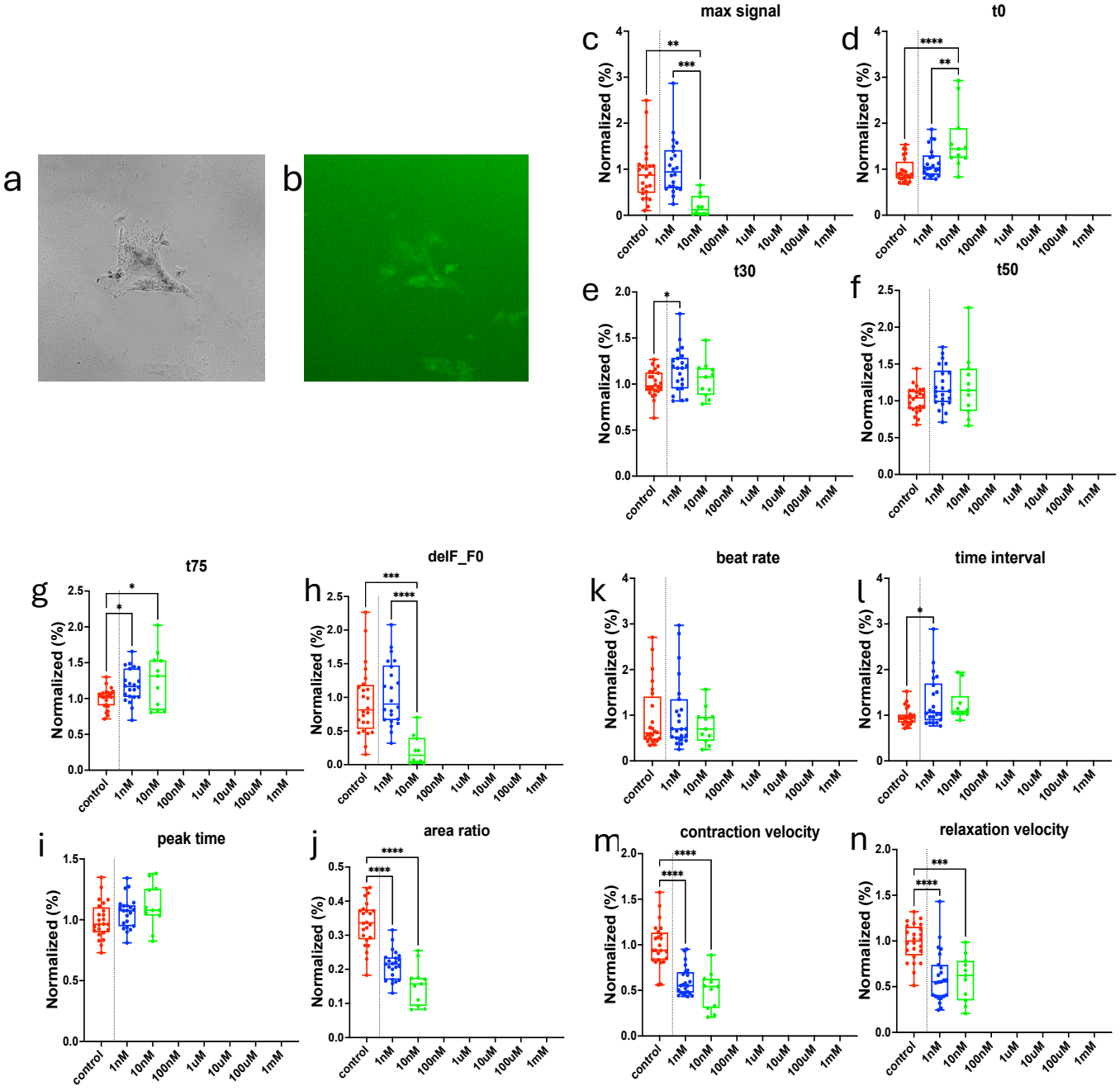

Figure 15. Functionality readouts of cardiac organoids with methotrexate treatment. (a-b) Bright-field and GFP fluorescent images with 10 nM methotrexate treatment on Day 20. (c-n) Limited dataset of methotrexate-induced interruption of the cardiac differentiation process, including significantly reduced calcium tracing (c-i), impaired cardiac tissue area (j), and irregular and complex contractile motions (m-n) suggesting arrhythmia-like responses.

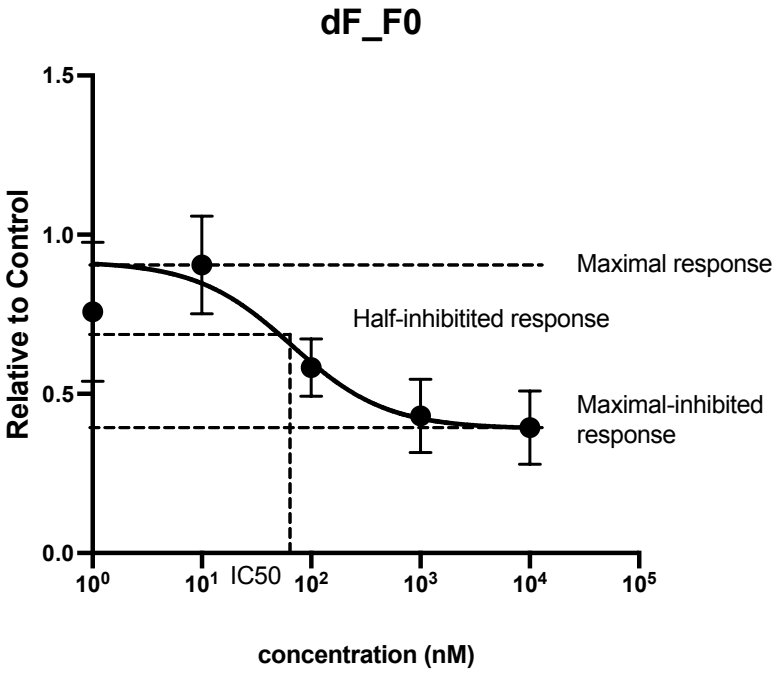

Figure 16. Dose-response curve of relative fluorescence intensity (df/f0) with dacarbazine treatment. The four-parameter logistic curve is fitted with y value of maximal drug response, half-inhibited response (IC50), maximally inhibited response, and Hill's slope. IC50 is the concentration of drug that gives a response to cardiac organoids halfway between the top and bottom plateaus, indicating the concentration of inducing cardiotoxicity.

Table 1. IC50 (nM) of functional readouts for each testing compound.

Drug	Beating rate	Time interval	Contraction velocity	Relaxation velocity	Max signal	t0	t30	t50	t75	df/f0	Peak time	Area ratio	Average	Cmax (nM)
Thiamine	5.65E+06	1.95E+07	8.50E+05	3.38E+06	4.96E+07	3.65E+06	1.00E+07	2.67E+07	1.28E+07	4.22E+07	7.49E+05	8.96E+05	1.47E+07	NA
Penicillin	6.80E+06	3.32E+05	5.08E+06	3.01E+06	2.98E+06	2.94E+07	1.00E+06	3.41E+08	4.29E+06	2.16E+06	1.83E+06	1.62E+07	3.45E+07	1.2E+06
Dacarbazine	26.38	11418	1.288	0.9062	15	1616	13602	5631	1134	65.88	29597	40.66	5262.34	3.4E+04
Hydroxyurea	0.2688	427.5	1.106	0.2506	1.394	808.5	838.1	2189	3759	2470	255.3	1.876	896.02	6.63E+05
Doxorubicin	0.2088	1.248	0.128	0.1999	0.1125	7.786	7.639	7.722	6.145	0.3803	4.995	0.4166	3.08	2.03E+03
Methotrexate	22.72	28.45	0.4004	0.08849	8.085	9.779	115.2	59.68	28.72	1.802	15.52	0.5786	24.25	4.6

4 CHAPTER 4 CONCLUSION AND FUTURE WORK

4.1 Conclusions

This study explores the development of engineered cardiac organoids as an innovative tool for modeling embryonic cardiac development and characterizing cardiac physiology, with a particular focus on enhancing diagnostic capabilities for chemotherapy-induced cardiotoxicity. The well-defined three-dimensional cardiac organoid architecture, which closely mimics the human physiological environment, is envisioned to serve as a pre-validation model for cardiotoxicity assessment in the early stages of assay development.

In Chapter 2, the study illustrates the methodology for generating biomaterial-based micropatterned cardiac organoids utilizing established protocols. This approach employs engineering-inspired techniques to guide self-organization through defined initial cellular density and spatial geometry. Methodological optimization was predicated on achieving control over the geometry of three-dimensional tissues by directly stamping micropatterns into a PEG-based hydrogel, with a focus on geometric shape and size as critical parameters guiding spatial cardiac differentiation into robust cardiac tissue.[204] The 600 μm circular geometry with low seeding density was identified as the optimized model, providing the largest area of cardiac tissue and highest motion velocities, indicative of higher cardiac differentiation efficiency compared to alternative shapes or sizes. By directing iPSC self-patterning through activation of the WNT pathway, cells are induced towards a mesoderm lineage and undergo self-migration to form an annulus shape characterized by a dense perimeter and dispersed center. At the differentiation endpoint, cardiac microchambers emerge in the center, surrounded by myofibroblasts at the

pattern periphery.[90]This phenomenon elucidates how the control of spatial boundary conditions through micropatterning illuminates fundamental mechanisms regulating stem cell differentiation. The application of a semi-automated imaging analysis with GCaMP-engineered iPSC reporter lines has replaced the traditional electrophysiological characterization methods for cardiac tissue, eliminating the need for stimulation and calcium dyes. This non-invasive approach is applicable to cardiomyocytes in various culture formats with minimal additional expertise required.[97]

Chapter 3 employs the optimized cardiac organoid model as a toxicity screening assay, precisely characterizing the embryotoxic potential of six pharmaceuticals through functional readouts, including parameters related to physiological kinetics and tissue morphology. From the perspective of assay development, this study can be considered as the method pre-validation phase, with results potentially serving as a compound training set and coded pharmaceuticals for subsequent assay development utilizing biostatistical models for predicting developmental toxicity. Given its capacity to recapitulate the human developmental and physiological environment, this three-dimensional cardiac organoid assay holds promise for high-throughput applications and potential replacement of traditional two-dimensional cell models in preclinical drug safety screening by enhancing data accuracy, efficiency, and reliability. Furthermore, the assay may provide evidence-based guidelines for healthcare professionals in conducting risk assessments and managing existing antineoplastic therapies in pregnant individuals.

The cardiac differentiation endpoint of this methodology is limited to Day 20, preceding epicardium formation, which indicates the inability of patterned cardiac organoids to achieve

further maturation due to geometrical constraints and insufficient cell population complexity. Indeed, the current cardiac organoid models lack several critical aspects of the human heart, including perfused vascularization, valves, and outflow tract.

Although chamber formation is observed, left-right asymmetry, conductance properties, and chamber delineation remain poorly defined, albeit present to some extent in this study. Furthermore, other significant cell populations, such as resident immune cells and neural crest contributions to innervation, are absent.[205] More importantly, this model primarily reflects embryonic or fetal cardiac development, lacking fidelity when compared to the adult human heart. This disparity is particularly significant given that adult-derived cardiac tissue is more structurally and functionally defined than fetal cardiac tissue. An additional constraint of the patterned organoids is their limited utility as "building blocks" for constructing larger engineered heart tissue (EHT) constructs. The firm attachment of organoids to the etched PEG gel on the solid substrate impedes the dissociation of intact organoid patterns for cryopreservation, thus compromising the reproducibility of the patterned structure. Consequently, this organoid construct is primarily suitable for recapitulating embryonic heart chamber development prior to the initiation of cardiac looping.

Notwithstanding these limitations, the immature, fetal-like microchambers offer valuable insights into studying early cardiac development and provide a promising platform for embryonic toxicological assessments. This applicability stems from the less differentiated nature of fetal cardiac tissue compared to adult cardiac tissue, potentially offering a more sensitive platform for detecting developmental perturbations induced by various compounds.

4.2 Future Improvement

In the context of developing a comprehensive toxicity assay for the successful implementation of a standardized human iPSC-based in vitro model, future methodological optimizations and the establishment of computational prediction models are imperative. For example, the development of a standardized protocol for imaging processing and camera optics optimization should be considered. This is crucial as the image-based algorithm's efficacy is highly dependent on the resolution achieved through optical flow. Parameter optimization should not only focus on ensuring high-quality videos for analytical accuracy but also consider video storage efficiency. Furthermore, diverse characterization scopes with advanced analytical techniques are necessary for in-depth toxicity evaluation across various aspects. The current assay involves multiple dosing of test compounds throughout the cardiac differentiation timeline from Day 0. To enhance reliability, it would be prudent to conduct exposure-based evaluations with multiple differentiation endpoints. For instance, since the addition of IWP4 (Day 2) is a critical step in observing a wide range of cell apoptosis, cytotoxicity assays could be performed around Day 4 prior to cardiac differentiation functionality assays. This approach is particularly relevant for agents demonstrating higher inhibition of organoid cell viability compared to cardiac differentiation inhibition, such as doxorubicin, in this study. Selecting appropriate compound concentrations can mitigate cytotoxicity-induced effects on differentiation readouts and provide a reliable range for subsequent concentration selections. However, cell death masked by dense viable cells may be challenging to detect within patterned organoids using direct Live/Dead staining. Consequently, luminescent staining of fine-lysed organoids may be offered as an alternative. Compound concentrations exhibiting cytotoxicity should be excluded from subsequent differentiation assays.

Additional electrophysiological evaluations, such as intracellular action potential measurements of cardiac tissue, can be implemented using automated fluorescence imaging analysis with membrane potential dyes. In conjunction with calcium flux tracing, this approach can further elucidate drug-induced cardiac repolarization-related responses. Moreover, flow cytometry-based measurements can serve as an alternative method for confirming differentiation efficiency by quantifying the expression of genes encoding cardiac differentiation markers, including MHC (myosin heavy chain), α-actinin (structural protein of sarcomere), and cTnT (cardiac troponin T). This technique could also be employed to investigate markers of signal transduction pathways regulating cardiac development, which have similar principles that apply to transcriptional analysis. Additionally, advanced techniques such as single-cell RNA sequencing or proteomics would complement the overall understanding of physiological pathways in this system beyond morphogenic effects. These high-throughput approaches would provide a more comprehensive molecular profile of the cardiac organoids, potentially revealing subtle drug-induced alterations in gene expression or protein abundance that may not be apparent through conventional assays.

The optimized organoid constructs have demonstrated their capacity to recapitulate in vivo developing heart characteristics and have exhibited sensitivity to drug exposure, with toxicity manifesting as unique impairments specific to each drug. These cardiac constructs show promise in classifying developmental toxicity and identifying cellular developmental processes targeted by drugs, potentially evolving into a proof-of-concept toxicity assay for preclinical screening practices. To ensure data integrity and reliability for preclinical practices, rigorous control of the quality differentiation testing system is imperative. The current assay employed only solvent

control, represented by culture media with 0.1% DMSO substituting for test compounds. Future iterations should incorporate positive-reference chemicals, such as 5-FU or methotrexate (as validated in this study), and negative controls, like penicillin, known to have no adverse effects on reproduction or differentiation. Moreover, the development of biostatistical models incorporating machine learning algorithms coupled with functional readouts is essential for predicting and classifying drug-induced embryotoxicity. The classification of embryotoxic effects can be further refined using a scoring system, ranking compounds as non-embryotoxic, weakly embryotoxic, or strongly embryotoxic. This approach could provide insights beyond the current IC50 estimation based on single parameters, evaluating the weighted importance of various factors contributing to induced toxicity. Additionally, the readouts from this study can serve as an initial validation set for future training of predictive learning models, necessitating further data collection to cover a broader chemical space.

In the early stages of pharmaceutical development, as exemplified in this study, assay concentrations are compared with effective pharmacological concentrations determined in cell-based assays or animal models. To develop a therapeutic exposure-based toxicity assay, the relationship between in vitro assay concentration and in vivo plasma exposure (C_{max}) must be established. As pharmaceutical development progresses, the predictive power of the assay for selected candidates can be optimized by incorporating actual human exposure data into the machine-learning prediction model. However, challenges remain in qualifying in vitro human-based data for regulatory safety testing. The scarcity of teratogens with sufficient human data makes it difficult to demonstrate the superiority of human-based tests over rodent-based in vivo tests. Moreover, the results of metabolism-independent testing systems may be less reliable for

drugs that serve as metabolites in vivo, such as dacarbazine, in this study. Therefore, cross-validation of this model with in vitro and in vivo study data requires further exploration.

The primary limitation of most in vitro assays for human-based teratogenicity is their inability to specify the mechanism of drug-induced toxicity – whether the drug crosses the placenta and acts directly on its molecular target in the fetus, or acts directly on the uterus and/or placenta.[206] To address this, the in vitro model would benefit from biostatistical characterization of effective intracellular concentrations combined with data on active metabolism or trans-placental barrier transfer. This approach would provide a more comprehensive explanation of compound distribution within the test system, enhancing our understanding of drug-induced developmental toxicity mechanisms.

In conclusion, while the optimized cardiac organoid model shows promise for developmental toxicity screening, further refinements in methodology, data analysis, and integration with complementary approaches are necessary to enhance its predictive power and regulatory acceptance.

REFERENCES

1. *Congenital disorders*. (n.d.). Retrieved June 5, 2024, from https://www.who.int/health-topics/congenital-anomalies

2. *Congenital disorders*. (n.d.). Retrieved June 5, 2024, from https://www.who.int/news-room/fact-sheets/detail/birth-defects

3. Broussard, C. S., Frey, M. T., Hernandez-Diaz, S., Greene, M. F., Chambers, C. D., Sahin, L., Sharp, B. A. C., & Honein, M. A. (2014). Developing a systematic approach to safer medication use during pregnancy: Summary of a Centers for Disease Control and Prevention–convened meeting. *American Journal of Obstetrics & Gynecology*, *211*(3), 208-214.e1. https://doi.org/10.1016/j.ajog.2014.05.040

4. Andrade, S. E., Raebel, M. A., Morse, A. N., Davis, R. L., Chan, K. A., Finkelstein, J. A., Fortman, K. K., McPhillips, H., Roblin, D., Smith, D. H., Yood, M. U., Platt, R., & Gurwitz, J. H. (2006). Use of prescription medications with a potential for fetal harm among pregnant women. *Pharmacoepidemiology and Drug Safety*, *15*(8), 546–554. https://doi.org/10.1002/pds.1235

5. Mitchell, A. A., Gilboa, S. M., Werler, M. M., Kelley, K. E., Louik, C., & Hernández-Díaz, S. (2011). Medication use during pregnancy, with particular focus on prescription drugs: 1976-2008. *American Journal of Obstetrics & Gynecology*, *205*(1), 51.e1-51.e8. https://doi.org/10.1016/j.ajog.2011.02.029

6. Demirtaş, M. S. (2020). The Pathogenesis of Congenital Anomalies: Roles of Teratogens and Infections. In *Congenital Anomalies in Newborn Infants—Clinical and Etiopathological Perspectives*. IntechOpen. https://doi.org/10.5772/intechopen.92580

7. Finnell, R. H. (1999). Teratology: General considerations and principles. *The Journal of Allergy and Clinical Immunology*, *103*(2 Pt 2), S337-342. https://doi.org/10.1016/s0091-6749(99)70259-9

8. Schaefer, C., Peters, P. W. J., & Miller, R. K. (2014). *Drugs during pregnancy and lactation: Treatment options and risk assessment* (3d Edition). Elsevier/Academic Press.

9. Li, M., Gong, J., Gao, L., Zou, T., Kang, J., & Xu, H. (2022). Advanced human developmental toxicity and teratogenicity assessment using human organoid models. *Ecotoxicology and Environmental Safety*, *235*, 113429. https://doi.org/10.1016/j.ecoenv.2022.113429

10. Sadough Shahmirzady, P., Esteghamati, A., Sadough, A., & Sarvi, F. (2020). The Risk Factors Associated with Congenital Anomalies in Newborns. *Journal of Comprehensive Pediatrics*, *11*(3). https://doi.org/10.5812/compreped.90136

11. Van Gelder, M. M. H. J., Van Rooij, I. A. L. M., Miller, R. K., Zielhuis, G. A., De Jong-van Den Berg, L. T. W., & Roeleveld, N. (2010). Teratogenic mechanisms of medical drugs. *Human Reproduction Update*, *16*(4), 378–394. https://doi.org/10.1093/humupd/dmp052

12. Thorpe, P. G., Gilboa, S. M., Hernandez-Diaz, S., Lind, J., Cragan, J. D., Briggs, G., Kweder, S., Friedman, J. M., Mitchell, A. A., Honein, M. A., & Study, T. N. B. D. P. (2013). Medications in the first trimester of pregnancy: Most common exposures and critical gaps in understanding fetal risk. *Pharmacoepidemiology and Drug Safety*, *22*(9), 1013–1018. https://doi.org/10.1002/pds.3495

13. Yeom, W., Kim, M.-N., Choi, S.-J., Oh, S., Roh, C.-R., & Kim, J.-H. (2015). Hyperplastic primary vitreous with hemorrhage manifested as a hyperechoic mass in the fetal orbit by prenatal ultrasound in a case of isolated unilateral microphthalmia. *Obstetrics & Gynecology Science*, *58*(4), 309–313. https://doi.org/10.5468/ogs.2015.58.4.309

14. Hatakeyama, S., Goto, M., Yamamoto, A., Ogura, J., Watanabe, N., Tsutsumi, S., Yakuwa, N., Yamane, R., Nagase, S., Takahashi, K., Kosaki, R., Murashima, A., & Yamaguchi, H. (2022). The safety of pranlukast and montelukast during the first trimester of pregnancy: A prospective, two-centered cohort study in Japan. *Congenital Anomalies*, *62*(4), 161–168. https://doi.org/10.1111/cga.12471

15. Therapontos, C., Erskine, L., Gardner, E. R., Figg, W. D., & Vargesson, N. (2009). Thalidomide induces limb defects by preventing angiogenic outgrowth during early limb formation. *Proceedings of the National Academy of Sciences*, *106*(21), 8573–8578. https://doi.org/10.1073/pnas.0901505106

16. Zomerdijk, I., Ruiter, R., Houweling, L., Herings, R., Straus, S., & Stricker, B. (2015). Dispensing of potentially teratogenic drugs before conception and during pregnancy: A population-based study. *BJOG: An International Journal of Obstetrics & Gynaecology*, *122*(8), 1119–1129. https://doi.org/10.1111/1471-0528.13128

17. Faiola, F., Yin, N., Yao, X., & Jiang, G. (2015). The Rise of Stem Cell Toxicology. *Environmental Science & Technology*, *49*(10), 5847–5848. https://doi.org/10.1021/acs.est.5b01549

18. Kimmel, C. B., Ballard, W. W., Kimmel, S. R., Ullmann, B., & Schilling, T. F. (1995). Stages of embryonic development of the zebrafish. *Developmental Dynamics*, *203*(3), 253–310. https://doi.org/10.1002/aja.1002030302

19. Legradi, J., Weiss, C., Reischl, M., Mikut, R., Liebel, U., & Müller, F. (2009). Zebrafish embryos as models for embryotoxic and teratological effects of chemicals. *Reproductive Toxicology*, *28*(2), 245–253. https://doi.org/10.1016/j.reprotox.2009.04.013

20. Milan, D. J., Peterson, T. A., Ruskin, J. N., Peterson, R. T., & MacRae, C. A. (2003). Drugs That Induce Repolarization Abnormalities Cause Bradycardia in Zebrafish. *Circulation*, *107*(10), 1355–1358. https://doi.org/10.1161/01.CIR.0000061912.88753.87

21. Bennekou, S. H. (2019). Moving towards a holistic approach for human health risk assessment – Is the current approach fit for purpose? *EFSA Journal*, *17*(S1), e170711. https://doi.org/10.2903/j.efsa.2019.e170711

22. Spielmann, H., Pohl, I., Doring, B., Liebsch, M., & Moldenhauer, F. (1997). The embryonic stem cell test (EST), an in vitro embryotoxicity test using two permanent mouse cell lines: 3T3 fibroblasts and embryonic stem cells. *In Vitro Toxicology: Journal of Molecular and Cellular Toxicology*, *10*, 119–127. https://doi.org/10.1007/978-3-7091-7500-2_69

23. Hong, E.-J., & Jeung, E.-B. (2013). Assessment of Developmental Toxicants using Human Embryonic Stem Cells. *Toxicological Research*, *29*(4), 221–227. https://doi.org/10.5487/TR.2013.29.4.221

24. Seiler, A. E. M., & Spielmann, H. (2011). The validated embryonic stem cell test to predict embryotoxicity in vitro. *Nature Protocols*, *6*(7), 961–978. https://doi.org/10.1038/nprot.2011.348

25. Genschow, E., Spielmann, H., Scholz, G., Pohl, I., Seiler, A., Clemann, N., Bremer, S., & Becker, K. (2004). Validation of the Embryonic Stem Cell Test in the International ECVAM Validation Study on Three *In Vitro* Embryotoxicity Tests. *Alternatives to Laboratory Animals*, *32*(3), 209–244. https://doi.org/10.1177/026119290403200305

26. de Miguel-Beriain, I. (2015). The ethics of stem cells revisited. *Advanced Drug Delivery Reviews*, *82–83*, 176–180. https://doi.org/10.1016/j.addr.2014.11.011

27. Hatani, T., Miki, K., & Yoshida, Y. (2018). Induction of Human Induced Pluripotent Stem Cells to Cardiomyocytes Using Embryoid Bodies. In K. Ishikawa (Ed.), *Experimental Models of Cardiovascular Diseases: Methods and Protocols* (pp. 79–92). Springer. https://doi.org/10.1007/978-1-4939-8597-5_6

28. Gorshkov, K., Aguisanda, F., Thorne, N., & Zheng, W. (2018). Astrocytes as targets for drug discovery. *Drug Discovery Today*, *23*(3), 673–680. https://doi.org/10.1016/j.drudis.2018.01.011

29. Cheng, W., Zhou, R., Liang, F., Wei, H., Feng, Y., & Wang, Y. (2016). Application of Mouse Embryonic Stem Cell Test to Detect Gender-Specific Effect of Chemicals: A Supplementary Tool for Embryotoxicity Prediction. *Chemical Research in Toxicology*, *29*(9), 1519–1533. https://doi.org/10.1021/acs.chemrestox.6b00197

30. Lam, C. K., & Wu, J. C. (2021). Clinical Trial in a Dish: Using Patient-Derived Induced Pluripotent Stem Cells to Identify Risks of Drug-Induced Cardiotoxicity. *Arteriosclerosis, Thrombosis, and Vascular Biology*, *41*(3), 1019–1031. https://doi.org/10.1161/ATVBAHA.120.314695

31. Grimm, F. A., Iwata, Y., Sirenko, O., Bittner, M., & Rusyn, I. (2015). High-Content Assay Multiplexing for Toxicity Screening in Induced Pluripotent Stem Cell-Derived Cardiomyocytes and Hepatocytes. *ASSAY and Drug Development Technologies*, *13*(9), 529–546. https://doi.org/10.1089/adt.2015.659

32. Cohen, J. D., Babiarz, J. E., Abrams, R. M., Guo, L., Kameoka, S., Chiao, E., Taunton, J., & Kolaja, K. L. (2011). Use of human stem cell derived cardiomyocytes to examine sunitinib mediated cardiotoxicity and electrophysiological alterations. *Toxicology and Applied Pharmacology*, *257*(1), 74–83. https://doi.org/10.1016/j.taap.2011.08.020

33. Logan, S., Arzua, T., Canfield, S. G., Seminary, E. R., Sison, S. L., Ebert, A. D., & Bai, X. (2019). Studying Human Neurological Disorders Using Induced Pluripotent Stem Cells: From 2D Monolayer to 3D Organoid and Blood Brain Barrier Models. In Y. S. Prakash (Ed.), *Comprehensive Physiology* (1st ed., pp. 565–611). Wiley. https://doi.org/10.1002/cphy.c180025

34. Sasai, Y. (2013). Cytosystems dynamics in self-organization of tissue architecture. *Nature*, *493*(7432), 318–326. https://doi.org/10.1038/nature11859

35. Fan, C., He, J., Xu, S., Yan, J., Jin, L., Dai, J., & Hu, B. (2023). Advances in biomaterial-based cardiac organoids. *Biomaterials Advances*, *153*, 213502. https://doi.org/10.1016/j.bioadv.2023.213502

36. Rossi, G., Manfrin, A., & Lutolf, M. P. (2018). Progress and potential in organoid research. *Nature Reviews Genetics*, *19*(11), 671–687. https://doi.org/10.1038/s41576-018-0051-9

37. Lewis-Israeli, Y. R., Wasserman, A. H., Gabalski, M. A., Volmert, B. D., Ming, Y., Ball, K. A., Yang, W., Zou, J., Ni, G., Pajares, N., Chatzistavrou, X., Li, W., Zhou, C., & Aguirre, A. (2021). Self-assembling human heart organoids for the modeling of cardiac development and congenital heart disease. *Nature Communications*, *12*(1), 5142. https://doi.org/10.1038/s41467-021-25329-5

38. Shi, Y., Inoue, H., Wu, J. C., & Yamanaka, S. (2017). Induced pluripotent stem cell technology: A decade of progress. *Nature Reviews Drug Discovery*, *16*(2), 115–130. https://doi.org/10.1038/nrd.2016.245

39. Funata, M., Nio, Y., Erion, D. M., Thompson, W. L., & Takebe, T. (2021). The promise of human organoids in the digestive system. *Cell Death & Differentiation*, *28*(1), 84–94. https://doi.org/10.1038/s41418-020-00661-3

40. Yousef Yengej, F. A., Jansen, J., Ammerlaan, C. M. E., Dilmen, E., Pou Casellas, C., Masereeuw, R., Hoenderop, J. G., Smeets, B., Rookmaaker, M. B., Verhaar, M. C., & Clevers, H. (2023). Tubuloid culture enables long-term expansion of functional human kidney tubule epithelium from iPSC-derived organoids. *Proceedings of the National Academy of Sciences*, *120*(6), e2216836120. https://doi.org/10.1073/pnas.2216836120

41. Lee, C.-T., Bendriem, R. M., Wu, W. W., & Shen, R.-F. (2017). 3D brain Organoids derived from pluripotent stem cells: Promising experimental models for brain development and neurodegenerative disorders. *Journal of Biomedical Science*, *24*(1), 59. https://doi.org/10.1186/s12929-017-0362-8

42. Buskin, A., Singh, P., Lorenz, O., Robson, C., Strand, D. W., & Heer, R. (2021). A Review of Prostate Organogenesis and a Role for iPSC-Derived Prostate Organoids to Study Prostate Development and Disease. *International Journal of Molecular Sciences*, *22*(23), Article 23. https://doi.org/10.3390/ijms222313097

43. De Santis, M., Carducci, B., Cavaliere, A. F., De Santis, L., Straface, G., & Caruso, A. (2001). Drug—Induced Congenital Defects. *Drug Safety*, *24*(12), 889–901. https://doi.org/10.2165/00002018-200124120-00003

44. Takasato, M., Er, P. X., Chiu, H. S., Maier, B., Baillie, G. J., Ferguson, C., Parton, R. G., Wolvetang, E. J., Roost, M. S., Chuva De Sousa Lopes, S. M., & Little, M. H. (2015). Kidney organoids from human iPS cells contain multiple lineages and model human nephrogenesis. *Nature*, *526*(7574), 564–568. https://doi.org/10.1038/nature15695

45. Czerniecki, S. M., Cruz, N. M., Harder, J. L., Menon, R., Annis, J., Otto, E. A., Gulieva, R. E., Islas, L. V., Kim, Y. K., Tran, L. M., Martins, T. J., Pippin, J. W., Fu, H., Kretzler, M., Shankland, S. J., Himmelfarb, J., Moon, R. T., Paragas, N., & Freedman, B. S.

(2018). High-Throughput Screening Enhances Kidney Organoid Differentiation from Human Pluripotent Stem Cells and Enables Automated Multidimensional Phenotyping. *Cell Stem Cell*, *22*(6), 929-940.e4. https://doi.org/10.1016/j.stem.2018.04.022

46. Morizane, R., Lam, A. Q., Freedman, B. S., Kishi, S., Valerius, M. T., & Bonventre, J. V. (2015). Nephron organoids derived from human pluripotent stem cells model kidney development and injury. *Nature Biotechnology*, *33*(11), 1193–1200. https://doi.org/10.1038/nbt.3392

47. Pendergraft, S. S., Sadri-Ardekani, H., Atala, A., & Bishop, C. E. (2017). Three-dimensional testicular organoid: A novel tool for the study of human spermatogenesis and gonadotoxicity in vitro†. *Biology of Reproduction*, *96*(3), 720–732. https://doi.org/10.1095/biolreprod.116.143446

48. Ross, E. J., Graham, D. L., Money, K. M., & Stanwood, G. D. (2015). Developmental Consequences of Fetal Exposure to Drugs: What We Know and What We Still Must Learn. *Neuropsychopharmacology*, *40*(1), 61–87. https://doi.org/10.1038/npp.2014.147

49. Frank, D. A., Augustyn, M., & Zuckerman, B. S. (1998). Neonatal Neurobehavioral and Neuroanatomic Correlates of Prenatal Cocaine Exposure: Problems of Dose and Confounding. *Annals of the New York Academy of Sciences*, *846*(1), 40–50. https://doi.org/10.1111/j.1749-6632.1998.tb09725.x

50. Bandstra, E. S., Vogel, A. L., Morrow, C. E., Xue, L., & Anthony, J. C. (2004). Severity of Prenatal Cocaine Exposure and Child Language Functioning Through Age Seven Years: A Longitudinal Latent Growth Curve Analysis. *Substance Use & Misuse*, *39*(1), 25–59. https://doi.org/10.1081/JA-120027765

51. Singer, L. T., Arendt, R., Minnes, S., Farkas, K., Salvator, A., Kirchner, H. L., & Kliegman, R. (2002). Cognitive and motor outcomes of cocaine-exposed infants. *JAMA*, *287*(15), 1952–1960. https://doi.org/10.1001/jama.287.15.1952

52. Kindberg, A. A., Bendriem, R. M., Spivak, C. E., Chen, J., Handreck, A., Lupica, C. R., Liu, J., Freed, W. J., & Lee, C.-T. (2014). An in vitro model of human neocortical development using pluripotent stem cells: Cocaine-induced cytoarchitectural alterations. *Disease Models & Mechanisms*, *7*(12), 1397–1405. https://doi.org/10.1242/dmm.017251

53. Lee, C.-T., Chen, J., Kindberg, A. A., Bendriem, R. M., Spivak, C. E., Williams, M. P., Richie, C. T., Handreck, A., Mallon, B. S., Lupica, C. R., Lin, D.-T., Harvey, B. K., Mash, D. C., & Freed, W. J. (2017). CYP3A5 Mediates Effects of Cocaine on Human Neocorticogenesis: Studies using an In Vitro 3D Self-Organized hPSC Model with a Single Cortex-Like Unit. *Neuropsychopharmacology*, *42*(3), 774–784. https://doi.org/10.1038/npp.2016.156

54. Johnson, N. M., Hoffmann, A. R., Behlen, J. C., Lau, C., Pendleton, D., Harvey, N., Shore, R., Li, Y., Chen, J., Tian, Y., & Zhang, R. (2021). Air pollution and children's health—A review of adverse effects associated with prenatal exposure from fine to ultrafine particulate matter. *Environmental Health and Preventive Medicine*, *26*(1), 72. https://doi.org/10.1186/s12199-021-00995-5

55. DeFranco, E., Hall, E., Hossain, M., Chen, A., Haynes, E. N., Jones, D., Ren, S., Lu, L., & Muglia, L. (2015). Air Pollution and Stillbirth Risk: Exposure to Airborne Particulate Matter during Pregnancy Is Associated with Fetal Death. *PLOS ONE*, *10*(3), e0120594. https://doi.org/10.1371/journal.pone.0120594

56. Kim, J.-H., Kim, J., Kim, W. J., Choi, Y. H., Yang, S.-R., & Hong, S.-H. (2020). Diesel Particulate Matter 2.5 Induces Epithelial-to-Mesenchymal Transition and Upregulation of SARS-CoV-2 Receptor during Human Pluripotent Stem Cell-Derived Alveolar Organoid Development. *International Journal of Environmental Research and Public Health*, *17*(22), Article 22. https://doi.org/10.3390/ijerph17228410

57. Paakkari, I. (2002). Cardiotoxicity of new antihistamines and cisapride. *Toxicology Letters*, *127*(1–3), 279–284. https://doi.org/10.1016/s0378-4274(01)00510-0

58. Ghigo, A., Li, M., & Hirsch, E. (2016). New signal transduction paradigms in anthracycline-induced cardiotoxicity. *Biochimica et Biophysica Acta*, *1863*(7 Pt B), 1916–1925. https://doi.org/10.1016/j.bbamcr.2016.01.021

59. Lee, S. W., Song, M., Woo, D.-H., & Jeong, G. S. (2024). Proposal for considerations during human iPSC-derived cardiac organoid generation for cardiotoxicity drug testing. *Biomedicine & Pharmacotherapy*, *174*, 116511. https://doi.org/10.1016/j.biopha.2024.116511

60. Chen, X., Lu, N., Huang, S., Zhang, Y., Liu, Z., & Wang, X. (2023). Assessment of doxorubicin toxicity using human cardiac organoids: A novel model for evaluating drug cardiotoxicity. *Chemico-Biological Interactions*, *386*, 110777. https://doi.org/10.1016/j.cbi.2023.110777

61. Motlagh, P. E., Novin, A. G., Ghahari, F., Nikzad, A., Khoshandam, M., Mardani, S., Khanbabaei, H., Farsinejad, A., Sathyapalan, T., Sahebkar, A., & Pourghadamyari, H. (2021). Evaluation of the Effect of Crocin on Doxorubicin-Induced Cardiotoxicity. In A. Sahebkar & T. Sathyapalan (Eds.), *Natural Products and Human Diseases:*

Pharmacology, Molecular Targets, and Therapeutic Benefits (pp. 143–153). Springer International Publishing. https://doi.org/10.1007/978-3-030-73234-9_10

62. Mills, R. J., Parker, B. L., Quaife-Ryan, G. A., Voges, H. K., Needham, E. J., Bornot, A., Ding, M., Andersson, H., Polla, M., Elliott, D. A., Drowley, L., Clausen, M., Plowright, A. T., Barrett, I. P., Wang, Q.-D., James, D. E., Porrello, E. R., & Hudson, J. E. (2019). Drug Screening in Human PSC-Cardiac Organoids Identifies Pro-proliferative Compounds Acting via the Mevalonate Pathway. *Cell Stem Cell*, *24*(6), 895-907.e6. https://doi.org/10.1016/j.stem.2019.03.009

63. Lee, M.-S., Hekimian, A., Doctorian, T., & Duan, L. (2018). Statin exposure during first trimester of pregnancy is associated with fetal ventricular septal defect. *International Journal of Cardiology*, *269*, 111–113. https://doi.org/10.1016/j.ijcard.2018.07.002

64. Drakhlis, L., Biswanath, S., Farr, C.-M., Lupanow, V., Teske, J., Ritzenhoff, K., Franke, A., Manstein, F., Bolesani, E., Kempf, H., Liebscher, S., Schenke-Layland, K., Hegermann, J., Nolte, L., Meyer, H., De La Roche, J., Thiemann, S., Wahl-Schott, C., Martin, U., & Zweigerdt, R. (2021). Human heart-forming organoids recapitulate early heart and foregut development. *Nature Biotechnology*, *39*(6), 737–746. https://doi.org/10.1038/s41587-021-00815-9

65. Hofbauer, P., Jahnel, S. M., Papai, N., Giesshammer, M., Deyett, A., Schmidt, C., Penc, M., Tavernini, K., Grdseloff, N., Meledeth, C., Ginistrelli, L. C., Ctortecka, C., Šalic, Š., Novatchkova, M., & Mendjan, S. (2021). Cardioids reveal self-organizing principles of human cardiogenesis. *Cell*, *184*(12), 3299-3317.e22. https://doi.org/10.1016/j.cell.2021.04.034

66. Li, S., Zhou, D., Lu, M. M., & Morrisey, E. E. (2004). Advanced Cardiac Morphogenesis Does Not Require Heart Tube Fusion. *Science*, *305*(5690), 1619–1622. https://doi.org/10.1126/science.1098674

67. Ivanovitch, K., Esteban, I., & Torres, M. (2017). Growth and Morphogenesis during Early Heart Development in Amniotes. *Journal of Cardiovascular Development and Disease*, *4*(4), Article 4. https://doi.org/10.3390/jcdd4040020

68. Cao, J., & Poss, K. D. (2018). The epicardium as a hub for heart regeneration. *Nature Reviews Cardiology*, *15*(10), 631–647. https://doi.org/10.1038/s41569-018-0046-4

69. Quijada, P., Trembley, M. A., & Small, E. M. (2020). The Role of the Epicardium During Heart Development and Repair. *Circulation Research*, *126*(3), 377–394. https://doi.org/10.1161/CIRCRESAHA.119.315857

70. Rossi, G., Broguiere, N., Miyamoto, M., Boni, A., Guiet, R., Girgin, M., Kelly, R. G., Kwon, C., & Lutolf, M. P. (2021). Capturing Cardiogenesis in Gastruloids. *Cell Stem Cell*, *28*(2), 230-240.e6. https://doi.org/10.1016/j.stem.2020.10.013

71. Miquerol, L., & Kelly, R. G. (2013). Organogenesis of the vertebrate heart. *WIREs Developmental Biology*, *2*(1), 17–29. https://doi.org/10.1002/wdev.68

72. Kim, H., Kamm, R. D., Vunjak-Novakovic, G., & Wu, J. C. (2022). Progress in multicellular human cardiac organoids for clinical applications. *Cell Stem Cell*, *29*(4), 503–514. https://doi.org/10.1016/j.stem.2022.03.012

73. Polonchuk, L., Chabria, M., Badi, L., Hoflack, J.-C., Figtree, G., Davies, M. J., & Gentile, C. (2017). Cardiac spheroids as promising in vitro models to study the human heart microenvironment. *Scientific Reports*, *7*(1), 7005. https://doi.org/10.1038/s41598-017-06385-8

74. Beauchamp, P., Moritz, W., Kelm, J. M., Ullrich, N. D., Agarkova, I., Anson, B. D., Suter, T. M., & Zuppinger, C. (2015). Development and Characterization of a Scaffold-Free 3D Spheroid Model of Induced Pluripotent Stem Cell-Derived Human Cardiomyocytes. *Tissue Engineering Part C: Methods*, *21*(8), 852–861. https://doi.org/10.1089/ten.tec.2014.0376

75. Eschenhagen, T., & Zimmermann, W. H. (2005). Engineering Myocardial Tissue. *Circulation Research*, *97*(12), 1220–1231. https://doi.org/10.1161/01.RES.0000196562.73231.7d

76. Jin, H., Xue, Z., Liu, J., Ma, B., Yang, J., & Lei, L. (n.d.). Advancing Organoid Engineering for Tissue Regeneration and Biofunctional Reconstruction. *Biomaterials Research*, *28*, 0016. https://doi.org/10.34133/bmr.0016

77. Zhu, L., Liu, K., Feng, Q., & Liao, Y. (2022). Cardiac Organoids: A 3D Technology for Modeling Heart Development and Disease. *Stem Cell Reviews and Reports*, *18*(8), 2593–2605. https://doi.org/10.1007/s12015-022-10385-1

78. Arai, K., Murata, D., Verissimo, A. R., Mukae, Y., Itoh, M., Nakamura, A., Morita, S., & Nakayama, K. (2018). Fabrication of scaffold-free tubular cardiac constructs using a Bio-3D printer. *PLOS ONE*, *13*(12), e0209162. https://doi.org/10.1371/journal.pone.0209162

79. Kupfer, M. E., Lin, W.-H., Ravikumar, V., Qiu, K., Wang, L., Gao, L., Bhuiyan, D. B., Lenz, M., Ai, J., Mahutga, R. R., Townsend, D., Zhang, J., McAlpine, M. C., Tolkacheva, E. G., & Ogle, B. M. (2020). In Situ Expansion, Differentiation, and Electromechanical Coupling of Human Cardiac Muscle in a 3D Bioprinted, Chambered Organoid. *Circulation Research*, *127*(2), 207–224. https://doi.org/10.1161/CIRCRESAHA.119.316155

80. Min, S., Kim, S., Sim, W.-S., Choi, Y. S., Joo, H., Park, J.-H., Lee, S.-J., Kim, H., Lee, M. J., Jeong, I., Cui, B., Jo, S.-H., Kim, J.-J., Hong, S. B., Choi, Y.-J., Ban, K., Kim, Y.-G., Park, J.-U., Lee, H.-A., … Cho, S.-W. (2024). Versatile human cardiac tissues engineered with perfusable heart extracellular microenvironment for biomedical applications. *Nature Communications*, *15*(1), 2564. https://doi.org/10.1038/s41467-024-46928-y

81. Eiraku, M., Takata, N., Ishibashi, H., Kawada, M., Sakakura, E., Okuda, S., Sekiguchi, K., Adachi, T., & Sasai, Y. (2011). Self-organizing optic-cup morphogenesis in three-dimensional culture. *Nature*, *472*(7341), 51–56. https://doi.org/10.1038/nature09941

82. Qian, X., Nguyen, H. N., Song, M. M., Hadiono, C., Ogden, S. C., Hammack, C., Yao, B., Hamersky, G. R., Jacob, F., Zhong, C., Yoon, K., Jeang, W., Lin, L., Li, Y., Thakor, J., Berg, D. A., Zhang, C., Kang, E., Chickering, M., … Ming, G. (2016). Brain-Region-Specific Organoids Using Mini-bioreactors for Modeling ZIKV Exposure. *Cell*, *165*(5), 1238–1254. https://doi.org/10.1016/j.cell.2016.04.032

83. Koike, H., Iwasawa, K., Ouchi, R., Maezawa, M., Giesbrecht, K., Saiki, N., Ferguson, A., Kimura, M., Thompson, W. L., Wells, J. M., Zorn, A. M., & Takebe, T. (2019). Modelling human hepato-biliary-pancreatic organogenesis from the foregut–midgut boundary. *Nature*, *574*(7776), 112–116. https://doi.org/10.1038/s41586-019-1598-0

84. Silva, A. C., Matthys, O. B., Joy, D. A., Kauss, M. A., Natarajan, V., Lai, M. H., Turaga, D., Blair, A. P., Alexanian, M., Bruneau, B. G., & McDevitt, T. C. (2021). Co-emergence of cardiac and gut tissues promotes cardiomyocyte maturation within human iPSC-derived organoids. *Cell Stem Cell*, *28*(12), 2137-2152.e6. https://doi.org/10.1016/j.stem.2021.11.007

85. Shinozawa, T., Kimura, M., Cai, Y., Saiki, N., Yoneyama, Y., Ouchi, R., Koike, H., Maezawa, M., Zhang, R.-R., Dunn, A., Ferguson, A., Togo, S., Lewis, K., Thompson, W. L., Asai, A., & Takebe, T. (2021). High-Fidelity Drug-Induced Liver Injury Screen Using Human Pluripotent Stem Cell–Derived Organoids. *Gastroenterology*, *160*(3), 831-846.e10. https://doi.org/10.1053/j.gastro.2020.10.002

86. Freedman, B. S., Brooks, C. R., Lam, A. Q., Fu, H., Morizane, R., Agrawal, V., Saad, A. F., Li, M. K., Hughes, M. R., Werff, R. V., Peters, D. T., Lu, J., Baccei, A., Siedlecki, A. M., Valerius, M. T., Musunuru, K., McNagny, K. M., Steinman, T. I., Zhou, J., … Bonventre, J. V. (2015). Modelling kidney disease with CRISPR-mutant kidney organoids derived from human pluripotent epiblast spheroids. *Nature Communications*, *6*, 8715. https://doi.org/10.1038/ncomms9715

87. *About us*. (n.d.). CYTOO. Retrieved June 23, 2024, from https://cytoo.com/about-us

88. Warmflash, A., Sorre, B., Etoc, F., Siggia, E. D., & Brivanlou, A. H. (2014). A method to recapitulate early embryonic spatial patterning in human embryonic stem cells. *Nature Methods*, *11*(8), 847–854. https://doi.org/10.1038/nmeth.3016

89. Etoc, F., Metzger, J., Ruzo, A., Kirst, C., Yoney, A., Ozair, M. Z., Brivanlou, A. H., & Siggia, E. D. (2016). A Balance between Secreted Inhibitors and Edge Sensing Controls Gastruloid Self-Organization. *Developmental Cell*, *39*(3), 302–315. https://doi.org/10.1016/j.devcel.2016.09.016

90. Laurent, J., Blin, G., Chatelain, F., Vanneaux, V., Fuchs, A., Larghero, J., & Théry, M. (2017). Convergence of microengineering and cellular self-organization towards functional tissue manufacturing. *Nature Biomedical Engineering*, *1*(12), 939–956. https://doi.org/10.1038/s41551-017-0166-x

91. Khademhosseini, A., Eng, G., Yeh, J., Kucharczyk, P. A., Langer, R., Vunjak-Novakovic, G., & Radisic, M. (2007). Microfluidic patterning for fabrication of contractile cardiac organoids. *Biomedical Microdevices*, *9*(2), 149–157. https://doi.org/10.1007/s10544-006-9013-7

92. Annabi, N., Tsang, K., Mithieux, S. M., Nikkhah, M., Ameri, A., Khademhosseini, A., & Weiss, A. S. (2013). Highly Elastic Micropatterned Hydrogel for Engineering Functional Cardiac Tissue. *Advanced Functional Materials*, *23*(39), 4950–4959. https://doi.org/10.1002/adfm.201300570

93. Ma, Z., Wang, J., Loskill, P., Huebsch, N., Koo, S., Svedlund, F. L., Marks, N. C., Hua, E. W., Grigoropoulos, C. P., Conklin, B. R., & Healy, K. E. (2015). Self-organizing human cardiac microchambers mediated by geometric confinement. *Nature Communications*, *6*(1), 7413. https://doi.org/10.1038/ncomms8413

94. Gomez, E. W., Chen, Q. K., Gjorevski, N., & Nelson, C. M. (2010). Tissue geometry patterns epithelial–mesenchymal transition via intercellular mechanotransduction. *Journal of Cellular Biochemistry*, *110*(1), 44–51. https://doi.org/10.1002/jcb.22545

95. Gjorevski, N., Sachs, N., Manfrin, A., Giger, S., Bragina, M. E., Ordóñez-Morán, P., Clevers, H., & Lutolf, M. P. (2016). Designer matrices for intestinal stem cell and organoid culture. *Nature*, *539*(7630), 560–564. https://doi.org/10.1038/nature20168

96. Ranga, A., Gobaa, S., Okawa, Y., Mosiewicz, K., Negro, A., & Lutolf, M. P. (2014). 3D niche microarrays for systems-level analyses of cell fate. *Nature Communications*, *5*(1), 4324. https://doi.org/10.1038/ncomms5324

97. Huebsch, N., Loskill, P., Mandegar, M. A., Marks, N. C., Sheehan, A. S., Ma, Z., Mathur, A., Nguyen, T. N., Yoo, J. C., Judge, L. M., Spencer, C. I., Chukka, A. C., Russell, C. R., So,

P.-L., Conklin, B. R., & Healy, K. E. (2015). Automated Video-Based Analysis of Contractility and Calcium Flux in Human-Induced Pluripotent Stem Cell-Derived Cardiomyocytes Cultured over Different Spatial Scales. *Tissue Engineering Part C: Methods*, *21*(5), 467–479. https://doi.org/10.1089/ten.tec.2014.0283

98. Hoang, P., Wang, J., Conklin, B. R., Healy, K. E., & Ma, Z. (2018). Generation of spatial-patterned early-developing cardiac organoids using human pluripotent stem cells. *Nature Protocols*, *13*(4), 723–737. https://doi.org/10.1038/nprot.2018.006

99. Framarino-dei-Malatesta, M., Perrone, G., Giancotti, A., Ventriglia, F., Derme, M., Iannini, I., Tibaldi, V., Galoppi, P., Sammartino, P., Cascialli, G., & Brunelli, R. (2015). Epirubicin: A new entry in the list of fetal cardiotoxic drugs? Intrauterine death of one fetus in a twin pregnancy. Case report and review of literature. *BMC Cancer*, *15*(1), 951. https://doi.org/10.1186/s12885-015-1976-4

100. Sadural, E., & Smith, L. G. J. (1995). Hematologic Malignancies During Pregnancy. *Clinical Obstetrics and Gynecology*, *38*(3), 535.

101. Framarino-dei-Malatesta, M., Sammartino, P., & Napoli, A. (2017). Does anthracycline-based chemotherapy in pregnant women with cancer offer safe cardiac and neurodevelopmental outcomes for the developing fetus? *BMC Cancer*, *17*(1), 777. https://doi.org/10.1186/s12885-017-3772-9

102. Miyamoto, S., Yamada, M., Kasai, Y., Miyauchi, A., & Andoh, K. (2016). Anticancer drugs during pregnancy. *Japanese Journal of Clinical Oncology*, *46*(9), 795–804. https://doi.org/10.1093/jjco/hyw073

103. Bassan, R., Gatta, G., Tondini, C., & Willemze, R. (2004). Adult acute lymphoblastic leukaemia. *Critical Reviews in Oncology/Hematology*, *50*(3), 223–261. https://doi.org/10.1016/j.critrevonc.2003.11.003

104. Yang, T., Walker, M. C., Krewski, D., Yang, Q., Nimrod, C., Garner, P., Fraser, W., Olatunbosun, O., & Wen, S. W. (2008). Maternal characteristics associated with pregnancy exposure to FDA category C, D, and X drugs in a Canadian population. *Pharmacoepidemiology and Drug Safety*, *17*(3), 270–277. https://doi.org/10.1002/pds.1538

105. *Indian Journal of Pharmaceutical Sciences*. (n.d.). Ijpsonline. Retrieved July 21, 2024, from https://www.ijpsonline.com/

106. Battula, P., Kommireddy, S., Lakshmi, K., Farhana, S., & Reddy, V. (2019). DRUG UTILIZATION ASSESSMENT IN PREGNANCY WOMEN: A CROSS SECTIONAL STUDY. *International Research Journal Of Pharmacy*, *10*, 109–113. https://doi.org/10.7897/2230-8407.100252

107. Öztürk, Z., Ölmez, E., Gürpınar, T., & Vural, K. (2018). Birth outcomes after inadvertent use of category X drugs contraindicated in pregnancy: Where is the real risk? *The Turkish Journal of Pediatrics*, *60*(3), 298–305. https://doi.org/10.24953/turkjped.2018.03.010

108. *Essential Medication Prescription and Associated Maternal Characteristic among Hospitalized Pregnant Women: A Retrospective Population Based Study | Journal of Young Pharmacists*. (2018, April 1). https://jyoungpharm.org/article/1119

109. Martel, J. L., Kerndt, C. C., Doshi, H., Sina, R. E., & Franklin, D. S. (2024). Vitamin B1 (Thiamine). In *StatPearls [Internet]*. StatPearls Publishing. https://www.ncbi.nlm.nih.gov/books/NBK482360/

110. Strandler, H. S., & Strand, T. A. (2023). Thiamin (Vitamin B_1) – A scoping review for Nordic Nutrition Recommendations 2023. *Food & Nutrition Research*. https://doi.org/10.29219/fnr.v67.10290

111. Jhala, S. S., & Hazell, A. S. (2011). Modeling neurodegenerative disease pathophysiology in thiamine deficiency: Consequences of impaired oxidative metabolism. *Neurochemistry International*, *58*(3), 248–260. https://doi.org/10.1016/j.neuint.2010.11.019

112. Nisar, S., Kareem, O., Muzaffer, U., Tanvir, M., Ganaie, Mohd. A., & Ahmed, R. N. (2024). Descriptive spectrum of thiamine deficiency in pregnancy: A potentially preventable condition. *International Journal of Gynecology & Obstetrics*, *164*(1), 157–165. https://doi.org/10.1002/ijgo.14989

113. Wang, X., Xu, M., Frank, J. A., Ke, Z., & Luo, J. (2017). Thiamine deficiency induces endoplasmic reticulum stress and oxidative stress in human neurons derived from induced pluripotent stem cells. *Toxicology and Applied Pharmacology*, *320*, 26–31. https://doi.org/10.1016/j.taap.2017.02.009

114. Bhanothu, V., Venkatesan, V., Kondapi, A., & Ajumeera, R. (2021). Restrictions and supplementations effects of vitamins B6, B9 and B12 on growth, vasculogenesis and senescence of BG01V human embryonic stem cell derived embryoid bodies. *Nutrition Clinique et Métabolisme*, *35*. https://doi.org/10.1016/j.nupar.2021.07.002

115. Noble, S., Saxena, V., Ekker, M., & Devlin, R. (2017). Expression of Thiaminase in Zebrafish (Danio rerio) is Lethal and Has Implications for Use as a Biocontainment Strategy in Aquaculture and Invasive Species. *Marine Biotechnology*, *19*(6), 563–569. https://doi.org/10.1007/s10126-017-9776-2

116. Ramanjulu, S., Sudhakar, C., Ramanjulu, S., & Sudhakar, C. (1997). Drought tolerance is partly related to amino acid accumulation and ammonia assimilation: A comparative study in two mulberry genotypes differing in drought sensitivity. *Journal of Plant Physiology*, *150*(3), Article 3. https://doi.org/10.1016/s0176-1617(97)80131-9

117. Hill, L. M., & Kleinberg, F. (1984). Effects of Drugs and Chemicals on the Fetus and Newborn (First of Two Parts). *Mayo Clinic Proceedings*, *59*(10), 707–716. https://doi.org/10.1016/S0025-6196(12)62060-6

118. Hesse, M. R., Prins, J. R., Hooge, M. N. L., Winter, H. L. J., Kosterink, J. G. W., Touw, D. J., & Mian, P. (2023). Pharmacokinetics and Target Attainment of Antimicrobial Drugs Throughout Pregnancy: Part I—Penicillins. *Clinical Pharmacokinetics*, *62*(2), 221–247. https://doi.org/10.1007/s40262-023-01211-z

119. Galvao, T. F., Silva, M. T., Serruya, S. J., Newman, L. M., Klausner, J. D., Pereira, M. G., & Fescina, R. (2013). Safety of Benzathine Penicillin for Preventing Congenital Syphilis: A Systematic Review. *PLOS ONE*, *8*(2), e56463. https://doi.org/10.1371/journal.pone.0056463

120. Desai, S. H., Kaplan, M. S., Chen, Q., & Macy, E. M. (2017). Morbidity in Pregnant Women Associated with Unverified Penicillin Allergies, Antibiotic Use, and Group B Streptococcus Infections. *The Permanente Journal*, *21*(1), 16–080. https://doi.org/10.7812/TPP/16-080

121. Källén, B. A. J., Otterblad Olausson, P., & Danielsson, B. R. (2005). Is erythromycin therapy teratogenic in humans? *Reproductive Toxicology*, *20*(2), 209–214. https://doi.org/10.1016/j.reprotox.2005.01.010

122. Hondeghem, L. M., & Hoffmann, P. (2003). Blinded Test in Isolated Female Rabbit Heart Reliably Identifies Action Potential Duration Prolongation and Proarrhythmic Drugs: Importance of Triangulation, Reverse Use Dependence, and Instability. *Journal of Cardiovascular Pharmacology*, *41*(1), 14.

123. Milberg, P., Eckardt, L., Bruns, H.-J., Biertz, J., Ramtin, S., Reinsch, N., Fleischer, D., Kirchhof, P., Fabritz, L., Breithardt, G., & Haverkamp, W. (2002). Divergent Proarrhythmic Potential of Macrolide Antibiotics Despite Similar QT Prolongation: Fast Phase 3 Repolarization Prevents Early Afterdepolarizations and Torsade de Pointes. *Journal of Pharmacology and Experimental Therapeutics*, *303*(1), 218–225. https://doi.org/10.1124/jpet.102.037911

124. Schoenwetter, A. H., & Silber, E. N. (1965). Penicillin Hypersensitivity, Acute Pericarditis, and Eosinophilia. *JAMA*, *191*(8), 672–673. https://doi.org/10.1001/jama.1965.03080080062023

125. Adler, S., Pellizzer, C., Hareng, L., Hartung, T., & Bremer, S. (2008). First steps in establishing a developmental toxicity test method based on human embryonic stem cells. *Toxicology in Vitro*, *22*(1), 200–211. https://doi.org/10.1016/j.tiv.2007.07.013

126. Cohen, S., Samadikuchaksaraei, A., Polak, J. M., & Bishop, A. E. (2006). Antibiotics Reduce the Growth Rate and Differentiation of Embryonic Stem Cell Cultures. *Tissue Engineering*, *12*(7), 2025–2030. https://doi.org/10.1089/ten.2006.12.2025

127. Varghese, D. S., Parween, S., Ardah, M. T., Emerald, B. S., & Ansari, S. A. (2017). Effects of Aminoglycoside Antibiotics on Human Embryonic Stem Cell Viability during Differentiation In Vitro. *Stem Cells International*, *2017*, 2451927. https://doi.org/10.1155/2017/2451927

128. Domínguez, A. R., Márquez, A., Gumá, J., Llanos, M., Herrero, J., Nieves, M. A. de las, Miramón, J., & Alba, E. (2004). Treatment of stage I and II Hodgkin's lymphoma with ABVD chemotherapy: Results after 7 years of a prospective study. *Annals of Oncology*, *15*(12), 1798–1804. https://doi.org/10.1093/annonc/mdh465

129. BHATIA, S., TYKODI, S. S., & THOMPSON, J. A. (2009). Treatment of Metastatic Melanoma: An Overview. *Oncology (Williston Park, N.Y.)*, *23*(6), 488–496.

130. Reid, J. M., Kuffel, M. J., Miller, J. K., Rios, R., & Ames, M. M. (1999). Metabolic Activation of Dacarbazine by Human Cytochromes P450: The Role of CYP1A1, CYP1A2, and CYP2E11. *Clinical Cancer Research*, *5*(8), 2192–2197.

131. Kewitz, S., Stiefel, M., Kramm, C. M., & Staege, M. S. (2014). Impact of O6-methylguanine-DNA methyltransferase (MGMT) promoter methylation and MGMT expression on dacarbazine resistance of Hodgkin's lymphoma cells. *Leukemia Research*, *38*(1), 138–143. https://doi.org/10.1016/j.leukres.2013.11.001

132. Program, N. T. (2021). Dacarbazine. In *15th Report on Carcinogens [Internet]*. National Toxicology Program. https://www.ncbi.nlm.nih.gov/books/NBK590888/

133. Binaghi, G., Congia, D., Cossa, S., Massidda, S., Pasqualucci, D., Pilo, F., Serra, E., Angelucci, E., & Porcu, M. (2017). Cardiogenic Shock during First Infusion of Anthracycline Chemotherapy in a Patient with Hodgkin Lymphoma: An Unusual Event. *Cardiology*, *139*(1), 7–10. https://doi.org/10.1159/000480291

134. Ali, N., Selim, M., Salah, Z., El Nabarawy, N. M., Hussein, H., & Sidhom, I. (2023). Cardiovascular and Thyroid Late Effects in Pediatric Patients With Hodgkin Lymphoma Treated With ABVD Protocol. *Journal of Pediatric Hematology/Oncology*, *45*(4), e455–e463. https://doi.org/10.1097/MPH.0000000000002638

135. Liu, W., Yang, M., Ping, L., Xie, Y., Wang, X., Zhu, J., & Song, Y. (2021). Chemotherapy with a Pegylated Liposomal Doxorubicin-Containing Regimen in Newly Diagnosed Hodgkin Lymphoma Patients. *Cardiovascular Toxicology*, *21*(1), 12–16. https://doi.org/10.1007/s12012-020-09589-z

136. Salvi, F., Luminari, S., Tucci, A., Massidda, S., Liberati, A. M., Stelitano, C., Zanni, M., Re, A., Centurioni, R., Freilone, R., Musuraca, G., Nassi, L., Patti, C., Arcari, A., Tani, M., Pulsoni, A., Pavone, V., Volpetti, S., Peli, A., … Merli, F. (2019). Bleomycin, vinblastine and dacarbazine combined with nonpegylated liposomal doxorubicin (MBVD) in elderly (≥70 years) or cardiopathic patients with Hodgkin lymphoma: A phase-II study from Fondazione Italiana Linfomi (FIL). *Leukemia & Lymphoma*, *60*(12), 2890–2898. https://doi.org/10.1080/10428194.2019.1608529

137. Adler, I.-D. (2002). Induction of chromosomal aberrations by dacarbazine in somatic and germinal cells of mice. *Mutagenesis*, *17*(5), 383–389. https://doi.org/10.1093/mutage/17.5.383

138. Maggen, C., Dierickx, D., Lugtenburg, P., Laenen, A., Cardonick, E., Smakov, R. G., Bellido, M., Cabrera-Garcia, A., Gziri, M. M., Halaska, M. J., Ottevanger, P. B., Calsteren, K. V., O'Laughlin, A., Polushkina, E., Dam, L. V., Avivi, I., Vandenberghe, P., Woei-A-Jin, F. J. S. H., & Amant, F. (2019). Obstetric and maternal outcomes in patients diagnosed with Hodgkin lymphoma during pregnancy: A multicentre, retrospective, cohort study. *The Lancet Haematology*, *6*(11), e551–e561. https://doi.org/10.1016/S2352-3026(19)30195-4

139. *The treatment of Hodgkin's and non-Hodgkin's lymphoma in pregnancy | Haematologica*. (n.d.). Retrieved July 21, 2024, from https://haematologica.org/article/view/4564

140. Avilès, A., Nambo, M.-J., & Neri, N. (2018). TREATMENT OF EARLY STAGES HODGKIN LYMPHOMA DURING PREGNANCY. *Mediterranean Journal of Hematology and Infectious Diseases*, *10*, e2018006–e2018006. https://doi.org/10.4084/mjhid.2018.006

141. Machet, A., Poudou, C., Tomowiak, C., Gastinne, T., Gardembas, M., Systchenko, T., Moya, N., Debiais, C., Levy, A., Gruchet, C., Sabirou, F., Noel, S., Bouyer, S., Leleu, X., Delwail, V., & Guidez, S. (2023). Hodgkin lymphoma and female fertility: A multicenter study in women treated with doxorubicin, bleomycin, vinblastine, and dacarbazine. *Blood Advances*, *7*(15), 3978–3983. https://doi.org/10.1182/bloodadvances.2021005557

142. Cotteret, C., Pham, Y.-V., Marcais, A., Driessen, M., Cisternino, S., & Schlatter, J. (2020). Maternal ABVD chemotherapy for Hodgkin lymphoma in a dichorionic diamniotic pregnancy: A case report. *BMC Pregnancy and Childbirth*, *20*(1), 231. https://doi.org/10.1186/s12884-020-02928-6

143. Triarico, S., Rivetti, S., Capozza, M. A., Romano, A., Maurizi, P., Mastrangelo, S., Attinà, G., & Ruggiero, A. (2022). Transplacental Passage and Fetal Effects of Antineoplastic Treatment during Pregnancy. *Cancers*, *14*(13), 3103. https://doi.org/10.3390/cancers14133103

144. Kantrowitz-Gordon, I., Hays, K., Kayode, O., Kumar, A. R., Kaplan, H. G., Reid, J. M., Safgren, S. L., Ames, M. M., Easterling, T. R., & Hebert, M. F. (2018). Pharmacokinetics of Dacarbazine (DTIC) in Pregnancy. *Cancer Chemotherapy and Pharmacology*, *81*(3), 455–460. https://doi.org/10.1007/s00280-017-3511-6

145. Cardonick, E., & Iacobucci, A. (2004). Use of chemotherapy during human pregnancy. *The Lancet. Oncology*, *5*(5), 283–291. https://doi.org/10.1016/S1470-2045(04)01466-4

146. Pagès, C., Robert, C., Thomas, L., Maubec, E., Sassolas, B., Granel-Brocard, F., Chevreau, C., De Raucourt, S., Leccia, M. -T., Fichet, D., Khammari, A., Boitier, F., Stoebner, P. -E., Dalac, S., Celerier, P., Aubin, F., & Viguier, M. (2010). Management and outcome of metastatic melanoma during pregnancy. *British Journal of Dermatology*, *162*(2), 274–281. https://doi.org/10.1111/j.1365-2133.2009.09240.x

147. Thompson, D. J., Molello, J. A., Strebing, R. J., & Dyke, I. L. (1978). Teratogenicity of adriamycin and daunomycin in the rat and rabbit,. *Teratology*, *17*(2), 151–157. https://doi.org/10.1002/tera.1420170207

148. Zhou, B., Hutson, J. M., Farmer, P. J., Hasthorpe, S., Myers, N. A., & Liu, M. (1999). Apoptosis in tracheoesophageal embryogenesis in rat embryos with or without adriamycin treatment. *Journal of Pediatric Surgery*, *34*(5), 872–876. https://doi.org/10.1016/S0022-3468(99)90390-1

149. Menegola, E., Broccia, M. L., & Renzo, F. D. (2001). Teratogenic effects of Doxorubicin in rats at midgestation and at term. *Teratogenesis, Carcinogenesis, and Mutagenesis*, *21*(4), 283–293. https://doi.org/10.1002/tcm.1016

150. Menegola, E., Broccia, M. L., Prati, M., Ricolfi, R., & Giavini, E. (1997). Comparative embryotoxicity of four anthracyclines: In Vitro study on their effects on glutathione status. *Toxicology in Vitro: An International Journal Published in Association with BIBRA*, *11*(1–2), 33–41. https://doi.org/10.1016/s0887-2333(96)00070-7

151. Germann, N., Goffinet, F., & Goldwasser, F. (2004). Anthracyclines during pregnancy: Embryo–fetal outcome in 160 patients. *Annals of Oncology*, *15*(1), 146–150. https://doi.org/10.1093/annonc/mdh009

152. Selig, B. P., Furr, J. R., Huey, R. W., Moran, C., Alluri, V. N., Medders, G. R., Mumm, C. D., Hallford, H. G., & Mulvihill, J. J. (2012). Cancer chemotherapeutic agents as human teratogens. *Birth Defects Research Part A: Clinical and Molecular Teratology*, *94*(8), 626–650. https://doi.org/10.1002/bdra.23063

153. *NTP Monograph: Developmental Effects and Pregnancy Outcomes Associated with Cancer Chemotherapy Use During Pregnancy; May 2013*. (n.d.).

154. Dilek, I., Topcu, N., Demir, C., Bay, A., Uzun, K., Gul, A., Faik Öner, A., & Ugras, S. (2006). Hematological malignancy and pregnancy: A single-institution experience of 21 cases. *Clinical & Laboratory Haematology*, *28*(3), 170–176. https://doi.org/10.1111/j.1365-2257.2006.00781.x

155. Hasselt, J. G. C. van, Calsteren, K. van, Heyns, L., Han, S., Gziri, M. M., Schellens, J. H. M., Beijnen, J. H., Huitema, A. D. R., & Amant, F. (2014). Optimizing anticancer drug treatment in pregnant cancer patients: Pharmacokinetic analysis of gestation-induced changes for doxorubicin, epirubicin, docetaxel and paclitaxel. *Annals of Oncology*, *25*(10), 2059–2065. https://doi.org/10.1093/annonc/mdu140

156. Ryu, R. J., Eyal, S., Kaplan, H. G., Akbarzadeh, A., Hays, K., Puhl, K., Easterling, T. R., Berg, S. L., Scorsone, K. A., Feldman, E. M., Umans, J. G., Miodovnik, M., & Hebert, M. F. (2014). Pharmacokinetics of doxorubicin in pregnant women. *Cancer Chemotherapy and Pharmacology*, *73*(4), 789–797. https://doi.org/10.1007/s00280-014-2406-z

157. Roboz, J., Gleicher, N., Wu, K., Chahinian, P., Kerenyi, T., & Holland, J. (1979). DOES DOXORUBICIN CROSS THE PLACENTA? *The Lancet*, *314*(8156), 1382–1383. https://doi.org/10.1016/S0140-6736(79)92878-2

158. Swain, S. M., Whaley, F. S., & Ewer, M. S. (2003). Congestive heart failure in patients treated with doxorubicin. *Cancer*, *97*(11), 2869–2879. https://doi.org/10.1002/cncr.11407

159. Force, T., & Kolaja, K. L. (2011). Cardiotoxicity of kinase inhibitors: The prediction and translation of preclinical models to clinical outcomes. *Nature Reviews Drug Discovery*, *10*(2), 111–126. https://doi.org/10.1038/nrd3252

160. Volkova, M., & Russell, R. (2012). Anthracycline Cardiotoxicity: Prevalence, Pathogenesis and Treatment. *Current Cardiology Reviews*, *7*(4), 214–220. https://doi.org/10.2174/157340311799960645

161. Ewer, M. S., & Ewer, S. M. (2015). Cardiotoxicity of anticancer treatments. *Nature Reviews Cardiology*, *12*(9), 547–558. https://doi.org/10.1038/nrcardio.2015.65

162. Zamorano, J. L., Lancellotti, P., Rodriguez Muñoz, D., Aboyans, V., Asteggiano, R., Galderisi, M., Habib, G., Lenihan, D. J., Lip, G. Y. H., Lyon, A. R., Lopez Fernandez, T., Mohty, D., Piepoli, M. F., Tamargo, J., Torbicki, A., Suter, T. M., & ESC Scientific Document Group. (2016). 2016 ESC Position Paper on cancer treatments and cardiovascular toxicity developed under the auspices of the ESC Committee for Practice Guidelines: The Task Force for cancer treatments and cardiovascular toxicity of the European Society of Cardiology (ESC). *European Heart Journal*, *37*(36), 2768–2801. https://doi.org/10.1093/eurheartj/ehw211

163. Azim, H. A., Peccatori, F. A., Scarfone, G., Acaia, B., Rossi, P., Cascio, R., & Goldhirsch, A. (2008). Anthracyclines for gestational breast cancer: Course and outcome of pregnancy. *Annals of Oncology*, *19*(8), 1511–1512. https://doi.org/10.1093/annonc/mdn396

164. Cardonick, E., Gilmandyar, D., & Somer, R. A. (2012). Maternal and Neonatal Outcomes of Dose-Dense Chemotherapy for Breast Cancer in Pregnancy. *Obstetrics & Gynecology*, *120*(6), 1267. https://doi.org/10.1097/AOG.0b013e31826c32d9

165. Siedner, S., Krüger, M., Schroeter, M., Metzler, D., Roell, W., Fleischmann, B. K., Hescheler, J., Pfitzer, G., & Stehle, R. (2003). Developmental changes in contractility and sarcomeric proteins from the early embryonic to the adult stage in the mouse heart. *The Journal of Physiology*, *548*(Pt 2), 493–505. https://doi.org/10.1113/jphysiol.2002.036509

166. Maillet, A., Tan, K., Chai, X., Sadananda, S. N., Mehta, A., Ooi, J., Hayden, M. R., Pouladi, M. A., Ghosh, S., Shim, W., & Brunham, L. R. (2016). Modeling Doxorubicin-Induced Cardiotoxicity in Human Pluripotent Stem Cell Derived-Cardiomyocytes. *Scientific Reports*, *6*(1), 25333. https://doi.org/10.1038/srep25333

167. Zhang, S., Liu, X., Bawa-Khalfe, T., Lu, L.-S., Lyu, Y. L., Liu, L. F., & Yeh, E. T. H. (2012). Identification of the molecular basis of doxorubicin-induced cardiotoxicity. *Nature Medicine*, *18*(11), 1639–1642. https://doi.org/10.1038/nm.2919

168. Zhao, L., & Zhang, B. (2017). Doxorubicin induces cardiotoxicity through upregulation of death receptors mediated apoptosis in cardiomyocytes. *Scientific Reports*, *7*(1), 44735. https://doi.org/10.1038/srep44735

169. Elford, H. L. (1968). Effect of hydroxyurea on ribonucleotide reductase. *Biochemical and Biophysical Research Communications*, *33*(1), 129–135. https://doi.org/10.1016/0006-291X(68)90266-0

170. Schmidt, C. W. P., & Otoni, K. M. (Eds.). (2021). *Chemotherapy and Pharmacology for Leukemia in Pregnancy: Guidelines and Strategies for Best Practices*. Springer International Publishing. https://doi.org/10.1007/978-3-030-54058-6

171. Reynoso, E. E., Keating, A., & Baker, M. A. (1987). Acute leukemia occurring 19 years after treatment of acute lymphoblastic leukemia. *Cancer*, *59*(11), 1963–1965. https://doi.org/10.1002/1097-0142(19870601)59:11<1963::AID-CNCR2820591121>3.0.CO;2-C

172. Tartakover Matalon, S., Ornoy, A., Fishman, A., Drucker, L., & Lishner, M. (2005). The effect of 6-mercaptopurine on early human placental explants. *Human Reproduction*, *20*(5), 1390–1397. https://doi.org/10.1093/humrep/deh721

173. Ticku, J., Oberoi, S., Friend, S., Busowski, J., Langenstroer, M., & Baidas, S. (2013). Acute lymphoblastic leukemia in pregnancy: A case report with literature review. *Therapeutic Advances in Hematology*, *4*(5), 313–319. https://doi.org/10.1177/2040620713492933

174. Palani, R., Milojkovic, D., & Apperley, J. F. (2015). Managing pregnancy in chronic myeloid leukaemia. *Annals of Hematology*, *94*(2), 167–176. https://doi.org/10.1007/s00277-015-2317-z

175. Abruzzese, E., Trawinska, M. M., de Fabritiis, P., & Baccarani, M. (2016). Management of pregnant chronic myeloid leukemia patients. *Expert Review of Hematology*, *9*(8), 781–791. https://doi.org/10.1080/17474086.2016.1205479

176. *Chronic Myelogenous Leukemia: Pregnancy in the Era of Stopping Tyrosine Kinase Inhibitor Therapy | Journal of Clinical Oncology*. (n.d.). Retrieved July 23, 2024, from https://ascopubs.org/doi/10.1200/JCO.2017.77.2574

177. Beckloff, G. L., Lerner, H. J., Frost, D., Russo-Alesi, F. M., & Gitomer, S. (1965). Hydroxyurea (NSC-32065) in biologic fluids: Dose-concentration relationship. *Cancer Chemotherapy Reports*, *48*, 57–58.

178. *S5-R3_Step4_Guideline_2020_0218_1.pdf*. (n.d.). Retrieved July 10, 2024, from https://database.ich.org/sites/default/files/S5-R3_Step4_Guideline_2020_0218_1.pdf

179. Sadler, T. W., & Cardell, R. R. (1977). Ultrastructural alterations in neuroepithelial cells of mouse embryos exposed to cytotoxic doses of hydroxyurea. *The Anatomical Record*, *188*(1), 103–123. https://doi.org/10.1002/ar.1091880110

180. Warner, C. W., Salder, T. W., Shockey, J., & Kate Smith, M. (1983). A comparison of the in vivo and in vitro response of mammalian embryos to a teratogenic insult. *Toxicology*, *28*(4), 271–282. https://doi.org/10.1016/0300-483X(83)90001-X

181. Jaklin, M., Zhang, J. D., Barrow, P., Ebeling, M., Clemann, N., Leist, M., & Kustermann, S. (2020). Focus on germ-layer markers: A human stem cell-based model for *in vitro* teratogenicity testing. *Reproductive Toxicology*, *98*, 286–298. https://doi.org/10.1016/j.reprotox.2020.10.011

182. Shah, S., Haeger-Overstreet, K., & Flynn, B. (2022). Methotrexate-induced acute cardiotoxicity requiring veno-arterial extracorporeal membrane oxygenation support: A case report. *Journal of Medical Case Reports*, *16*(1), 447. https://doi.org/10.1186/s13256-022-03644-9

183. Thunuguntla, S. (2020). Cardiotoxicity: An Unusual Case of Methotrexate Overdose. *Archives of Clinical Case Studies*, *2*(5), 1–3.

184. National Toxicology Program. (2013). NTP Monograph: Developmental Effects and Pregnancy Outcomes Associated With Cancer Chemotherapy Use During Pregnancy. *NTP Monograph*, *2*, i–214.

185. Campbell, M. A., Perrier, D. G., Dorr, R. T., Alberts, D. S., & Finley, P. R. (1985). Methotrexate: Bioavailability and pharmacokinetics. *Cancer Treatment Reports*, *69*(7–8), 833–838.

186. *Methotrexate Dosage Guide + Max Dose, Adjustments*. (n.d.). Drugs.Com. Retrieved July 23, 2024, from https://www.drugs.com/dosage/methotrexate.html

187. Piggott, K. D., Sorbello, A., Riddle, E., & DeCampli, W. (2011). Congenital Cardiac Defects: A Possible Association of Aminopterin Syndrome and In Utero Methotrexate Exposure? *Pediatric Cardiology*, *32*(4), 518–520. https://doi.org/10.1007/s00246-011-9913-z

188. Feldkamp, M., & Carey, J. C. (1993). Clinical teratology counseling and consultation case report: Low dose methotrexate exposure in the early weeks of pregnancy. *Teratology*, *47*(6), 533–539. https://doi.org/10.1002/tera.1420470605

189. Perez-Verdia, A., Angulo, F., Hardwicke, F. L., & Nugent, K. M. (2005). Acute Cardiac Toxicity Associated with High-Dose Intravenous Methotrexate Therapy: Case Report and Review of the Literature. *Pharmacotherapy: The Journal of Human Pharmacology and Drug Therapy*, *25*(9), 1271–1276. https://doi.org/10.1592/phco.2005.25.9.1271

190. Dawson, A. L., Riehle-Colarusso, T., Reefhuis, J., & Arena, J. F. (2014). Maternal Exposure to Methotrexate and Birth Defects: A Population-Based Study. *American Journal of Medical Genetics. Part A*, *0*(9), 2212–2216. https://doi.org/10.1002/ajmg.a.36625

191. Cerychova, R., & Pavlinkova, G. (2018). HIF-1, Metabolism, and Diabetes in the Embryonic and Adult Heart. *Frontiers in Endocrinology*, *9*, 460. https://doi.org/10.3389/fendo.2018.00460

192. Nakamura, Z. M., Deal, A. M., Rosenstein, D. L., Quillen, L. J., Chien, S. A., Wood, W. A., Shea, T. C., & Park, E. M. (2020). Design of a randomized placebo controlled trial of high dose intravenous thiamine for the prevention of delirium in allogeneic hematopoietic stem cell transplantation. *Contemporary Clinical Trials*, *95*, 106076. https://doi.org/10.1016/j.cct.2020.106076

193. Mantziou, V., Baillie-Benson, P., Jaklin, M., Kustermann, S., Arias, A. M., & Moris, N. (2021). *In vitro* teratogenicity testing using a 3D, embryo-like gastruloid system. *Reproductive Toxicology*, *105*, 72–90. https://doi.org/10.1016/j.reprotox.2021.08.003

194. Sparrow, A. J., Sievert, K., Patel, S., Chang, Y.-F., Broyles, C. N., Brook, F. A., Watkins, H., Geeves, M. A., Redwood, C. S., Robinson, P., & Daniels, M. J. (2019). Measurement of Myofilament-Localized Calcium Dynamics in Adult Cardiomyocytes and the Effect of Hypertrophic Cardiomyopathy Mutations. *Circulation Research*, *124*(8), 1228–1239. https://doi.org/10.1161/CIRCRESAHA.118.314600

195. Robinson, P., Liu, X., Sparrow, A., Patel, S., Zhang, Y.-H., Casadei, B., Watkins, H., & Redwood, C. (2018). Hypertrophic cardiomyopathy mutations increase myofilament Ca2+ buffering, alter intracellular Ca2+ handling, and stimulate Ca2+-dependent signaling. *The Journal of Biological Chemistry*, *293*(27), 10487–10499. https://doi.org/10.1074/jbc.RA118.002081

196. Piersma, A. H., Baker, N. C., Daston, G. P., Flick, B., Fujiwara, M., Knudsen, T. B., Spielmann, H., Suzuki, N., Tsaioun, K., & Kojima, H. (2022). Pluripotent stem cell assays: Modalities and applications for predictive developmental toxicity. *Current Research in Toxicology*, *3*, 100074. https://doi.org/10.1016/j.crtox.2022.100074

197. Robinson, J. F., & Piersma, A. H. (2013). Toxicogenomic Approaches in Developmental Toxicology Testing. In P. C. Barrow (Ed.), *Teratogenicity Testing: Methods and Protocols* (pp. 451–473). Humana Press. https://doi.org/10.1007/978-1-62703-131-8_31

198. West, P. R., Weir, A. M., Smith, A. M., Donley, E. L. R., & Cezar, G. G. (2010). Predicting human developmental toxicity of pharmaceuticals using human embryonic stem cells and metabolomics. *Toxicology and Applied Pharmacology*, *247*(1), 18–27. https://doi.org/10.1016/j.taap.2010.05.007

199. Aikawa, N., Kunisato, A., Nagao, K., Kusaka, H., Takaba, K., & Ohgami, K. (2014). Detection of Thalidomide Embryotoxicity by In Vitro Embryotoxicity Testing Based on Human iPS Cells. *Journal of Pharmacological Sciences*, *124*(2), 201–207. https://doi.org/10.1254/jphs.13162FP

200. Shinozawa, T., Furukawa, H., Sato, E., & Takami, K. (2012). A Novel Purification Method of Murine Embryonic Stem Cell– and Human-Induced Pluripotent Stem Cell–Derived Cardiomyocytes by Simple Manual Dissociation. *Journal of Biomolecular Screening*, *17*(5), 683–691. https://doi.org/10.1177/1087057111434145

201. Dehghani, L., Nasr Esfahani, M.-H., & Tahani, S. (2014). Genetically Engineered Mouse Embryonic Stem Cell – derived Cardiomyocytes as a Suitable Model on Drugs Toxicity In vitro. *International Journal of Pediatrics*, *2*(2.3), 73–73. https://doi.org/10.22038/ijp.2014.2736

202. Cunha-Oliveira, T., Ferreira, L. L., Coelho, A. R., Deus, C. M., & Oliveira, P. J. (2018). Doxorubicin triggers bioenergetic failure and p53 activation in mouse stem cell-derived cardiomyocytes. *Toxicology and Applied Pharmacology*, *348*, 1–13. https://doi.org/10.1016/j.taap.2018.04.009

203. Lagerqvist, E. L., Finnin, B. A., Elliott, D. A., Anderson, D. J., Wu, S. M., Pouton, C. W., & Haynes, J. M. (2015). Comparing mouse and human pluripotent stem cell derived cardiac cells: Both systems have advantages for pharmacological and toxicological screening. *Journal of Pharmacological and Toxicological Methods*, *74*, 17–25. https://doi.org/10.1016/j.vascn.2015.04.009

204. Hoang, P., Sun, S., Tarris, B. A., & Ma, Z. (2023). Controlling Morphology and Functions of Cardiac Organoids by Two-Dimensional Geometrical Templates. *Cells Tissues Organs*, *212*(1), 64–73. https://doi.org/10.1159/000521787

205. Kostina, A., Volmert, B., & Aguirre, A. (2024). Human heart organoids: Current applications and future perspectives. *European Heart Journal*, *45*(10), 751–753. https://doi.org/10.1093/eurheartj/ehad841

206. Sheffield, J. S., Siegel, D., Mirochnick, M., Heine, R. P., Nguyen, C., Bergman, K. L., Savic, R. M., Long, J., Dooley, K. E., & Nesin, M. (2014). Designing Drug Trials: Considerations for Pregnant Women. *Clinical Infectious Diseases*, *59*(suppl_7), S437–S444. https://doi.org/10.1093/cid/ciu709

Meng Chai

Email: mechai@syr.edu , Tel:+1-786-5213546

SUMMARY

A versatile person with diverse backgrounds from cell biology to analytical process development. Demonstrate proficiency in stem cell maintenance, differentiation, and cell-based functional assays on establishing advanced human iPSCs 2D/3D platforms. Proficient in organoid technology, molecular biology, and analytical chemistry. In-progress master thesis featured in embryotoxicity screening assay using iPSC-based cardiac organoids. Extensive experience in developing state-of-the-art analytical tools for small molecule/nanoparticle-based pharmaceutical characterization. Currently a research intern in a leading bioprocessing company, Sartorius Stedim Biotech. Highly independent and collaborative in conducting experiments, quality control, and data interpretation.

SKILLS

- Cell biology: human-induced pluripotent stem cells (iPSC), embryonic stem cells (ESC), mesenchymal stem cells (MSC), mammalian cells (fibroblasts, cardiomyocytes)
- Molecular biology: PCR/qPCR, ELISA, western blotting, RNA transfection
- Polymer fabrication: photolithography, soft lithography, microcontact patterning
- Analytical instrumentation: Flow cytometry, High-performance liquid chromatography (HPLC), Size exclusion chromatography-multiangle scattering(SEC-MALS), Field flow filtration (FFF), Liquid chromatography-mass spectrometry (LC-MS)
- Data analysis: GraphPad-Prism, Image-J, FlowJo, Matlab, Excel

RESEARCH EXPERIENCE

Research Intern, Sartorius Stedim Biotech, MA *Sep. 2023 – Present*

- Contributed as part of the Advanced Bio-analytics team in analytical method development for various nanoparticle (extracellular vesicles (EV), liposomes, lipid nanoparticles) characterization, quantification, and purification
- Focused on developing and optimizing orthogonal techniques for nanoparticle characterization using nanoparticle tracking analysis, flow cytometry, and analytical HPLC
- Experienced in designing and executing size-exclusion chromatography (SEC) to support crude mesenchymal stem cell-produced extracellular vesicles (MSC-EV) characterization using orthogonal chromatographic methods; supported Process Development team in optimizing and transferring methods for crude sample purification and final product characterization
- Proficient in troubleshooting and performing routine maintenance of the analytical instrumentations

Research Technician, BioMarin Inc, CA *Dec. 2022 – Aug. 2023*

- Focused on studying the mutations of a congenital disease-induced hypertrophic cardiomyopathy (HCM) using iPSC-derived cardiomyocytes
- Recapitulated disease pathologies in HCM with iPSC-derived mutants and CRISPR-Cas9-corrected isogenic control cardiomyocytes by exhibiting structural defects
- Developed a congenital HCM disease model with verified signal pathways; evaluated the underdeveloped therapeutic solutions to attenuate HCM phenotypes

Research Assistant, Syracuse Bioinspired Institute, NY *Advisor: Dr. Zhen Ma* *Sep. 2021 – Aug. 2023*

Thesis: Embryotoxicity of Chemotherapeutic Agents Tested Using Engineered Cardiac Organoids

- Conducted routine iPSC culture and differentiation; supported cryopreservation; established improved new and existing protocols for lab operations and provided SOP manuals for the stem cell differentiation workflow

- Engineered 3D cardiac organoids with geometric confinements provided by a biomaterial-based micropatterning method to study the human cardio genesis and cardiac developmental toxicity
- Evaluated cardiac embryotoxicity by characterizing drugs' effects on organoids based on cardiac differentiation, contractile behaviors, and tissue morphology
- Provided training for new team members in cell culture, differentiation, in vitro assays, and lab safety procedures

PUBLICATION

- **Manuscript in progress; *targeted journal: Cell Reports***

Hoang P., Mckellar D., Mai N., **Chai M.,** et al. "Size-Driven Mesoderm-Endoderm Lineage Divergence in Engineered Cardiac Organoids"

CONFERENCE

- ***International Society for Cell & Gene Therapy*** *June. 2024*

Dehghani M., Keselman P., Mukherjee P., Speidel J., Olszowy M., **Chai M**. et al. "Analytical Toolbox for Biophysical Characterization of Extracellular Vesicles Samples"

EDUCATION

- Syracuse University (SU) — Syracuse, NY

Master of Science in Bioengineering, GPA: 3.74/4.0 — Expected in Aug. 2024

- University of Miami (UM) — Miami, FL

Master of Science in Industrial Engineering, GPA: 3.37/4.0 — Sep. 2019 - May. 2021

- China University of Petroleum (East China) (UPC) — Qingdao, China

Bachelor of Engineering in Chemical Engineering, GPA: 3.45/4.0 — Sep. 2015 - Jun. 2019